

# Statistical physics of inference: Thresholds and algorithms

Lenka Zdeborová<sup>1,\*</sup>, and Florent Krzakala<sup>2,\*</sup>

<sup>1</sup> *Institut de Physique Théorique,*

*CEA Saclay and CNRS, 91191, Gif-sur-Yvette, France.*

<sup>2</sup> *Sorbonne Universités, Université Pierre et Marie Curie Paris 6 and Ecole Normale Supérieure, 75005 Paris, France.*

*\* lenka.zdeborova@cea.fr and florent.krzakala@ens.fr*

Many questions of fundamental interest in today's science can be formulated as inference problems: Some partial, or noisy, observations are performed over a set of variables and the goal is to recover, or infer, the values of the variables based on the indirect information contained in the measurements. For such problems, the central scientific questions are: Under what conditions is the information contained in the measurements sufficient for a satisfactory inference to be possible? What are the most efficient algorithms for this task? A growing body of work has shown that often we can understand and locate these fundamental barriers by thinking of them as phase transitions in the sense of statistical physics. Moreover, it turned out that we can use the gained physical insight to develop new promising algorithms. Connection between inference and statistical physics is currently witnessing an impressive renaissance and we review here the current state-of-the-art, with a pedagogical focus on the Ising model which formulated as an inference problem we call the planted spin glass. In terms of applications we review two classes of problems: (i) inference of clusters on graphs and networks, with community detection as a special case and (ii) estimating a signal from its noisy linear measurements, with compressed sensing as a case of sparse estimation. Our goal is to provide a pedagogical review for researchers in physics and other fields interested in this fascinating topic.

## CONTENTS

A. What is statistical inference?	4
1. What do we want to know	4
2. Terminology and a simple example	5
3. Teacher-student scenario	6
4. Bayes optimal versus mismatched	6
5. Estimators	7
6. The high-dimensional limit	8
B. Statistical physics and inference	9
1. Basic dictionary	10
2. Useful statistical physics concepts	10
II. Inference as the planted ensemble	12
A. Example of the planted spin glass	12
1. Definition of planted spin glass	12
2. Nishimori's mapping via gauge transformation	14
3. Bayes-optimality on the Nishimori line	14
4. Parameter mismatch and learning	15
B. Averaging and the planted ensemble	16
1. The quenched and annealed ensembles	16
2. Planting as an ensemble	18
3. Quiet planting	18
4. No replica symmetry breaking on the Nishimori line.	19
C. Phase diagram from the cavity method	20
1. Properties of the random ensemble	21
2. Phase diagram of the planted spin glass	22
3. Systems with first order phase transitions	22
4. Comments on the phase transitions in various problems	23
D. Applications of planting for studies of glasses	24
1. Equilibration for free in glasses	24
2. Following states and analyzing slow annealing	25
3. Melting and glass transition	26
III. From physics insight to new algorithmic ideas	27
A. Non-backtracking spectral method	27
B. On computational hardness of the hard phase	28
C. Spatial coupling	29
1. Spatially coupled Curie-Weiss model	30
D. A brief history of time indices in the TAP equations	30
IV. Clustering of networks and community detection	33
A. Biased overview of community detection	33
B. Asymptotically exact analysis of the SBM	34
C. Examples of phase transitions in the SBM	36
D. Spectral redemption in clustering sparse networks	38
E. More on the non-backtracking operator	40
F. Deceptiveness of the variational Bayes method	41
G. Real networks are not generated by the SBM	41
V. Linear estimation and compressed sensing	43
A. Compressed sensing	44
B. Approximate message passing	44
1. Note of convergence and parameter learning	46
2. Examples of priors and outputs	47
C. State evolution and phase transitions	48
D. Spatial coupling	49
E. Non-random matrices and non-separable priors	51

	3
1. Structured priors	51
2. Orthogonal matrices	51
3. Reconstruction in discrete tomography	52
F. Optics in complex media	52
Acknowledgements	55
Fundings	55
References	55

## I. INTRODUCTION

Our goal in this review is to describe recent developments in a rapidly evolving field at the interface between statistical inference and statistical physics.

This review being written mostly for physics audience, we shall assume some rudimentary familiarity with concepts of statistical physics, such as the canonical ensemble, partition function and Hamiltonian. We shall start by reminding some text-book material for statistical inference and by describing the connection between the two. Statistical physics was developed to derive macroscopic properties of material from microscopic physical laws. Inference aims to discover structure in data. On the first look, these goals seem quite different. Yet, it was the very same man, Pierre Simon, Marquis de Laplace (1749–1827), who did one of the first very sophisticated derivation of the gas laws within the caloric theory, and who also created the field of statistical inference [159]. This suggests there may be a link after all. Methods and tools of statistical physics are designed to describe large assemblies of small elements - such as atoms or molecules. These atoms can quite readily be replaced by other elementary constituents - bits, nodes, agents, neurons, data points. This simple fact, and the richness and the power of the methods invented by physicists over the last century, is at the roots of the connection.

There is a number of books discussing this interdisciplinary connection, without pretention of exhaustivity, see e.g. [72, 89, 138, 165]. Our focus here is to present the recent contributions that were obtained using methodology that originated in the field of spin glasses [163, 215]. In particular the replica and cavity method with related message passing algorithm are at the roots of our toll box.

The present contribution is organized as follow. First, the present chapter introduces the subject and necessary concepts. Next, in Sec. II, we present an example of an inference problem – the planted spin glass. This will allow to introduce the generic approach to inference in a setting familiar to all physicists. Armed with the statistical physics understanding of inference, we discuss related recent algorithmic ideas in Sec. III. Finally we study and review two different timely applications: the clustering of networks in Sec. IV and linear estimation with compressed sensing as its example in Sec. V.

### A. What is statistical inference?

According to common wisdom as collected by Wikipedia, inference is the act or process of deriving logical conclusions from premises known or assumed to be true. Statistical inference is the process of deducing properties of an underlying distribution by analysis of data. A way to think about inference problems, that is particularly relevant in the context of today’s data deluge (often referred to as *big data*), are procedures to extract useful information from large amounts of data.

As the boundaries between fields are breaking, nowadays inference problems appear literally everywhere, in machine learning, artificial intelligence, signal processing, quantitative biology, medicine, neuroscience and many others.

A more formal way to set an inference problem is the following, one considers a set of variables  $\mathbf{x} = \{x_i\}_{i=1,\dots,N}$  on which one is able to perform some partial observations or measurements  $\mathbf{y} = \{y_\mu\}_{\mu=1,\dots,M}$ . The goal is to deduce or infer the values of variables  $\mathbf{x}$  based on the perhaps indirect and noisy information contained in the observed data  $\mathbf{y}$ . To give a couple of examples the variables may correspond for instance to image pixels, an acoustic signal, assignment of data points into clusters while the corresponding observations would correspond for instance to a blurred photograph, recording of a song performed on a platform while the metro was arriving, or positions of points in space.

#### 1. What do we want to know

For inference problems the two scientific questions of interest are:

- The question of sufficient information – Under what conditions is the information contained in the observations sufficient for satisfactory recovery of the variables to be possible?
- The question of computational efficiency – Can the inference be done in an algorithmically efficient way? What are the most optimal algorithms for this task?

These two questions are of very different nature. The first one is a question that belongs to the realm of statistics and information theory. The second one, instead, is in the realm of computer science and computational complexity. Before the era of big data, statistics was often not concerned with computational tractability, because the number of parameters to estimate was usually small. Today the tradeoff between statistical and computational efficiency is changing and studying the two above questions jointly seems as the most reasonable option.

We will see that these two questions have a very clear interpretation in terms of phase transitions in physics. Or better, the first one is connected to a genuine phase transitions while the second one is connected to the type of the transition (first or second order), and to the metastability associated with first order phase transitions.

## 2. Terminology and a simple example

Let us turn to a concrete example in physics, which is actually taken from Ref. [153]. Unstable particles are emitted from a source and decay at a distance  $y$  from the source. Unfortunately, we cannot build a perfect infinite length detector, and decay events can only be observed if they occur in a window extending from distances  $y = 1$  cm to  $y = 20$  cm from the source.

We run the experiments for some time, and we observe  $M$  decays at locations  $\mathbf{y} = \{y_1, \dots, y_M\}$ . We also know that we should expect an exponential probability distribution with characteristic length  $x$  for the event. Writing things in the inference language,  $\mathbf{y}$  are the observations and  $x$  is the unknown signal (of dimension  $N = 1$ ). The question we would like to answer is: Given the observations, how to estimate  $x$ ?

In this review, we will follow the approach of Bayesian inference. Developed by Thomas Bayes and Laplace, it concentrates on conditional probabilities and denotes  $P(A|B)$  the probability of having an event  $A$  conditioned to the event  $B$ . The central point of the approach is the so-called Bayes formula:

$$P(\mathbf{x}|\mathbf{y}) = \frac{P(\mathbf{y}|\mathbf{x})}{P(\mathbf{y})}P(\mathbf{x}). \quad (1)$$

There is a precise terminology for all the terms entering this equation, so we shall start by discussing the Bayesian inference vernacular:

- $P(\mathbf{x}|\mathbf{y})$  is called the *posterior* probability for  $\mathbf{x}$  given all the data  $\mathbf{y}$ .
- $P(\mathbf{y}|\mathbf{x})$  is called the *likelihood*.
- The  $P(\mathbf{y})$ , also denoted as a normalisation  $Z(\mathbf{y})$ , is called the *evidence*.
- $P(\mathbf{x})$  is called the *prior* probability for  $\mathbf{x}$ . It should reflect our belief over what  $\mathbf{x}$  should be before we received any data.

Let us see how this applies in the above problem of decaying particles. We know that the likelihood for one observation is

$$P(y|x) = \begin{cases} \frac{1}{x\mathcal{N}(x)}e^{-y/x} & \text{if } 1 < y < 20, \\ 0 & \text{otherwise,} \end{cases} \quad (2)$$

with a normalisation  $\mathcal{N}(x) = \int_1^{20} dz \frac{1}{x} e^{-z/x} = e^{-1/x} - e^{-20/x}$ . The observations are independent. From eq. (2) we can now extract  $P(x|\mathbf{y})$  using the Bayes formula we get

$$P(x|\mathbf{y}) = \frac{P(x)}{Z(\mathbf{y}) [x\mathcal{N}(x)]^M} e^{-\sum_{i=1}^M y_i/x}. \quad (3)$$

Looking to this equation, we see that we have  $P(x)$  on the right. If we do not have any prior information on  $x$ , we assume that  $P(x)$  is a constant that just enters in the  $x$ -independent normalization, and in this case we obtain

$$P(x|\mathbf{y}) = \frac{1}{\bar{Z}(\mathbf{y}) [x\mathcal{N}(x)]^M} e^{-\sum_{i=1}^M y_i/x} \quad (4)$$

This is the final answer from Bayesian statistics. It contains all the information that we have on  $x$  in this approach. For a dataset consisting of several points, for instance the six points  $y = 1.5, 2, 3, 4, 5, 12$  cm, one can compute the most probable value of  $x$  to be around  $\hat{x} = 3.7$  cm, note that this is considerably different from the mere average of the points which is  $\bar{y} = 4.6$  cm.

Let us make some important comments on these considerations, which have been at the roots of the Bayesian approach to inference from the very start. First, we notice that probabilities are used here to quantify degrees of belief. To avoid possible confusions, it must thus be emphasized that the true  $\mathbf{x}$  in the real world *is not* a random variable, and the fact that Bayesians use probability distribution  $P(\mathbf{x}|\mathbf{y})$  does not mean that they think of the world

as stochastically changing its nature between the states described by the different hypotheses. The notation of probabilities is used here to represent the beliefs about the mutually exclusive hypotheses (here, values of  $x$ ), of which only one is actually true. The fact that probabilities can denote degrees of belief is at the heart of Bayesian inference. The reader interested in these considerations is referred to the very influential work of Bruno de Finetti [58] (who famously once said that “Probability does not exist!”).

Another subtle point is how to choose the prior distribution  $P(\mathbf{x})$ . In fact, discussions around this point have been extremely controversial in the beginning of the history of statistical inference, and even now there are many school of thoughts such as empirical, subjective and objective Bayesians (not to mention frequentists or likelihoodists). We shall here adopt a very pragmatic point of view, avoid these discussions and let the debates asides. We introduce the following teacher-student scenario in which we know what the prior really is, so that the use of the Bayes formula will be straightforward and justified. Cases that deviate from this scenario will be discussed but not in the main line.

### 3. Teacher-student scenario

As we said, traditional statistics tries to cope with the fact that processes used to generate the observed data  $\mathbf{y}$  from unknown variables  $\mathbf{x}$  are not fully known, and moreover no information is available about how the values of the variables  $\mathbf{x}$  were chosen. The so-called *frequentist* approach to inference aims to draw conclusions from data while making the least number of explicit assumptions on how the data were created. Next to it in the *Bayesian* approach one uses Bayes’ theorem to update the probability for a hypothesis as more evidence is acquired. It is not the point of this manuscript to enter into subtleties of these different approaches to statistical inference. For this reason and for the sake of clarity all the main concepts here will be explained in the so-called *teacher-student scenario*.

- Teacher: In a first step the teacher generates variables/parameters  $\mathbf{x}^*$  from some probability distribution  $P_{\text{tp}}(\mathbf{x}^*)$ , where tp stand for teacher’s prior. In a second step she uses these *ground truth* values  $\mathbf{x}^*$  to generate the data  $\mathbf{y}$  from some statistical model characterized by a likelihood of  $\mathbf{y}$  given  $\mathbf{x}^*$ , which we denote as  $P_{\text{tm}}(\mathbf{y}|\mathbf{x}^*)$ , where tm stands for teacher’s model. Finally the teacher hands the data  $\mathbf{y}$  to the student together with some information about the distributions  $P_{\text{tp}}(\mathbf{x}^*)$  and  $P_{\text{tm}}(\mathbf{y}|\mathbf{x}^*)$ .
- Student: The goal of the student is to infer as precisely as possible (and tractably, when computational complexity is included into considerations) the original values of variables  $\mathbf{x}$  from the information provided by the teacher, i.e. from the data  $\mathbf{y}$  and the available information about the distributions  $P_{\text{tp}}(\mathbf{x}^*)$  and  $P_{\text{tm}}(\mathbf{y}|\mathbf{x}^*)$ .

The variables with a \* (e.g.  $\mathbf{x}^*$ ) denote the ground truth that was used by the teacher, but that is not available to the student.

### 4. Bayes optimal versus mismatched

Throughout this manuscript we will be distinguishing two main cases depending on what information about the distributions  $P_{\text{tp}}(\mathbf{x}^*)$  and  $P_{\text{tm}}(\mathbf{y}|\mathbf{x}^*)$  the teacher gave to the student

- Bayes optimal case: In this case the teacher hands to the student the full and correct form of both the prior distribution  $P_{\text{tp}}(\mathbf{x})$  and the likelihood  $P_{\text{tm}}(\mathbf{y}|\mathbf{x})$ .
- Mismatching prior and/or model: In this case the teacher hands no or only partial information about the prior distribution  $P_{\text{tp}}(\mathbf{x})$  and/or the statistical model  $P_{\text{tm}}(\mathbf{y}|\mathbf{x})$ . In most of the present manuscript we will assume that the teacher’s prior  $P_{\text{tp}}(\mathbf{x})$  (model  $P_{\text{tm}}(\mathbf{y}|\mathbf{x})$ ) was a function parameterized by some values  $\theta^*$  ( $\Delta^*$ ), the teacher handed the correct functional form of the prior distribution, but not the values of the parameters.

Given the information available to her, the student then basically follows the strategy of Bayesian statistics. The prior information she has from the teacher is denoted as  $P(\mathbf{x})$ , where  $\mathbf{x}$  are the variables to be inferred. The statistical model is represented by its likelihood  $P(\mathbf{y}|\mathbf{x})$ . She then considers the Bayes’s theorem (1) and writes the posterior probability which contains all the information available to her.

Let us now consider the following exercise. Take  $\mathbf{x}^*$  to the ground truth values of the variables generated by the teacher and take  $\mathbf{x}, \mathbf{x}_1, \mathbf{x}_2$  to be three independent samples from the posterior probability distribution  $P(\mathbf{x}|\mathbf{y})$ . We

then consider some function  $f(\mathbf{a}, \mathbf{b})$  of two configurations of the variables  $\mathbf{a}, \mathbf{b}$ . Consider the following two expectations

$$\mathbb{E}[f(\mathbf{x}_1, \mathbf{x}_2)] = \int f(\mathbf{x}_1, \mathbf{x}_2) P(\mathbf{y}) P(\mathbf{x}_1|\mathbf{y}) P(\mathbf{x}_2|\mathbf{y}) d\mathbf{x}_1 d\mathbf{x}_2 d\mathbf{y}, \quad (5)$$

$$\begin{aligned} \mathbb{E}[f(\mathbf{x}^*, \mathbf{x})] &= \int f(\mathbf{x}^*, \mathbf{x}) P(\mathbf{x}^*, \mathbf{x}) d\mathbf{x} d\mathbf{x}^* = \int f(\mathbf{x}^*, \mathbf{x}) P(\mathbf{x}^*, \mathbf{x}, \mathbf{y}) d\mathbf{x} d\mathbf{x}^* d\mathbf{y} \\ &= \int f(\mathbf{x}^*, \mathbf{x}) P(\mathbf{x}|\mathbf{y}, \mathbf{x}^*) P_{\text{tm}}(\mathbf{y}|\mathbf{x}^*) P_{\text{tp}}(\mathbf{x}^*) d\mathbf{x} d\mathbf{x}^* d\mathbf{y}. \end{aligned} \quad (6)$$

where we used the Bayes formula. We further observe that  $P(\mathbf{x}|\mathbf{y}, \mathbf{x}^*) = P(\mathbf{x}|\mathbf{y})$  because  $\mathbf{x}$  is conditionally on  $\mathbf{y}$  independent of  $\mathbf{x}^*$ . Remarkably, in the Bayes optimal case, i.e. when  $P(\mathbf{x}) = P_{\text{tp}}(\mathbf{x})$  and  $P(\mathbf{y}|\mathbf{x}) = P_{\text{tm}}(\mathbf{y}|\mathbf{x})$ , we then obtain

$$\text{Bayes optimal : } \quad \mathbb{E}[f(\mathbf{x}_1, \mathbf{x}_2)] = \mathbb{E}[f(\mathbf{x}^*, \mathbf{x})], \quad (7)$$

meaning that under expectations there is no statistical difference between the ground truth assignment of variables  $\mathbf{x}^*$  and an assignment sampled uniformly at random from the posterior probability distribution. This is a simple yet immensely important property that will lead to numerous simplifications in the Bayes optimal case and it will be used on several places of this manuscript, mostly under the name *Nishimori condition*.

In the case of mismatching prior or model the equality (7) in general does not hold.

## 5. Estimators

What is the optimal estimator  $\hat{\mathbf{x}}$  for the variables  $\mathbf{x}$ ? The answer naturally depends on what is the quantity we aim to optimize. The most commonly considered estimators are:

*Maximum a posteriori (MAP) estimator.* MAP simply maximizes the posterior distribution and is given by

$$\hat{\mathbf{x}}^{\text{MAP}} = \operatorname{argmax}_{\mathbf{x}} P(\mathbf{x}|\mathbf{y}). \quad (8)$$

The main disadvantage of the MAP estimator is the lack of a confidence interval and related issues with overfitting.

*Minimum mean squared error (MMSE).* Ideally we would like to minimize the squared error between  $\hat{\mathbf{x}}$  and  $\mathbf{x}^*$

$$\text{SE}(\hat{\mathbf{x}}, \mathbf{x}^*) = \frac{1}{N} \sum_{i=1}^N (\hat{x}_i - x_i^*)^2. \quad (9)$$

In general, however, we do not know the ground truth values of the variables  $\mathbf{x}^*$ . Our best possibility within Bayesian statistics is to assume that  $\mathbf{x}^*$  is distributed according to the posterior probability distribution. We then want to find an estimator  $\hat{\mathbf{x}}$  that minimizes the squared error average over the posterior

$$\text{MSE}(\hat{\mathbf{x}}) = \frac{1}{N} \int P(\mathbf{x}|\mathbf{y}) \sum_{i=1}^N (\hat{x}_i - x_i)^2 d\mathbf{x}. \quad (10)$$

By a simple derivative with respect to  $\hat{x}_i$  we see that the minimum of this quadratic function is achieved when

$$\hat{x}_i^{\text{MMSE}} = \int P(\mathbf{x}|\mathbf{y}) x_i d\mathbf{x} = \int \mu_i(x_i) x_i dx_i, \quad (11)$$

where the right hand side is actually the mean of the marginal on the  $i$ 'th variable defined as

$$\mu_i(x_i) = \int P(\mathbf{x}|\mathbf{y}) \prod_{j \neq i} dx_j. \quad (12)$$

The value of the MMSE is then computed as the MSE (10) evaluated at  $\hat{x}_i$  (11).

*Maximum mean overlap (MMO).* In cases where the support of the variables is discrete and the variables represent indices of types rather than continuous values, the mean-squared error is not very meaningful. In that case we would rather count how many of the  $N$  positions we obtained the correct type. We define the overlap  $O$  as the fraction of variables where the estimator  $\hat{\mathbf{x}}$  agrees with the ground truth

$$O(\hat{\mathbf{x}}, \mathbf{x}^*) = \frac{1}{N} \sum_i \delta_{x_i^*, \hat{x}_i}. \quad (13)$$

As in the case of MMSE, when we do not have the knowledge of the ground truth, the best Bayesian estimate of the overlap is its average over the posterior distribution

$$\text{MO}(\hat{\mathbf{x}}) = \frac{1}{N} \int P(\mathbf{x}|\mathbf{y}) \sum_i \delta_{x_i, \hat{x}_i} d\mathbf{x}. \quad (14)$$

Mean overlap MO maximized over the estimator  $\hat{\mathbf{x}}$  leads to the maximum mean overlap estimator

$$\hat{x}_i^{\text{MMO}} = \operatorname{argmax}_{x_i} \mu_i(x_i), \quad (15)$$

where  $\mu(x_i)$  is the marginal probability of variable  $i$  having type  $x_i$ , eq. (12). We should note that MMO is not an estimator very commonly considered in statistics, but given that statistical physics often deals with discrete variables, and anticipating the close relation, MMO will turn out instrumental.

To compare the MAP estimator with the ones based on marginals. In most cases the MAP estimator is easier to approach algorithmically (optimization is generically easier than enumeration). Moreover in many traditional settings, where the number of samples is much higher than the number of variables, there is usually very little difference between the two since the marginal probabilities are basically peaked around the value corresponding to the MAP estimator. However, in the setting of high-dimensional statistics (see Sec. IA 6), where the number of samples is small and noise is therefore important, it is quite common that the MAP estimator provides crude overfitting. A nice example of such overfitting could be seen, for instance, in particle tracking [50]. Bayesians, in general, thus tends to favor marginalization based estimators. One reason is because they come directly with a notion of statistical significance of the estimate. A second reason is because, from the point of view of methodology coming from theory of spin glasses, there might even be computational advantage (ground states might be glassy, whereas Bayes-optimal computations are not, see sec IIB 4).

Let us now investigate the MMSE (and the MMO) estimator in the Bayes optimal case in the view of the equality (7). In section IA 4 we concluded that in the Bayes optimal case (i.e. when the teacher handed to the student the precise form of the prior distribution and of the model likelihood) and in expectation, a random sample  $\mathbf{x}$  from the posterior distribution can be replaced by the ground truth assignment  $\mathbf{x}^*$  without changing the values of the quantity under consideration. It hence follows that

$$\text{Bayes optimal : } \quad \text{MMSE} = \mathbb{E}[\text{SE}(\hat{\mathbf{x}}, \mathbf{x}^*)]. \quad (16)$$

In words, the MMSE computed solely using the posterior distribution is on average equal to the squared error between the MMSE estimator and the ground truth value of the variables  $\mathbf{x}^*$ . This is a very nice property. An analogous identity holds between the MMO and the average of the overlap between the MMO estimator and the ground truth assignment

$$\text{Bayes optimal : } \quad \text{MMO} = \mathbb{E}[O(\hat{\mathbf{x}}, \mathbf{x}^*)]. \quad (17)$$

## 6. The high-dimensional limit

Let us denote by  $N$  the number of variables  $\mathbf{x} = \{x_i\}_{i=1, \dots, N}$  (sometimes referred to as dimensionality in statistics), and by  $M$  the number of observations (or samples)  $\mathbf{y} = \{y_i\}_{i=1, \dots, M}$ . Traditionally, statistical theory would consider the case of a finite number  $N$  of variables/parameters to estimate and a diverging number of samples  $M$ . Think for instance of the canonical case of regression of points in 2D by a line, where there are two parameters to estimate and a lot of points, or about the example of decaying particles from sec. IA 2.

In today's data deluge more than ever, it is crucial to extract as much information as possible from available data. From the information theoretic perspective we would expect that useful information is extractable even when the number of variables (dimensionality)  $N$  is comparably large (or even somewhat larger) than the number of observations (samples)  $M$ . In that case separating the useful information about  $\mathbf{x}$  from noise is much more challenging. This is



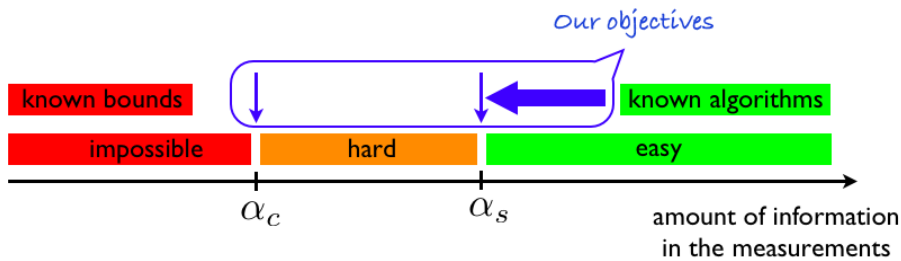


FIG. 1. Schematic representation of a typical high-dimensional inference problem.

referred to as the *high-dimensional statistical theory*. It is in particular in this high-dimensional framework, where the amount of data to analyze is huge, that we need to pay attention not only to solvability but also to computational efficiency, keeping in mind both questions from section I A.

Typically, we will consider the limit where  $\alpha = M/N$  is fixed, whereas  $N \rightarrow \infty$ . In this limit the following scenario, illustrated schematically in Fig. 1, very often applies: For low values of  $\alpha < \alpha_c$ , successful inference of the variables is not possible for any algorithm, the corresponding observed information is simply insufficient. For high values of  $\alpha > \alpha_s$ , computationally efficient inference algorithms do exist. In an intermediate regime  $\alpha_c < \alpha < \alpha_s$ , a successful inference is in principal possible but algorithmically considerably harder than above  $\alpha_s$ . In many settings, the values  $\alpha_c$  and  $\alpha_s$  can be defined in a precise mathematical way as values at which some measure of performance (or its first derivative) presents a discontinuity in the limit of large size. In such a case we talk about thresholds or phase transitions (see section IB 2 for a more precise meaning of the second). In many problems the intermediate hard phase is missing and  $\alpha_c = \alpha_s$ . On the other hand, settings and examples where the hard phase exists ( $\alpha_c < \alpha_s$ ) are theoretically very interesting and challenging many researchers to prove some formal results about this hardness. For a general inference problem, the values of  $\alpha_c$ , and  $\alpha_s$  are not known, and neither are efficient algorithms that would work down to  $\alpha_s$ . The state-of-the-art results usually give only a lower bound on  $\alpha_c$ , and an algorithmic upper bound on  $\alpha_s$ .

The objective of a large part of the statistical physicists interested in these directions and included in this manuscript could be summarized as follows (see also the schema Fig. 1): Determine the threshold  $\alpha_c$  between the *inference-impossible* and *inference-possible* region, and the threshold  $\alpha_s$  between the *inference-hard* and *inference-easy* region. Develop efficient algorithms that would be able to infer the variables successfully with as little information contained in the observations as corresponds to  $\alpha_s$ .

## B. Statistical physics and inference

The connection between statistical physics and statistical inference has a long history. Arguably, the most influential early works are due to E. T. Jaynes, starting with his *Statistical mechanics and information theory* in 1957 [110] where he develops the maximum entropy principle thus building upon the pioneering work of C. Shannon [214], who named the amount of information as entropy inspired by mathematically analogous formulas in thermodynamics. Jaynes actually suggests that statistical mechanics does not have to be regarded as a physical theory dependent on its assumptions, but simply as a special case of a more general theory of Bayesian inference. An inspiring reference is a collection of lecture notes *Statistical Physics to Statistical Inference and Back* from a meeting held in Cargèse 1992. The goal of that meeting was precisely to revise the foundational connections between the two fields. This close connection leads to a continued cross-fertilization between the two fields. Important methodological developments in one field find numerous applications in the other, and a new applicational area in one field profits greatly from the methodology more common to the other.

The present manuscript is mainly concerned with recent applications of methods from spin glasses and glasses [163] into inference problem and associated algorithms. This direction is also relatively well explored and illustrated on a number of problems as seen from classical books such as the one by H. Nishimori *Statistical Physics of Spin Glasses and Information Processing An Introduction*, or more recently *Information, Physics, and Computation* [165].

Data processing is, however, a very fast developing field with many emerging yet far reaching applications. On top of that, there was an important development in the theory of spin glasses on sparse random graphs in early 2000 [160, 161]. This manuscript aims at exposing this recent development.

### 1. Basic dictionary

Let us first establish a dictionary between statistical inference and statistical physics. We will in particular be interested in inference problems where the prior distribution is separable, i.e. can be written as a product over elements

$$P(\mathbf{x}) = \prod_{i=1}^N P(x_i). \quad (18)$$

Further we are mostly interested in case where observations  $\{y_\mu\}_{\mu=1,\dots,M}$  are also independent and each of them depends on a subset of variables denoted  $\partial\mu$ , the likelihood of the statistical model is then written as

$$P(\mathbf{y}|\mathbf{x}) = \prod_{\mu=1}^M P(y_\mu|\{x_i\}_{i\in\partial\mu}). \quad (19)$$

The posterior probability (1) is finally

$$P(\mathbf{x}|\mathbf{y}) = \frac{1}{Z(\mathbf{y})} \exp \left\{ \beta \sum_{\mu=1}^M \log P(y_\mu|\{x_i\}_{i\in\partial\mu}) + \beta \sum_{i=1}^N \log P(x_i) \right\}. \quad (20)$$

We have written the exponential form to note that it takes the form of the Boltzmann probability distribution on spin-like variables (discrete or continuous) with  $Z$  being the partition function,  $\log P(x_i)$  the local magnetic field, and  $\log P(y_\mu|\{x_i\}_{i\in\partial\mu})$  being the interaction between spins. We also introduced the auxiliary parameter  $\beta$ , that previously was  $\beta = 1$ , that plays the role of the inverse temperature. The whole exponent multiplying the inverse temperature is then minus the Hamiltonian  $\mathcal{H}$  of the physical system.

The marginal probabilities (12) are nothing else than local magnetizations. The MMSE (or the MMO) estimator is then computed using these local magnetizations (at  $\beta = 1$ ). On the other hand the MAP estimator can be viewed as the ground state of the physical system, i.e. the minimum of the Hamiltonian. Another way to think about the MAP estimator is as the zero temperature limit  $\beta \rightarrow \infty$  of MMSE estimator.

### 2. Useful statistical physics concepts

Traditional physical systems are composed of a number of spins or molecules that is comparable to the Avogadro number  $N_A \approx 10^{23}$ . It is hence almost always relevant to investigate the limit of section IA 6 that is in statistical physics referred to as the *thermodynamic limit*.

In the analogy between inference and statistical physics, the observations  $\mathbf{y}$  play the role of the so called *quenched disorder* in the Hamiltonian in eq. (20). Generically, quantities of interest, e.g. the magnetization of variable number 10, do depend on the realization of this quenched disorder.

*Self-averaging.* Statistical physics, however, mostly focuses on quantities that have the so-called *self-averaging* property, i.e. in the thermodynamic limit their value does not depend on the realization of the disorder (only on its statistical properties). More formally, a quantity  $A(\mathbf{y})$  is self-averaging if for every  $\epsilon > 0$

$$\lim_{N \rightarrow \infty} \text{Prob} \{ |A(\mathbf{y}) - \mathbb{E}[A(\mathbf{y})]| > \epsilon \} = 0. \quad (21)$$

One of the most important quantities that we expect to be self-averaging is the free energy density

$$f(\beta, \mathbf{y}, N) = -\frac{1}{N\beta} \log Z(\mathbf{y}) \quad (22)$$

that is assumed to have a thermodynamic limit

$$f(\beta) = \lim_{N \rightarrow \infty} f(\beta, \mathbf{y}, N) \quad (23)$$

that does not depend on the realization of  $\mathbf{y}$ . From a rigorous point of view, even this first simple assumptions poses a non-trivial technical challenge. A recurring discrepancy between theoretical physics and rigorous approach.

From the quantities discussed previously in this manuscript, the ones for which self-averaging property is particularly interesting are the MMSE and MMO. Under self-averaging the equalities (16-17) hold not only on average, but also when the averages on the r.h.s. are removed. This means that the typical squared distance between the ground truth and the MMSE (MMO) estimator is equal, in the thermodynamic limit, to the one evaluated without the knowledge of the ground truth. Clearly, focusing on the analysis on the self-averaging quantities greatly simplifies the description of the behavior in the thermodynamic limit.

*Phase transitions.* Another concept borrowed from physics that will turn out as well very influential in the analysis of high-dimensional inference are phase transition. Intuitively a phase transition is a rather abrupt change in behavior as a parameter (commonly the temperature) is tuned. Since by far not everything that is termed *phase transition* in computer science or engineering literature is a genuine phase transition from a physics point of view, it is useful to make some reminders.

First of all, a phase transition does not exist at finite system size. In mathematical physics a phase transition is defined as a non-analyticity in the free energy density  $f(\beta)$  (23). Since the finite  $N$  free energy density is a logarithm of a sum of exponentials, it is always an analytical function. Only when the limit  $N \rightarrow \infty$  is taken the non-analyticities can appear. Therefore when we talk about a phase transition, we should always make sure that it indeed corresponds to a non-analyticity and not to a smooth (even though perhaps very abrupt) change.

Secondly, a traditional phase transition is always associated to either a *critical slowing down* or *metastability*. According to the Ehrenfest classification of phase transitions there are two main types

- *1st order phase transition* is associated to a discontinuity in the first derivative of the free energy. The first derivative of the free energy is usually related to some measurable quantity that consequently have a discontinuity. Since a number of quantities, including e.g. the MMSE or magnetization, are related to this first derivative, they also display a discontinuity at a first order phase transition. The mechanism behind a 1st order phase transition is a competition between two states of the system, for the sake of vocabulary let us call the two states as paramagnet and ferromagnet. Around the phase transition there is a so-called metastable region where the properties of the system are ruled by properties of both the states. In systems that cannot be embedded into a finite dimensional Euclidean space we can define sharp boundaries of this region, called the *spinodal* points. Metastability has a profound consequence on the behavior of dynamics and algorithms. We will come back to this in detail.
- *2nd order phase transition* is associated to a discontinuity in the second derivative of the free energy. This type of phase transition is associated to a so-called *critical slowing down*, meaning that dynamical processes become divergingly slow next to the phase transition. Diverging timescales are closely linked to diverging length-scales and diverging strength of fluctuations. These are described by the theory of criticality and critical exponents that ruled statistical physics in the second half of last century.

Genuine phase transitions are quite peculiar creatures, and this is largely why they fascinate many physicist. To make a distinction in vocabulary in physics we use *cross-over* for a more generic rather abrupt change in behavior as a parameter is tuned. And the term *phase transition* or *threshold* for what is described above. Going back to the scheme 1, a physicist mind becomes very intrigued when for a given inference problem we find that  $\alpha_c$  and  $\alpha_s$  are genuine phase transitions. For a physicist a phase transition is something intrinsic, we immediately expect a profound meaning and non-trivial consequences for the system under investigation.

## II. INFERENCE AS THE PLANTED ENSEMBLE

In our opinion, the most transparent way to look at inference problems from the point of view of statistical physics is to think about them as a particular type of statistical ensemble - the planted ensemble. This point of view will be explained and developed in this section.

### A. Example of the planted spin glass

As biology has its drosophila, or computational complexity its K-SAT problems, in statistical physics the canonical example is the Ising model

$$\mathcal{H}(\mathbf{S}) = - \sum_{(ij) \in E} J_{ij} S_i S_j - \sum_{i=1}^N h_i S_i, \quad (24)$$

where  $\mathbf{S} = \{S_i\}_{i=1, \dots, N}$  and the spins are  $S_i \in \{-1, 1\}$ ,  $E$  is the set of interacting pairs,  $J_{ij}$  is the interaction strength between spins and  $h_i$  is the magnetic field. Statistical physics is the study of the Boltzmann probability measure on configurations of spins

$$\mu(\mathbf{S}) = \frac{1}{Z(\beta, \mathbf{J}, \mathbf{h})} e^{-\beta \mathcal{H}(\mathbf{S})}. \quad (25)$$

The Ising model with the Hamiltonian (24) is presented in numerous textbooks. The most commonly considered geometries of interactions are finite dimensional lattices, fully connected graphs, random graphs, or for instance social networks. Interactions  $J_{ij}$  are chosen such that  $J_{ij} \geq 0$  in the ferromagnetic case (most commonly  $J_{ij} = J$  for all  $(ij) \in E$ ) while in antiferromagnetic case  $J_{ij} \leq 0$ . In the random field Ising model the fields  $h_i$  are random. Perhaps the most intriguing case of an Ising model is the spin glass when the interactions  $J_{ij}$  are taken independently random from some distribution including both negative and positive numbers. In all these situations the interaction couplings  $\mathbf{J}$  are chosen independently of any specific configuration  $\mathbf{S}$ .

#### 1. Definition of planted spin glass

In the *planted* spin glass this is different. To define the planted spin glass we consider the following scenario: We have a (large) number  $N$  of people who are divided into two groups of friends of equal size, say group  $A$  and group  $B$ . We ask a question to  $M$  randomly chosen pairs of people: "Are you two friends?". Most of the people will answer truthfully, but a fraction of the collected answers will be lies [186]. We want to model this system, and one of the questions we have is whether and how we can estimate which person was part of group  $A$  and which was part of group  $B$ .

Mathematically, we can define the planted spin glass problem as follows: We have  $N$  nodes, each of them carrying a latent variables  $S_i^* = \pm 1$ ,  $1 \leq i \leq N$ . We then have selected a graph (for instance an Erdős-Rényi random graph) with  $M$  edges. Each of the edges carries a label  $J_{ij} = \pm 1$ ,  $(ij) \in E$  taken from the following distribution:

$$P(J_{ij} | S_i^*, S_j^*) = \rho \mathbb{I}(J_{ij} = S_i^* S_j^*) + (1 - \rho) \mathbb{I}(J_{ij} = -S_i^* S_j^*), \quad (26)$$

where  $\rho$  is a "truthfulness" parameter (i.e. the probability we obtained the correct information).

The latent values  $S_i^*$  are then hidden and the goal is to infer from the values of  $\mathbf{J}$  as precisely as possible which node was in which group. Obviously, the above riddle recalls us the teacher-student scenario that we discussed in sec. IA 3. The teacher here is the generative process that created the values  $\mathbf{J}$ . Depending on the situation the teacher revealed or not the value  $\rho$  he used, for the moment we will assume  $\rho$  is known.

Let us look at the simplest cases: In the noiseless case  $\rho = 1$ , each connected component of the graph should be in the same group. When the graph is largely connected one can easily recover the two groups. When  $\rho = 1/2$ , it is as if we chose the couplings independently at random just as in the standard (quenched) spin glass model. The values  $\mathbf{J}$  do not contain any information about the latent variables  $S_i^*$ , and recovery is clearly impossible. What is happening in between, for  $1/2 < \rho < 1$ ?

The above model is simple to state, but its solution is very interesting, and rather non-trivial. This problem appeared in several different context in the literature, it is called *censored block model* in [1, 2, 206], and *planted spin glass* in [141, 142]. From a rigorous point of view this problem is still a subject of current research. Here we will call

the above problem the planted spin-glass model to differentiate from the standard spin-glass model, where we chose all the interactions  $\mathbf{J}$  randomly and uncorrelated.

More formally defined, to create an instance of the planted spin glass we proceed as follows

- We consider that the hidden assignment  $S_i^*$ , called the *planted configuration* of spins, is chosen uniformly at random from all the  $2^N$  different possibilities.
- We then have chosen a graph of interactions  $G = (V, E)$ , but not yet the associated values of  $J_{ij}$ , independently of the planted configuration  $\mathbf{S}^*$ .
- For each edge  $E \in G$ , the value of  $J_{ij}$  are chosen to be either  $+1$  or  $-1$  with probability taken from (26). The signs of the couplings then carry information about the planted configuration.

So far the relation with the Ising model may not be very clear. To see it very explicitly we write eq. (26) differently. Without loosing generality, we can define a parameter  $\beta^*$  by

$$\rho = \frac{e^{\beta^*}}{2 \cosh \beta^*} \quad \text{and} \quad 1 - \rho = \frac{e^{-\beta^*}}{2 \cosh \beta^*} \quad \text{with} \quad \beta^* = \frac{1}{2} \log \left( \frac{\rho}{1 - \rho} \right), \quad (27)$$

so that eq. (26) reads

$$P(J_{ij} | S_i^*, S_j^*) = \frac{e^{\beta^* J_{ij} S_i^* S_j^*}}{2 \cosh \beta^*}. \quad (28)$$

Since we want to know the values of the spins  $\mathbf{S}$  given the knowledge of the couplings  $\mathbf{J}$ , we write the Bayes formula

$$P(\mathbf{S} | \mathbf{J}) = \frac{P(\mathbf{J} | \mathbf{S}) P(\mathbf{S})}{P(\mathbf{J})} = \frac{\prod_{(ij) \in E} e^{\beta^* J_{ij} S_i S_j}}{2^N (2 \cosh \beta^*)^M P(\mathbf{J})} \quad (29)$$

where we used (28). The posterior probability distribution has to be normalized, therefore

$$P(\mathbf{J}) = \frac{Z(\beta^*, \mathbf{J})}{2^N (2 \cosh \beta^*)^M}, \quad (30)$$

where  $Z(\beta^*, \mathbf{J})$  is the partition function of the Ising model (25) at temperature  $\beta^*$  (in zero magnetic field). In other words, the posterior distribution is simply the standard Boltzmann measure of the Ising model at a particular temperature  $\beta^*$ . In general we shall consider this Ising model at a generic temperature  $\beta \neq \beta^*$ . This is because a priori we do not know how many people lied. In the teacher-student setting, the teacher may not have handed the student the value  $\beta^*$ .

The special case  $\beta = \beta^*$  corresponds to the Bayes optimal inference as discussed in section IA 4. One of the most physically important properties of the Bayes-optimal case is that the planted configuration can be exchanged (under averages, or in the thermodynamic limit) for a random configuration taken from the posterior measure, which is in physics simply called an *equilibrium configuration*. This property will turn out as crucial in the present context.

As discussed in Sec. IA 5, since we are dealing with a problem with discrete variables (spins), it is desirable to minimize the number of mismatches in the estimation of the planted assignment. We hence aim to evaluate the maximum mean overlap (MMO) estimator (15) which in the case of an Ising model is simply

$$\hat{S}_i = \text{sign } m_i, \quad (31)$$

where  $m_i$  is the equilibrium value of the magnetization of node  $i$  in the Ising model. We reduced the inference of the planted configuration to the problem of computing the magnetizations in a disordered Ising model as a function of temperature.

An off-the-shelf method for this that every physicist has in her handbag is a Monte-Carlo simulation, with for instance the Metropolis algorithm. In Sec. II C we shall see that for the mean-field setting (i.e. the underlying graph being random or fully connected) there exists an exact solution of this problem via the cavity method. However, before turning to the mean-field setting we want to discuss concepts that are more generic and we will hence keep Monte-Carlo in our mind as a simple and universal method to evaluate phase diagrams of Hamiltonians with discrete degrees of freedom.

## 2. Nishimori's mapping via gauge transformation

For the planted spin glass there is an alternative way that provides understanding of its phase diagram and quite interesting additional insights [183–185]. One takes advantage of the so-called gauge transformation

$$S_i S_i^* \rightarrow \tilde{S}_i, \quad J_{ij} S_i^* S_j^* \rightarrow \tilde{J}_{ij}. \quad (32)$$

If this transformation is applied, the Ising Hamiltonian is conserved since all  $S_i = \pm 1$ . In the new variables the planted configuration becomes ferromagnetic  $\tilde{S}_i^* = (S_i^*)^2 = 1$ . What happened to the couplings? The energy of each link in the planted configuration has not been changed by the gauge transform. Since the frustrated interactions were chosen independently at random in the planting, after the gauge transformation we end up with a standard spin glass with a fraction

$$\rho = \frac{e^{\beta^*}}{2 \cosh \beta^*} \quad (33)$$

of positive  $J_{ij} = +1$  couplings and the rest  $-1$ , where the  $-1$  are chosen independently at random.

After the gauge transformation, the planted assignment has been transformed to the ferromagnetic one where all spins are positive. The system is now a standard spin glass with iid interactions, albeit with a ferromagnetic bias  $\rho$ . The question of the identification of the hidden assignment is now simply mapped to the question of finding the ferromagnetic “all spins up” configuration. Clearly, this is a step that from the physics point of view simplifies the discussion.

The phase diagram of the spin glass models, with a ferromagnetic bias  $\rho$ , versus a temperature  $1/\beta$ , has been determined and one has simply to look it up in the literature [42, 43, 146]. In a remarkable contribution, Nishimori realized that the physics on the line  $\rho = e^{\beta}/(2 \cosh \beta)$  is particularly simple and quite different from a generic  $\beta$ . This line is now called the *Nishimori line* and corresponds to nothing else but the condition for Bayes optimality  $\beta = \beta^*$ .

Consequently, number of interesting properties, that are false in general, hold on the Nishimori line, these are called *Nishimori conditions*. In general, Nishimori conditions are properties that hold in the Bayes optimal case, such as (16) and (17). Another useful Nishimori identity concerns the average energy  $E = \langle \mathcal{H} \rangle / N$  (24). Using again the property that the planted configuration can under averages replace an equilibrium configuration we obtain immediately

$$E = -c \tanh \beta^* / 2. \quad (34)$$

In Fig. 2 we give the phase diagram of the spin glass at temperature  $T = 1/\beta$  with ferromagnetic bias  $\rho$ . As an example we use the spin glass on a random graph in which case an exact solutions exists (see sec. II C). However, on a generic geometry the phase diagram could be obtained using Monte-Carlo simulation and would be qualitatively similar. The phenomenology of Bayesian inference can be directly read off from this phase diagram.

## 3. Bayes-optimality on the Nishimori line

First, let us assume that we know (or that we learn from data, see next section) the true value of  $\beta^*$  (or equivalently  $\rho$ ) from which the couplings  $\mathbf{J}$  have been generated. Then, our consideration is restricted to the Nishimori line. If the temperature is large enough,  $\beta^*$  low enough, we are in the paramagnetic phase, and we find that all marginals (magnetizations) are zero. It would thus be difficult to find their signs. In fact, this simply means that, in the paramagnetic phase, inference of the hidden configuration is impossible. There is just not enough information to say anything about the hidden/planted assignment.

As the temperature is lowered,  $\beta^*$  increased, the situation changes. If we used  $\beta^*$  corresponding to a temperature below a certain critical value  $\beta_c$ , then a Monte-Carlo simulation would rapidly discover the ferromagnetic phase where local magnetizations are (mostly) positive. Applying rule (31) would give at this point a decent overlap with the true assignment (which is, after the gauge transformation, all  $+1$ ).

In terms of inference of the planted configuration these two phases have the following interpretation

- Undetectable. For  $\beta^* < \beta_c$ ,  $\rho < \rho_c$ , the planted spin glass system is in the paramagnetic state meaning that the set of observed variables  $\mathbf{J}$  does not contain any information about the planted configurations and its inference is hence information-theoretically impossible.
- Detectable. For  $\beta^* > \beta_c$ ,  $\rho > \rho_c$ , the planted spin glass is in a ferromagnetic phase where equilibrium configurations are all correlated with the planted one and inference is possible, and algorithmically tractable e.g. via Monte-Carlo sampling.

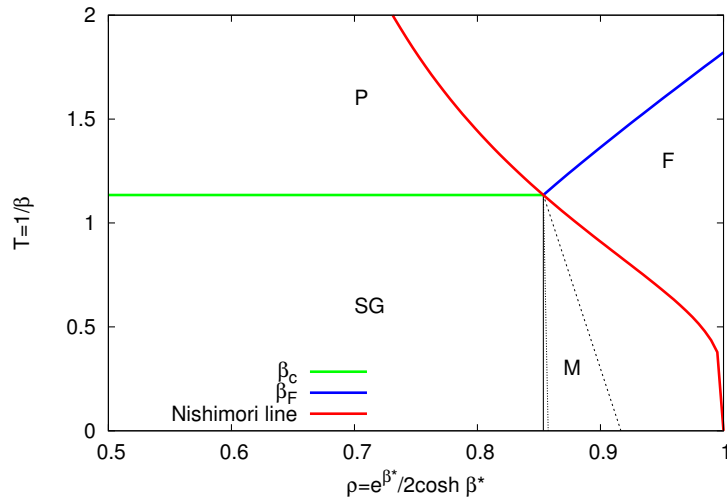


FIG. 2. Phase diagram of the spin glass as a function of temperature  $T = 1/\beta$  and density of ferromagnetic  $J = +1$  bonds  $\rho$ . This phase diagram is for random regular graph of degree  $c = 3$ . The Nishimori line,  $\rho = e^\beta / (2 \cosh \beta)$ , corresponds to the Bayes optimal inference. There is the spin glass (SG) phase where the system is in a glassy state, the ferromagnetic (F) phase, the paramagnetic (P) phase and the mixed (M) one where the system is both SG and F. The boundary of the mixed phase (black dashed) is only a guide for the eye between the multi-critical point and the zero-temperature point from [44]. The same for the boundary of the SG phase (black dotted) that is obtained from the inexact 1RSB approximation and is hardly distinguishable from the vertical line (black full).

For the planted spin glass of a random graph the critical temperature  $T_c = 1/\beta_c$  where one goes from *impossible inference* to *easy inference* can be taken from the literature [42, 43, 221] (we will show how to compute it for this case in Sec. II C) and in the case of random Erdős-Rényi graph with average degree  $c$  it reads

$$T_c^{\text{ER}}(c) = \left[ \text{atanh} \frac{1}{\sqrt{c}} \right]^{-1}, \quad (35)$$

while for regular random graphs it reads

$$T_c^{\text{REG}}(c) = \left[ \text{atanh} \frac{1}{\sqrt{c-1}} \right]^{-1}. \quad (36)$$

On a Erdős-Rényi random graph, this indicates that it is only possible to infer something about the planted assignment if

$$c > c_{\text{detect}} = \frac{1}{(2\rho - 1)^2}. \quad (37)$$

If this is not satisfied, the system is in the paramagnetic phase and nothing can be said about the planted configuration. If, on the other hand, (37) is satisfied, then the magnetization aligns partly with the planted configuration. This is a very generic situation in Bayesian optimal inference when we encounter a second order phase transition. We go from a phase where inference is impossible, to a phase where it is rather straightforward. Note that this is not only a statistical physics prediction, but one that can be proven rigorously. The impossibility result has been shown in [101, 148] and the possibility one (if (37) is satisfied) in [206].

#### 4. Parameter mismatch and learning

Let us now discuss what happens if one does not know the value  $\beta^*$ . One approach that seems reasonable is to use  $\beta \rightarrow \infty$ , so that we look for the most probable assignment (this would correspond to the MAP estimator) which is the ground state of the corresponding Ising model. We observe from the phase diagram that for  $\rho < \rho_c$  at  $T = 0$  the system is in the spin glass phase. In terms of Monte-Carlo the presence of such a phase manifests itself via a

drastic growth of the equilibration time. Computing the corresponding magnetizations becomes very hard. Moreover, even in the undetectable phase,  $\rho < \rho_c$ , the zero-temperature local magnetizations will not be zero. This is a sign of overfitting that the MAP estimator suffers from.

In the detectable phase,  $\rho > \rho_c$ , the ferromagnetic phase extends only up to a temperature that for an Erdős-Rényi random graph corresponds to a certain

$$\beta_F = \operatorname{atanh} \left( \frac{1}{c \tanh \beta^*} \right). \quad (38)$$

Hence if we chose too low  $\beta$  as a starting point we could miss the detectability. At low temperatures we again might encounter a spin glass phase that might or not be correlated to the planted configuration. In either case, such a phase causes convergence and equilibration problems and should better be avoided. Fortunately, there is no such glassy phase on the Nishimori line as we shall explain in sec. II B 4.

The above considerations highlight the necessity of learning parameters (in this case  $\beta^*$ ). Within the theory described above there is one particularly natural strategy for learning such parameters closely related to the well known algorithm of expectation maximization (EM) [62]. Let us illustrate this parameter learning on the example of the planted Ising model where we assume that the parameter  $\beta^*$  is not known.

In Bayesian inference, we always aim to write a posterior probability distribution of what we do not know conditioned to what we do know. In the present case we need  $P(\beta|\mathbf{J})$ . Using the Bayes formula we obtain

$$P(\beta|\mathbf{J}) = \sum_{\mathbf{S}} P(\mathbf{S}, \beta|\mathbf{J}) = \frac{P(\beta)}{2^N P(\mathbf{J})} \frac{Z(\beta, \mathbf{J})}{(2 \cosh \beta)^M}. \quad (39)$$

We notice that as long as the hyper-prior  $P(\beta)$  is independent of  $N$ , in the thermodynamic limit this probability distribution  $P(\beta|\mathbf{J})$  converges to a Dirac delta function on the maximum of the second fraction on the right hand side. This maximum is achieved at

$$E = - \left\langle \sum_{(ij) \in E} J_{ij} S_i S_j \right\rangle = - \frac{c}{2} \tanh \beta. \quad (40)$$

The corresponding iterative algorithm for learning  $\beta$  is as follows. We start with some initial choice of  $\beta$  and compute the average energy to update the value of  $\beta$  according to (40) until a fixed point is reached. In case there is more than one fixed point of (40) we choose the one that is the global maximum of (39).

Notice now a very useful property, the condition for stationarity of (39) is the same as the Nishimori condition (34) and indeed  $\beta = \beta^*$  is a fixed point of (40). This strategy is very reasonable, in the Bayes-optimal case all the parameters are the ground truth one and a number of *Nishimori conditions* hold only in this case. Hence in order to learn the right values of parameters we iteratively impose the Nishimori conditions to hold.

Finally, let us note that in the above planted Ising model the underlying phase transition is of second order, therefore there is no particular computational issue. Inference is either impossible or possible and tractable. The hard phase outlined in section (I A 6) is absent. The picture is richer in problems where in the random case there is a discontinuous phase transition. An example of such a case is described in detail in Sec. II C 3.

## B. Averaging and the planted ensemble

From the early works, it sometimes seems necessary to have a gauge transformation (and consequently a special form of the Hamiltonian) to be able to speak about the Nishimori conditions or other properties of the Nishimori line [85, 184, 185]. Importantly, this is not the case. The properties of the Nishimori line are more general and apply to every case where it makes sense to talk about planting and Bayes optimal inference. In fact a more general notion of the Nishimori line can be identified with the notion of Bayes-optimality in a planted ensemble. A nice article about the connection between Bayes optimality and Nishimori's work is by Iba [109].

In this section, we shall discuss properties of the planted ensemble, and its relation with the more usual ensembles of statistical mechanics of disordered systems - the quenched and the annealed one. This will show the generic connection between statistical physics spin glasses and Bayesian inference problems. We stress again that none of this requires a gauge symmetry of the underlying Hamiltonian.

### 1. The quenched and annealed ensembles

Let us consider back the Hamiltonian of the Ising system (24). For a given system, e.g. the magnet on the fridge in your house, the set of couplings  $J_{ij}$  is a given fixed finite set of numbers. In the planted spin glass above, this set



were the data we observed about the system, again data are presented as a given fixed set of numbers.

In statistical physics, where in vast majority of cases we can take advantage of self-averaging, see sec. IB2, we often do not think of a given set of numbers  $J_{ij}$  but instead about a probability distribution over such sets. For instance

$$P(J_{ij}) = \frac{1}{2}\delta(J_{ij} - 1) + \frac{1}{2}\delta(J_{ij} + 1) \quad (41)$$

for all  $(ij) \in E$ , where  $E$  are the edges of the graph of interactions. In this way we do not have a given Hamiltonian, but rather the probability of a given one. Properties of the system then have to be averaged over the disorder (41). This view is adopted in statistical physics because theory is then easier to develop. This notion of averaging over disorder is so well ingrained into a physicist mind that going away from this framework and starting to use the related (replica and cavity) calculations for a single realization of the disorder has led to a major paradigm shift and to a development of revolutionary algorithm such as the survey propagation [164]. In this section we do want to stay in the mindset of averaging over the disorder and explain how to fit in the notion of the *planted ensemble*.

How to do the average over disorder of  $J_{ij}$  meaningfully is a problem that was solved a long time ago by Edwards himself in his work on spin glasses and vulcanization (see the wonderful book *Stealing the gold* [87]). If one takes a large enough system, he suggested, then the system becomes *self-averaging*: all extensive thermodynamic quantities have the same values (in densities) for almost all realizations of the Hamiltonian. Therefore, one needs to compute the average free energy

$$f_{\text{quenched}} = \left[ \frac{F}{N} \right] = \lim_{N \rightarrow \infty} -\frac{1}{\beta N} [\log Z], \quad (42)$$

where here  $[\cdot]$  denotes the average over the disorder. Edwards did not stop here and also suggested (and gave credit to Mark Kac for the original idea) a way to compute the average of the (very tricky) logarithm of  $Z$ , known today as the *replica trick*, using the identity

$$\log Z = \lim_{n \rightarrow 0} \frac{Z^n - 1}{n}. \quad (43)$$

The idea here is that, if averaging the logarithm of  $Z$  turns out to be difficult, the average of  $Z^n$  is maybe doable for any integer value of  $n$ , and performing a (risky) analytic continuation to  $n = 0$ , one might compute the averaged free energy over the disorder as

$$f_{\text{quenched}} = -\frac{1}{N\beta} \lim_{n \rightarrow 0} \frac{[Z^n] - 1}{n}. \quad (44)$$

This is called the quenched average, and the corresponding computations are the quenched computations, the ensemble is referred to as the *quenched* or simply as the *random ensemble*. In fact, the self-averaging hypothesis for the free energy has been proven now rigorously in many cases, in particular for all lattices in finite dimension [229] and for some mean-field models [93]. However, the computation of the average free energy is in general very difficult and this problem is at the core of studies in statistical physics of disordered systems.

It is *much easier* to consider the so-called annealed ensemble. In the annealed ensemble, one simply averages the partition sum and only *then* takes the logarithm

$$f_{\text{annealed}} = -\frac{1}{N\beta} \log [Z]. \quad (45)$$

This is a very different computation, and of course, it has no reason to be equal to the quenched computation.

For the example of Ising model with binary uniformly distributed couplings (41) we obtain (independently of the dimension or geometry)

$$-\beta f_{\text{annealed}}^{\text{Ising}} = \log 2 + \frac{c}{2} \log(\cosh \beta), \quad (46)$$

where  $c$  is the average coordination number (degree) of the interaction graphs.

It is important to see that the annealed average is *wrong* if one wants to do physics. The point is that the free energy is an extensive quantity, so that the free energy per variable should be a quantity of  $O(1)$  with fluctuations going in most situations as  $\propto (1/\sqrt{N})$  (the exponent can be different, but the idea is that fluctuations are going to zero as  $N \rightarrow \infty$ ). The partition sum  $Z$ , however, is exponentially large in  $N$ , and so its fluctuations can be huge. The average can be easily dominated by rare, but large, fluctuations.

Consider for instance the situation where  $Z$  is  $\exp(-\beta N)$  with probability  $1/N$  and  $\exp(-2\beta N)$  with probability  $1 - 1/N$ . With high probability, if one picks up a large system, its free energy should be  $f_{\text{quenched}} = 2$ , however in the annealed computation one finds

$$[Z] = \frac{1}{N} \exp(-\beta N) + \left(1 - \frac{1}{N}\right) \exp(-2\beta N) \quad (47)$$

and to the leading order, the annealed free energy turns out to be  $f_{\text{annealed}} = 1$ .

One should not throw away the annealed computation right away, as we shall see, it might be a good approximation in some cases. Moreover, it turns out to be very convenient to prove theorems. Indeed, since the logarithm is a concave function, the average of the logarithm is always smaller or equal to the logarithm of the average, so that

$$f_{\text{annealed}} \leq f_{\text{quenched}}. \quad (48)$$

This is in fact a crucial property in the demonstrations of many results in the physics of disordered systems, and in computer science this is the inequality behind the “first moment method” [173].

Furthermore, there is a reason why, in physics, one should sometimes consider the annealed ensemble instead of the quenched one. When the disorder is changing quickly in time, on timescales similar to those of configuration changes, then we indeed need to average both over configurations and disorder and the annealed average is the correct physical one. This is actually the origin of the name *annealed* and *quenched* averages.

## 2. Planting as an ensemble

In sec. II A 1 we described the planted spin glass, where we first consider the planted configuration  $\mathbf{S}^*$  and then consider the probability over interactions  $P(\mathbf{J}|\mathbf{S}^*)$  eq. (28).

From a physics point of view the two most important properties of the planted ensemble, the two golden rules, are

- The planted configuration is an equilibrium configuration of the corresponding Hamiltonian (derived from the posterior distribution). Indeed, when we view planting as an inference problem, we can write the corresponding posterior probability distribution as in eq. (29). In section IA 4 we derived that in the Bayes optimal inference the planted configuration behaves exactly in the same way as a configuration sampled from the posterior. This is very interesting from a physics point of view, as we are generating at the same time an equilibrium configuration and a realization of the disorder (while doing the opposite is in general a difficult high dimensional sampling problem).
- The realization of the disorder of the planted problem is not chosen uniformly, as in the quenched ensemble, but instead each planted problem appears with a probability proportional to its partition sum. This can be seen from eq. (30) where the probability distribution over  $\mathbf{J}$  in the planted ensemble is related to the partition function of the planted system  $Z(\mathbf{J})$ . A more precise formula can be obtained using the annealed partition function (46)

$$P_{\text{planted}}(\mathbf{J}) = \frac{Z(\mathbf{J})}{\Lambda Z_{\text{annealed}}}, \quad (49)$$

where  $\Lambda$  is the number all possible realizations of the disorder,  $\Lambda = 2^M$  for the Ising model. Note the  $1/\Lambda$  can also be interpreted as the probability to generate a given set of couplings in the quenched ensemble where the couplings are chosen uniformly at random.

The planted ensemble might seem related to the annealed ensemble because for instance the planted energy (34) is always equal to the annealed average energy, which is easily derived from the annealed free energy (46). However, the free energy of the planted ensemble is in general different from the annealed free energy (46), as illustrated e.g. in Fig. 3.

## 3. Quiet planting

Let us now imagine we have found a system where the free energy (non-averaged one) is exactly equal to the annealed free energy. Then according to eq. (49) we see that for such a system  $P_{\text{planted}}(\mathbf{J}) = 1/\Lambda = P_{\text{quenched}}(\mathbf{J})$ , meaning that generating instances from the planted ensemble is the same thing as generating from the quenched

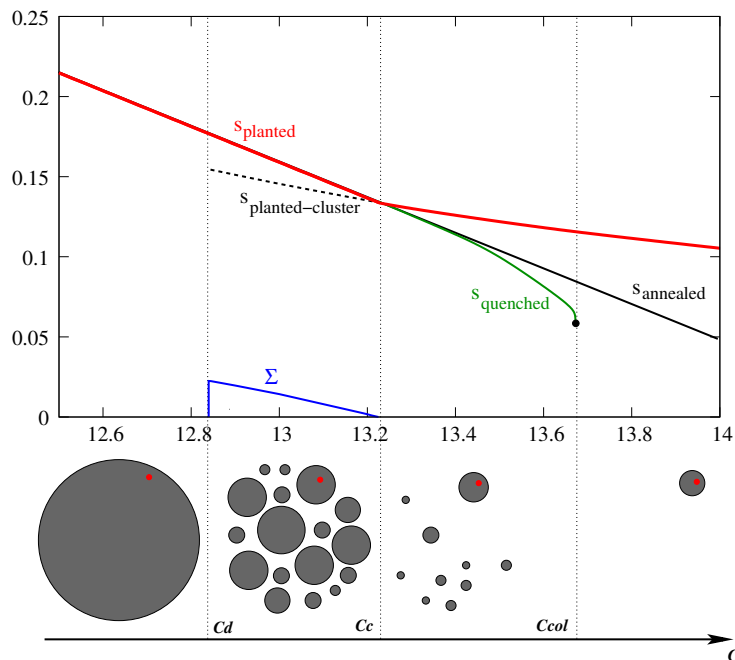


FIG. 3. Entropy density (which is equal to the free energy at zero temperature) for the 5-coloring problem on an Erdős-Rényi random graph of average degree  $c$ . The planted entropy (in red) is compared to the quenched one (in green) and the annealed one (in black). For  $c < c_c$  the three curves agree. The quenched entropy goes to  $-\infty$  at the colorability threshold  $c_{\text{col}}$ . The region between  $c_d$  and  $c_c$  is relevant only for cases with a first order phase transition as discussed in Sec. II C 3. In mean field theory of spin glasses this region is called the d1RSB phase. We also show the entropy of the planted cluster below  $c_c$  (black dashed), which is less than the total entropy, the difference is called the “complexity”  $\Sigma$  (in blue) and is the logarithm of the number of equilibrium clusters. Bottom: Sketch of the shape of the space of all valid colorings in the planted case. At an average degree  $c_d$  the space of solutions shatters into exponentially many clusters, the planted cluster being one of them. Beyond  $c_c$  the planted cluster contains more solutions than all the others together. At  $c_s$  the last non-planted cluster disappears (this is the coloring threshold in a non planted, purely random model). Figure taken from [139].

ensemble. Such planting is denoted as *quiet*. In fact, we do not even need the free energies to be exactly equal, it is sufficient that the free energy densities are the same. This is because atypical instances are usually exponentially rare and hence any difference in the free energies that does not show up in the leading order will not generate atypical instance.

It so happens that on mean-field systems the (self-averaging) free energies of paramagnets are indeed equal to the annealed free energies. The equilibrium in these systems can hence be studied using the planted ensemble and this is greatly advantageous as we will see in section II D 1.

The idea of quiet planting comes from a rigorous work [3] where the above notion was proven rigorously. In mathematics this property is formalized and the two ensembles termed *contiguous* [3, 177]. The paper that pioneered the usage of quiet planting in physics, and that also established the name “quiet”, is *Hiding quiet solutions in random constraint satisfaction problems* [139].

#### 4. No replica symmetry breaking on the Nishimori line.

From the methodological point of view the Nishimori line has one absolutely crucial property: the absence of glass phase at equilibrium. In the words of the mean-field theory of spin glasses, there is no static replica symmetry breaking on the Nishimori line. Note that there might be, and indeed is in all the cases where the underlying transition is of the 1st order, the dynamical one-step RSB phase (d1RSB). The marginals in the d1RSB phase are, however, still exactly described by the belief propagation, and this is what matters to us in the Bayes-optimal inference.

Replica symmetry breaking phase (or equivalently the static spin glass phase) can be defined by the non-self-averaging of the overlap  $q$  between two configurations randomly sampled from the Boltzmann distribution. Depending on the realization of the sampling, the Hamming distance between the two configurations is with nonzero probability different from its average.

In section IA 4 we derived that the overlap  $m$  between a typical configuration and the planted one is equal to the overlap between two typical configurations  $q$ . With similar arguments one can derive equality of the distribution (over realizations of the sampling) of overlap  $P(q)$  between two configurations randomly sampled from the posterior and the distribution of the magnetization  $P(m)$ , which is overlap between the planted configuration and a random sample from the posterior [183]. In physics magnetization is always argued to be self-averaging (the same is true for the free energy density and magnetization is its derivative with respect to the magnetic field), and hence on the Nishimori line the overlap is also self-averaging. From this, one argues that the  $P(q)$  is trivial, which in mean-field spin glasses indicates the absence of a spin glass phase. However, from a rigorous point of view self-averaging of the magnetization is an open problem.

Another way to see the problem is to remark that, given the spin glass susceptibility is equal to the ferromagnetic one for planted systems (see for instance [141, 142]), then it is hard to reconcile the presence of an equilibrium ferromagnet phase (where the susceptibility is finite) with an equilibrium spin glass phase (where the susceptibility diverges).

A complementary (rigorous) argument was presented by Montanari [168] who showed that in sparse systems (i.e. each observations depends on a bounded number of variables) in the Bayes-optimal setting two point correlations decay. In the static spin glass phase these correlations could not decay.

This means that we should not fear the presence of a static equilibrium transition to a glass phase on the Nishimori line. Note however that the dynamics can still be complicated, and in fact as we mentioned a dynamic spin glass (dIRSB) phase can appear. As soon as we depart from the Bayes optimal setting and mismatch the prior, the model or their parameters, the stage for glassiness to arrive is open. And indeed as we see in Fig. 2 there are regions with RSB when  $\beta \neq \beta^*$ , typically when we take the temperature too small. When studying inference with mismatched prior or model we thus always have to keep this in mind before making claims about exactness.

### C. Phase diagram from the cavity method

Now we move to special cases of inference problems where the phase diagram and phase transitions can be computed analytically exactly, and related algorithms more efficient than the Monte-Carlo derived. We achieve this using extended mean-field methods, slightly abusively we will call mean-field systems those where these methods lead to exact results.

Mean-field methods are often the first step in the understanding of systems in physics, and disordered systems are no exception. In spin glasses, in particular, the mean-field model proposed in 1975 by D. Sherrington and S. Kirkpatrick [215] has been particularly important. We refer to the classical literature [163] for the replica solution, involving the so-called replica symmetry breaking, devised by Parisi. It is not that we are not interested in the replica method, quite the contrary, the replica method is at the roots of many results in this review. We shall, however, specialize here to the alternative cavity method [160–162] since this leads more naturally to specific algorithms and algorithmic ideas. Development of more efficient algorithms is our goal in inference problems.

There are two main types of lattices for which the mean-field theory is exact. The first type is the fully connected lattice underlying the canonical Sherrington–Kirkpatrick model. Similar solutions have been derived for the  $p$ -spin model [92] and for the Potts glass model [90], and these played a major role in the development of the mean-field theory of the structural glass transition [125–127]. The linear estimation problem that we treat in Sec. V is an example of a problem on a fully connected lattice.

The second type of lattice for which the mean-field theory is exact is given by large random graphs with constant average degree (or connectivity), a case commonly referred to as “Bethe lattice” in the physics literature [225]. In 2001 Mézard and Parisi [160, 161], using the cavity method, adapted the replica symmetry breaking scheme to solve models on such sparse lattices. There is a number of reasons why Bethe lattices are interesting, the two major ones are: a) because of the finite connectivity, they provide a better approximation of the finite dimensional case and because the notions of distance and neighboring can be naturally defined, and b) the related random graphs are fundamental in many interdisciplinary cases, for instance in computer science problems, which is our main motivation here.

The cavity method is a generalization of the Bethe and Onsager ideas [23, 187] for disordered systems. It was developed initially by Mézard, Parisi and Virasoro [162] as a tool to recover the solution of the Sherrington–Kirkpatrick model without the use of replicas. It was subsequently developed by Mézard and Parisi to deal with the statistical physics of disordered systems on random graphs [160]. There is a global connection between the Bethe approximation and the so-called belief propagation approach in computer science (in error correction [82] and Bayesian networks [189]) as was realized in connection to error correcting codes by Kabashima and Saad [119], and was put in a more general setting by [233]. For a more recent textbook that covers in detail the cavity method and belief propagation see [165], for a very comprehensive explanation of belief propagation see [233]. We shall use the name belief propagation to refer to the corresponding iterative equations.

1. *Properties of the random ensemble*

The first system on which we will illustrate how to use the cavity method and related belief propagation to compute its phase diagram is the Viana-Bray (V-B) model for diluted spin glass [225]. Viana and Bray studied the Ising spin glass Hamiltonian (24) with the lattice being an Erdős-Rényi (ER) random graph with average degree  $c$ . The interactions  $J_{ij}$  are chosen from  $\pm 1$  uniformly at random. For simplicity we consider zero magnetic field.

In order to describe properties of the V-B model one uses the Bethe approximation as was originally done by [31]. The Bethe approximation here is written in terms of iterative equations for the so-called messages  $u_t^{i \rightarrow j}$  going from node  $i$  to node  $j$  along the edge  $(ij)$ , index  $t$  stands for time iteration,

$$u_t^{i \rightarrow j} = \frac{1}{\beta} \operatorname{atanh} \left[ \tanh(\beta J_{ij}) \tanh \left( \beta \sum_{k \in \partial i \setminus j} u_{t-1}^{k \rightarrow i} \right) \right], \quad (50)$$

where we denoted by  $\partial i$  the set of neighbors of node  $i$ .

In order to derive the above equation, the reader should consider the following exercise. Take a spin, denoted  $i$ , which is connected with  $k = 1, \dots, d_i - 1$  independent spins, each of them in a local field denoted  $u^{k \rightarrow i}$ . Summing over all possibilities of the all  $(d_i - 1)$  neighboring spins, simple algebra shows that the system is equivalent to a spin  $i$  with local field  $u_t^{i \rightarrow j}$  as given in eq. (50). Iterating this procedure allows to actually solve the problem on a tree, which is at the root of the cavity method. Here, however, we apply this procedure on the graph, iteratively, hence the time indices in eq. (50).

The local magnetization is computed from the BP fixed point using, as always, the hyperbolic tangent of the local field acting on the spin, and thus reads

$$m_i = \tanh \left( \beta \sum_{j \in \partial i} u^{j \rightarrow i} \right). \quad (51)$$

Interestingly, the same approach allows to also compute the free energy, again to derive it we assume that we work on a tree. With this approximation, it is called the Bethe free energy and reads

$$\beta F = \sum_i (d_i - 1) \log [2 \cosh(\beta h^i)] - \sum_{(ij) \in E} \log \left[ \sum_{S=\pm 1} 2e^{S\beta J_{ij}} \cosh(\beta h^{j \rightarrow i} + S\beta h^{i \rightarrow j}) \right], \quad (52)$$

where  $h^i = \sum_{k \in \partial i} u^{k \rightarrow i}$  and  $h^{i \rightarrow j} = \sum_{k \in \partial i \setminus j} u^{k \rightarrow i}$ , and  $d_i$  in degree of node  $i$ .

The physical properties of the system are computed from the fixed points of the BP equations (50). The fixed points can be investigated either numerically on a given realization of the problem or on average via the so-called population dynamics [160]. Depending on the value of the inverse temperature  $\beta$  in the Viana-Bray model we observe one of the two following possibilities: Either at low  $\beta$  there is a stable *paramagnetic* fixed point  $u^{i \rightarrow j} = 0$  for all  $(ij) \in E$ , or at high  $\beta$  the iterations of (50) do not converge. The corresponding paramagnetic free energy density reads

$$-\beta f(\beta, \mathbf{J}) = \log 2 + \frac{c}{2} [\log(2 \cosh \beta) - \log 2]. \quad (53)$$

We do notice that the same expression is obtained for the annealed free energy for this model.

Thouless [221] analyzed the threshold value of  $\beta_c$  by linearizing the update (50) around the uniform fixed point, thus getting

$$u_t^{i \rightarrow j} = \tanh(\beta J_{ij}) \sum_{k \in \partial i \setminus j} u_{t-1}^{k \rightarrow i}. \quad (54)$$

Thouless then argues that averaged over the disorder  $J_{ij}$  the above equation gives zero, and when its square is averaged we get

$$\langle u_t^2 \rangle = c \tanh^2 \beta \langle u_{t-1}^2 \rangle, \quad (55)$$

where we remind  $c$  is the average degree of the ER graph, that is also equal to the average branching factor. The critical temperature is then given by

$$\beta_c = \operatorname{atanh} \left( \frac{1}{\sqrt{c}} \right). \quad (56)$$

It follows that for  $\beta < \beta_c$  the state of the Viana-Bray model is correctly described by the paramagnetic fixed point. For  $\beta > \beta_c$  the Bethe approximation fails and the correct physical description is via the so-called replica symmetry breaking [160].

## 2. Phase diagram of the planted spin glass

Now we aim to compute the phase diagram of the planted spin glass, where the interactions  $\mathbf{J}$  are chosen conditionally to the planted configuration  $\mathbf{S}^*$ , following eq. (28). In this case the Bethe approximation and its linearization are still described by (50) and (54). On the planted model the stability analysis of the paramagnetic fixed point is slightly different since the distribution from which the interactions  $J_{ij}$  are taken is not random but depends on the planted configuration. When taking the average of (54) and counting properly the probability of  $J_{ij}$  given  $S_i^*$  and  $S_j^*$  we get

$$\langle u_t \rangle = c(\tanh \beta^*)(\tanh \beta) \langle u_{t-1} \rangle. \quad (57)$$

According to this the system starts to polarize towards the planted configuration for

$$\beta > \beta_F = \operatorname{atanh} \left( \frac{1}{c \tanh \beta^*} \right). \quad (58)$$

Note that as  $\beta^* \rightarrow \infty$  we recover the ordinary ferromagnetic Ising model with its well known critical temperature. Observe that there is one point, the so-called multi-critical points, at  $\beta = \operatorname{atanh}(1/\sqrt{c})$  where all the three conditions (56), (58) and Bayes-optimality,  $\beta = \beta^*$ , meet.

For the Bayes-optimal case,  $\beta^* = \beta$ , we obtain that for  $\beta^* < \beta_c$  the paramagnetic fixed point and the corresponding free energy is the only fixed point of the recursion (50). Since the paramagnetic and annealed free energies are equal, this is a case where the planting is quiet, as defined in section II B 3. This means that in the whole region  $\beta^* < \beta_c$  the planted ensemble behaves exactly the same as the random ensemble. This is indeed reflected in the phase diagram in Fig. 2 where everything on the left from the multi-critical point is independent of the value of  $\rho$ .

Out of the Bayes-optimal case, i.e. when  $\beta^* \neq \beta$ , at very low temperature (large  $\beta$ ) there exists a so-called mixed phase where equilibrium configurations are correlated to the planted one but the recursion (50) does not converge (analyzing the convergence is also how the phase boundary is determined). There might also be a genuine spin glass phase with no correlations to the planted configuration, but the exact boundary of this one is not known since a full-step replica symmetry breaking calculation would be needed and has not yet been developed for sparse Ising models.

The phase diagram is summarized in Fig. 2 where the boundary between the paramagnet (P) and the spin glass (SG) is plotted in green, between the paramagnet (P) and ferromagnet (F) in blue, and the Nishimori line corresponding to the Bayes-optimal inference is in red. We also sketch the position of the mixed phase (M).

## 3. Systems with first order phase transitions

In the above planted Ising spin glass model the underlying phase transition is of second order. In that case there is no particular computational issue. Either inference is impossible or possible and tractable. The hard phase outlined in section (I A 6) is absent.

The picture is richer in problems where in the random ensemble there is a discontinuous phase transition. Famously, this is the case in the low density parity check error correcting codes as described e.g. in [165, 183]. The examples of clustering of networks and compressed sensing (to which we consecrate sections IV and V) also fall in this category. For the material presented in this review the most vital paper in this category is *Hiding quiet solutions in random constraint satisfaction problems* [139] where the concept (or at least the name) of quiet planting was introduced on the example of planted coloring. Closely related ideas were already present in [78] for the ferromagnetic  $p$ -spin model, which is a little special in the sense that the easy detectable phase (see below) is missing.

In planted coloring one first chooses a random assignment of  $q$  colors out of the  $q^N$  possible ones. And then one puts  $M = cN/2$  edges at random among all those edges that do not have the same color on their two adjacent nodes. The Bayes optimal inference in this setting evaluates marginals over the set of all valid colorings of the created graph. Computation of these marginals builds on previous works [180, 235], where the problem of coloring random graphs was studied, and goes as follows: One considers belief propagation initialized in two different ways. In the random initialization the messages are chosen at random but close to the paramagnetic ones. In the planted initialization the initial values of the messages are set to point in the direction of the planted configurations. Fixed point is reached from both these initializations and its free energy evaluated. We obtain the following picture, illustrated in Figs. 3 and 4 for planted 5-coloring

- Undetectable paramagnetic phase, for average degree  $c < c_d$ . The planting is quiet and belief propagation converges to the uniform fixed point both from random and planted initialization. We will call  $c_d$  the *dynamical* or the *clustering* phase transition [236].

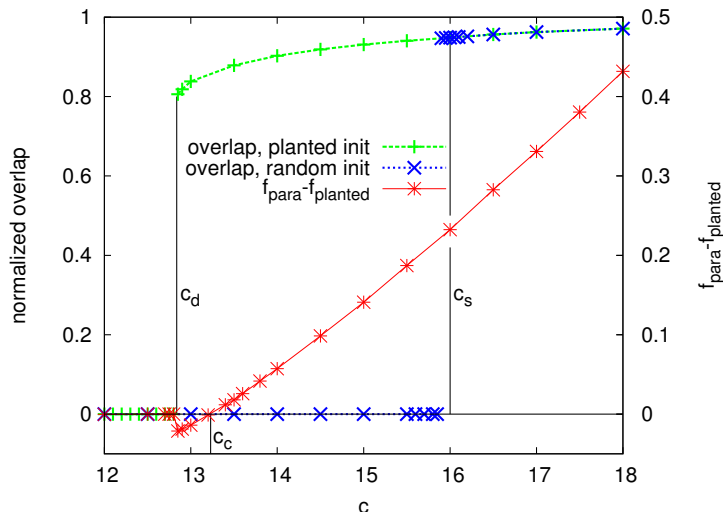


FIG. 4. The phase transitions for planted 5-coloring. The overlap (normalized in such a way that for a random configuration it is zero) achieved by BP initialized in the random and planted configuration. The difference between the corresponding free energies is also plotted. Figure taken from [59].

- Undetectable clustered phase, or dynamic one-step replica symmetry breaking (d1RSB) phase, for average degree  $c_d < c < c_c$ . The planting is still quiet, but the set of solutions is split into exponentially many clusters that are uncorrelated and all look the same as the one containing the planted solutions. We will refer to  $c_c$  as the *detectability* phase transition. In the random ensemble  $c_c$  is the condensation transition [236].
- Hard detectable phase, for average degree  $c_c < c < c_s$ . This is arguably the most peculiar phase of the four. The Bayes optimal marginals are correlated to the planted configuration, however, there is a metastable paramagnetic phase to which belief propagation converges from a random initialization. A ghost of the quiet planting is visible even for  $c > c_c$  in the sense that the space of configurations looks exactly like the one of the random ensemble except for the planted cluster.
- Easy detectable phase, for average degree  $c > c_s$ . Belief propagation finds a configuration correlated to the planted coloring. The phase transition  $c_s$  can be located doing a local stability analysis of the uniform BP fixed point, along the same lines as done for the planted spin glass in section IIC 2. We will refer to  $c_s$  as the *spinodal* or the *hard-easy* phase transition. In the random ensemble,  $c_s$  is the point starting from which belief propagation stops converging, related to the local instability towards the spin glass phase [236].

#### 4. Comments on the phase transitions in various problems

One question we want to clarify is whether the concept quiet planting works for every inference problem. Here the answer is both yes and no. First of all for quiet planting to work we need to be in a setting where belief propagation has the uniform (sometimes confusingly called factorized) fixed point, where the messages in the fixed point do not depend on the indices of the edge. If such a fixed point exists then the annealed free energy density equals the quenched one [174], and consequently the argument about planting being quiet works. There are many problems where for the random ensemble BP does not have a factorized fixed point, the most studied examples are perhaps the problem of  $K$ -satisfiability, or Ising model in a random external magnetic field  $h_i$ .

Even in problems such as  $K$ -SAT where the canonical BP does not have a uniform fixed point [166] we can introduce a reweighted Boltzmann measure, as done in [136], in such a way that the corresponding BP fixed point is uniform. Planting according to this reweighted measure then leads to instances that are contiguous to the random ones. Note that this reweighting and corresponding planted instances were used in the proof of [4, 5] and studied also in [16, 112]. The planted solution is not an equilibrium solution with respect to the canonical Boltzmann measure but with respect to the reweighted measure. Studying this reweighting for planted  $K$ -SAT one obtains several interesting results. For instance, one can put in direct evidence the existence of purely entropic barrier between clusters of solutions.

Another result is related to the following natural question: How to distinguish between problems where the transition is continuous or discontinuous. And when it is discontinuous, how wide is the hard phase. Is there some criteria simpler than performing the whole analysis? To distinguish between the first and second order transition, we do not know of any other way. We only have a couple of rules of thumb - in Potts model with sufficient number of states continuous transitions become discontinuous, and in models where more than two variables interact, e.g. the  $p$ -spin model or  $K$ -SAT, the continuous transition becomes discontinuous for sufficiently large  $K$  and  $p$ . But there are binary pairwise problems such as the independent set where at sufficiently large average degree the continuous transition also becomes discontinuous.

Interestingly, one can identify a class of constraint satisfaction problems where the hard phase is very wide. In [136] these problems were identified as those with  $\alpha_s \rightarrow \infty$ . Previously only XOR-SAT was known to have this property [78], but in [73, 136] a whole hierarchy of such problems was identified and is related to  $k$ -transitivity of the constraints. A constraint is  $k$ -transitive if and only if the number of satisfying assignments compatible with any given assignment of any  $k$  variables is the same. For all CSPs that are at least 2-transitive the hard phase extends over the whole region of linearly many constraints, equivalently  $\alpha_s \rightarrow \infty$ . Calling  $r$  the smallest number such that a constraint is not  $r$ -transitive, the number of constraints predicted to render the problem tractable scales as  $N^{r/2}$  [73]. Interestingly, this classification makes the  $K$ -XOR-SAT the hardest of all CSPs (despite the fact that it can be solved by Gaussian elimination, which is not robust to any kind of noise). The notion of 2-transitivity and consequently infinitely large hard phase extends also to continuous variables, and as it was recently pointed out renders tensor factorization and completion very difficult [201]. Physically, the corresponding systems are such where the paramagnetic phase is locally stable down to zero temperature [78]. Examples of such systems indeed include the Ising  $p$ -spin (related to  $K$ -XOR-SAT) or the spherical  $p$ -spin model related to tensor factorization.

Having examples where the hard phase is this extremely huge is very useful when thinking about formal reasons of why this phase is hard. In [73] the authors proved hardness for a class of so called *statistical algorithms* using precisely this kind of constraint satisfaction problems. Arguably, the class of statistical algorithms is too restrictive, but we believe that the instances of CSP with such a large hard phase should be instrumental for other attempts in this direction. We shall summarize in section IIIB arguments for why we think there is something fundamentally hard in this phase.

In [239] we discussed the example of planted locked constraint satisfaction problems (CSP). These are particularly interesting for a couple of reasons. First of all, the valid solutions are separated by extensive Hamming distance from each other and therefore either BP converges to a paramagnet or points exactly towards the planted configuration. Note that low-density parity check (LDPC) error correcting codes have precisely this property. Locked CSP can be thought of as non-linear generalization of LDPC. A second reason why locked CSPs are interesting is that in some cases the hard phase is very wide and moreover the planted assignment is with high probability the only one (perhaps up to a global flip symmetry). The planted locked CSP are hence attractive candidates for a one-way function that could find applications in cryptography. Having hard CSP instances that have exactly one valid assignment was used in studies of quantum annealing where having non-degenerate ground state is greatly advantageous, see e.g. [102].

#### D. Applications of planting for studies of glasses

Now that we explored the concept of planting and quiet planting we realize that it also has a number of consequences for the study of structural glasses. In this section these are summarized.

##### 1. Equilibration for free in glasses

Let us discuss the physical consequences of the fact that in quietly planted systems the planted configuration behaves exactly the same as any other equilibrium configuration. We can hence literally equilibrate for free. This is particularly interesting in the study of glassy models. As a matter of fact, the very concept of glassiness can be defined as super-fast growth of the equilibration time as the glass transition temperature is approached [28].

The core of the interest in glasses is concerned by finite (usually three) dimensional models. In those cases the annealed and quenched free energies are known not to coincide. A class of theories of glasses is, however, based on mean-field (i.e. systems living on random geometries of fully connected graphs) disordered systems that present a discontinuous phase transition. The analog of  $c_d$  in these systems is called the dynamical glass transition, and the analog of  $c_c$  is the Kauzmann glass temperature. Properties of the equilibration time are well studied and it turns out that equilibration time (i.e. number of Monte Carlo steps per variable in the thermodynamic limit) diverges as the dynamical temperature is approached [170] and is exponentially large in the system size between the dynamical and Kauzmann temperature. This in practice means that numerical simulations of these models are very cumbersome.



In most of the mean-field models used for studies of glasses the quiet planting works. Numerical simulation on which dynamics is studied from equilibrium can hence be speeded up considerably by initializing in the planted configuration. This trick was used first in [169], but popularized by [139] it has been now used in a considerable number of works. Without being exhaustive let us mention Refs. [10, 46, 47, 76, 155, 156].

Also if one does not care about the equivalence to the random ensemble one can use planting to obtain equilibrium configurations even in general finite dimensional systems. Indeed the property of planted configuration being the equilibrium one for a corresponding Boltzmann measure is general. This has been used in numerical studies of so-called pinning in glasses, see e.g. [105].

## 2. Following states and analyzing slow annealing

Ref. [139] studied the state that is created in the planted coloring around the planted configuration. Adding to this the concept of quiet planting, we realize that this framework allows us to study the *shape* of states in mean-field glassy systems. A plot that illustrates well our aim here is in Fig. 5 where the blue line is the equilibrium (one-step replica symmetry breaking) energy of the regular (i.e. every variables has the same degree) 3-XOR-SAT problem as a function of temperature  $T$ . Quiet planting works for this system at all temperatures. The red lines are energies that we obtain when we plant quietly (at temperature where the red lines crosses the blue one) and then lower or increase the temperature and monitor the corresponding Bethe energy given by the corresponding belief propagation fixed point. We call this procedure *state following* [140, 238], because physically this is a study of the corresponding state at temperature at which the state is no longer among the equilibrium ones.

Note that such state following was often described in physics of glasses on the level of a thought-experiment. Methods for quantitative analysis existed only for the particular case of spherical  $p$ -spin model, via an exact solution of the dynamics [28, 55, 56]. For other systems, in particular diluted ones, state following was considered as an open problem, see e.g. the concept suggested but not analyzed in [131]. Although the method for state following is mathematically very much related to the concept of Franz-Parisi potential [79], in our opinion the precise relation between the two concepts and the full physical interpretation was greatly clarified by refs. [140, 238]. The state following was applied in a number of settings involving glassy dynamics, see e.g. [46, 48, 193].

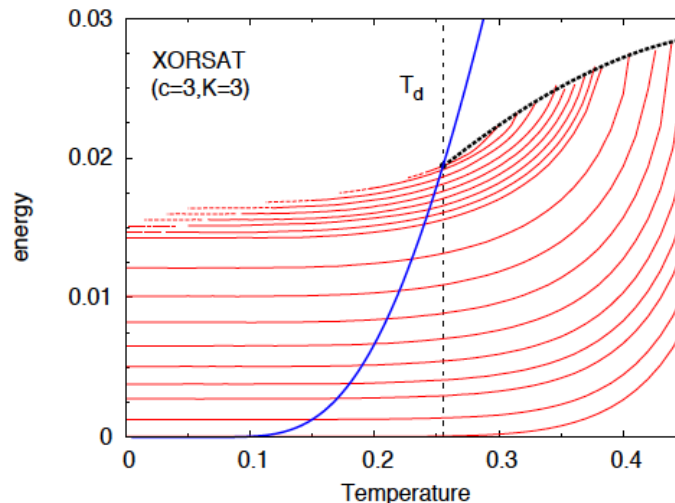


FIG. 5. State following in regular 3-XOR-SAT. Figure taken from [238].

From an algorithmic point of view, the method of state following opens the exciting possibility of analyzing limiting energy of very slow annealing. It is well known that on a finite size system annealing always finds the ground state, in time that is in general exponential in the system size. Crucially interesting question is: What is the lowest achievable energy when the annealing rate scales linearly with the size of the system? In mean-field models of glasses equilibration is possible in time that is linear in the system size down to the dynamical temperature  $T_d$  (or equivalently up to  $c_d$ ), after that the dynamics gets blocked in one of the exponentially many states. If we take an equilibrium state at  $T_d - \epsilon$  and follow it down to zero temperature the resulting energy is a very good candidate for the behavior and for the

limiting energy of very slow simulated annealing. Very slow annealing for the Ising  $p$ -spin model was analyzed in [143] and compared to the theoretical prediction from state following.

*Paradox in state following.* There is, however, a problem that appears when one tries to carry out the calculation for following of states that are at equilibrium close to  $T_d$ . When following the state down in temperature, the replica symmetry gets broken at some point (the boundary between full and dashed lines in Fig. 5). Moreover, at yet lower temperature the solution correlated to the planted configuration disappears (in a mathematically analogous way as when a spinodal line is encountered). Even using the 1RSB computation to describe the internal structure of the state we were not able to follow it down to zero temperature. A possible explanation is that the correct description of this region is the full-step replica symmetry breaking (FRSB). To test this hypothesis Ref. [218] analyzed the mixed spherical  $p$ -spin model where the FRSB is tractable.

The findings of [218], however, raised even more questions. We found by the Nishimori mapping to the model with a ferromagnetic bias (as described in section II A 2) that there is no FRSB solution to the problem, yet there is no magnetized 1RSB solution at very low temperature either. Yet in MCMC simulation one always confirms the expectation that as temperature is lowered the bottom of the state is correlated to the reference configuration. In other words, using the Nishimori mapping, the non-magnetized spin glass phase that is assumed to exist at low temperature for  $\rho > \rho_c$  in Fig. 2 is not physical in the context of state following. These observations are hence an inconsistency in the theory. Loose ends such as this one are always interesting and basically always eventually lead to new theoretical development. This state following paradox should hence not be forgotten and should be revisited as often as new possibilities open.

One such possibility might be related to the calculation involving a chain of reference (planted) configurations at lower and lower temperatures as suggested in [80].

### 3. Melting and glass transition

Using the planted models and extended form of the Nishimori conditions the analogy between glassy dynamics and melting was studied in [141, 142]. Perhaps the theoretically most intriguing and very fundamental question in theory of glasses is: Is there a true glass transition in a finite-dimensional system (i.e. system where the graph of interactions can be embedded into finite-dimensional Euclidean space)? Such an ideal glass transition has to come with diverging time and length scales when approaching the transition. A definitive answer to this question is difficult to obtain as both simulations and experiments are faced with the extremely slow dynamics. According to the random first order theory of the glass transition [128, 129], there are time and length scales with a genuine divergence at the ideal glass transition temperature, although the random first order theory is not free from criticisms, see for instance [24] and references therein.

The question of existence of the ideal glass transition remains open, but in [142] it was derived that if there is a finite-dimensional model with a first order phase transition on the Nishimori line (or equivalently in the Bayes optimal inference) then there is an ideal glass transition as well. This result was reached by using the Nishimori mapping from a planted model to a ferromagnet, sec. II A 2, and comparing their dynamical properties. In particular, if there is a first order phase transition on the Nishimori line then it comes with two quite uncommon properties - absent latent heat, and the melting dynamics being equivalent to the stationary equilibrium dynamics. Arguably first order phase transition are easier to describe or exclude than the tricky glass transition. This is hence an interesting path towards the fundamental question of existence of ideal glass transition.

Inspired by the theoretical analyses Ref. [142] devised a 3-dimensional 5-spin model that numerically shows up all the characteristics of a first order phase transition. This is interesting, because some previous works pointed out a difficulty in design of such a model because many of the models that are first order in the mean-field case seem to become clearly second order in 3 dimensions. Mathematically, the main question of course stays open, because it might be that even here there is a crossover to a second order phase transition at sizes much larger than those used for simulations.

### III. FROM PHYSICS INSIGHT TO NEW ALGORITHMIC IDEAS

In the introduction, sec. IA 1, we presented two main questions about inference we aim to answer. One more fundamental, about phase diagrams, phase transitions and related insight, second more practical, about development of algorithms. This section is about algorithmic contributions obtained using the insight resulting from statistical physics analysis. For clarity, all is again illustrated on the planted spin glass model.

With the work of Mézard, Parisi and Zecchina on survey propagation [164], the statistical physics community learned that the replica and cavity calculations are as powerful when used as algorithms as they are when used as tools for analyzing the phase diagram. The connection between the Bethe approximation and belief propagation was noticed earlier in connection to error correcting codes by Kabashima and Saad [119], and in a more general setting by [233]. But looking at the volume of related literature it is only after survey propagation that the whole statistical physics community started to look for explicit algorithmic applications of the Bethe approximation.

#### A. Non-backtracking spectral method

Notice, within the historical perspective, that the Bethe solution for the spin glass on a random graph was written by Bowman and Levin [31], i.e. about 16 years before realizing that the same equation is called belief propagation that can be used as an iterative algorithm in a number of applications.

The paper by Thouless [221], who analyzed the spin glass critical temperature, implicitly includes another very interesting algorithm, that can be summarized by equation (54) where BP is linearized. The fact that this equations has far-reaching implications when viewed as a basis for a spectral algorithm waited for its discovery even longer. Notably till 2013 when the methodologically same algorithm was suggested for clustering of networks [137], this work will be discussed in sec. IV D. We now turn back to our pedagogical example, the  $\pm J$  planted spin glass, and related spectral algorithm as described and analyzed in [206]. Related ideas also appeared in [240].

First note that a large class of inference algorithms is based on a spectral method of some kind. Probably the most widely used is the so-called principal component analysis (PCA). Citing Wikipedia, its operation can be thought of as revealing the internal structure of the data in a way that best explains the variance in the data. In PCA the information is contained in singular vectors (or eigenvectors for symmetric matrices) corresponding to the largest singular values. Resulting spectral algorithms are used everyday to solve numerous real world problems. The same strategy of computing leading singular (or eigen-) vector of some matrix related to the data is applied in many settings including the planted partitioning problem closely related to the planted spin glass model [52, 53], or in understanding financial data [29, 147].

A natural question that arises is whether a spectral algorithm can find a configuration correlated to the planted assignment in the planted spin glass in the whole region  $\beta^* > \beta_c$  where belief propagation can asymptotically do so. Facing this question, many experts would probably suggest to take the matrix  $J_{ij}$  (with  $J_{ij} = 0$  when  $(ij) \notin E$ ) or its associated Laplacian (perhaps normalized in some way) and compute the leading eigenvector. This is indeed a good strategy, but on Erdős-Rényi random graphs it does not work down to the threshold  $\beta_c$ . The problem is that for large Ising model living on an Erdős-Rényi graph the tail of the spectra of the commonly considered matrices is dominated by eigenvectors localized on some small subgraphs (e.g. around high-degree nodes or on some kind of hanging sub-trees).

The strategy in designing spectral method that does not have the problem with localized eigenvectors (at least on a much larger class of graphs) is to try to mimic what BP is doing when departing from the paramagnetic fixed point. Eq. (54) is precisely the linearization of BP around that fixed point and suggests a definition of a so-called *non-backtracking matrix*  $B$  defined on directed edges as

$$B_{i \rightarrow j, k \rightarrow l} = J_{ij} \delta_{il} (1 - \delta_{jk}). \quad (59)$$

Denoting  $M$  the number of edges in the non-directed graph, this is a  $2M \times 2M$  matrix. The term  $(1 - \delta_{jk})$  means that a walk that follows non-zero elements of the matrix is not going back on its steps, this motivates the name of the matrix. Building on [27, 137], we proved in [206] that the planted configuration is indeed correlated with the signs of elements of the eigenvector of  $B$  corresponding to the largest (in module) eigenvalue as soon as  $\beta^* > \beta_c$ .

Fig. 6 depicts the spectrum on the matrix  $B$  (59) for a planted spin glass model on an ER graph of average degree  $c$  and having  $N = 2000$  nodes. The  $J_{ij} = \pm 1$  were generated following the procedure described in sec. IIA 1 with  $\beta^* = 0.55$ . We observe (and proved in [206]) that

- For  $\beta^* < \beta_c = \text{atanh}(1/\sqrt{c})$ , corresponding to the paramagnetic phase of the planted spin glass model. The spectrum of  $B$  is the same as it would be for  $\beta^* = 0$ , bounded by a circle of radius  $\sqrt{c}$ .

- For  $\beta^* > \beta_c = \operatorname{atanh}(1/\sqrt{c})$ , corresponding to the ferromagnetic phase of the planted spin glass model. The spectrum of  $B$  has the same property as in the previous case, except for two eigenvalues of the real axes. One of them is out of the circle and has value  $c \tanh \beta^*$ . Its corresponding eigenvector is correlated positively with the planted assignment.

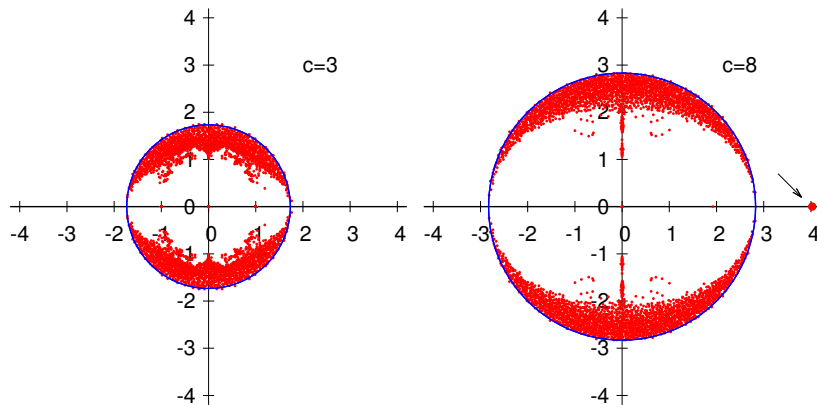


FIG. 6. Spectrum of the non-backtracking operator for the  $\pm J$  planted spin glass model. Right: In the undetectable phase where all eigenvalues are inside a circle of radius  $\sqrt{c}$ . Left: In the detectable phase where one eigenvalues is outside the circle on the real axes, its value is  $c \tanh \beta^*$ . Figure taken from [206].

### B. On computational hardness of the hard phase

In section II C 3 we described the four phases that we observe in the Bayes optimal setting of inference problems. The most theoretically intriguing is the hard detectable phase that appears between the detectability transition  $c_c$ , and the spinodal transition  $c_s$ . In this phase both Monte Carlo and belief propagation, that aim to sample the Bayes-optimal (i.e. prior distribution, the model and all their parameters are known) posterior distribution, fail and get blocked in the metastable paramagnetic phase. The spinodal transition  $c_s$  is also a barrier for all known spectral algorithms. Some of the spectral methods including the one based on the non-backtracking matrix saturate this threshold.

There are many other problems where a phase having the same physical origin was discovered. Among them the best known are the LDPC error correcting codes [165] and the planted clique problem [8, 63, 111, 114]. Some recent works prove hardness in other problems assuming the hardness of planted clique (in the corresponding region) [22, 33, 95, 152]. There is a lot of current interest in this kind of results.

When a physicist sees a phenomenon as the one above she immediately thinks about universality and tends to conjecture that the spinodal transition in inference problems will be a barrier for all polynomial algorithms. There is, however, the case of planted XOR-SAT that presents the same phenomenology as described in section II C 3. Moreover, the hard phase in planted XOR-SAT extends to infinity (the paramagnetic state is always locally stable). The work of [73] actually suggest that the right scaling for the number of clauses at which planted K-XOR-SAT becomes easy is when the number of clauses is at least  $O(N^{K/2})$ . Yet, thanks to its linearity planted K-XOR-SAT can be solved in polynomial time by Gaussian elimination. Hence the above conjecture about the hard phase is false. But the physicist's intuition is rarely entirely wrong, and in that rare cases when it was indeed entirely wrong it was for absolutely fundamental reasons. In our opinion, the question:

In which exact sense is the hard phase hard?

is the most fundamental question related to the interface between statistical physics, statistical inference and average computational complexity.

A line of research that should be explored, and seems quite accesible, is proving of disproving that there is no way to use belief propagation or Gibbs sampling with a mismatched prior or model in order to improve the position of the spinodal transition.

Let us also note here that the spinodals of first order phase transition in Bayes-optimal inference problems create a much cleaner algorithmic barrier than phase transitions described in optimization or in constraint satisfaction problems such as  $K$ -satisfiability. In  $K$ -SAT the idea of hard instances being close to the satisfiability threshold goes back to the works by [49, 167, 213]. However, even after more than 20 years of study it is still not clear what is the limiting constraint density up to which polynomial algorithms are able to find satisfiable solutions in random  $K$ -SAT (even at very large  $K$ ). For a related discussion see [236].

### C. Spatial coupling

Spatial coupling is, from a physics point of view, very natural strategy how to beat the hard-easy spinodal transition in systems where the structure of the graphical model can be designed. It is closely related to nucleation in physics. We mentioned above that exponentially long living metastability is only possible in mean-field systems. Let us describe here why it is not possible in systems embedded in finite Euclidean dimension  $d$ . Metastability means that there are two competing phases. Let us call  $\Delta f$  the free energy difference between them. Let us consider a large system in the metastable state with a droplet of radius  $L$  (small compared to the size of the whole system) that by random fluctuation appears to be in the stable state. Creating such a droplet will cost some energy due to its interface where the two phases do not match. This is quantified by the surface tension  $\Gamma$ . The total energy balance can be written as

$$E(L) = \Gamma L^{d-1} - \Delta f L^d. \quad (60)$$

Physical dynamics can be roughly thought of as gradient descent in this energy. Notice that  $E(L)$  is increasing for  $L < L^* = \Gamma(d-1)/(\Delta f)$  and decreasing for  $L > L^*$ . This means that if fluctuations created a droplet larger than the critical size  $L^*$  it will continue growing until it invades the whole system. The above argument works only in geometries where surface of a large droplet is much smaller than its volume. On random sparse graphs or fully connected geometries it does not work. This is why nucleation does not exist in mean-field systems. Notice also that nucleation is simpler for lower dimensions  $d$ , the lowest meaningful case being  $d = 1$ .

We can conclude that in order to avoid long living metastability we need to work with finite-dimensional systems. But the situation is not so simple either. In systems where the mean-field geometries are used they are used for a good reason. In LDPC codes they assure large distance from spurious codewords, in compressed sensing random projections are known to conserve well the available information, etc. To avoid metastability we need to mix the mean-field geometry on a local scale with the finite dimensional geometry on the global scale. This is exactly what spatial coupling is doing. Originally developed for LDPC error correcting codes [145, 149] and closely related to convolutional LDPC that have longer history [74], spatial coupling has been applied to numerous other settings. Again we will discuss some in more detail in section V D. To introduce the concept here, we restrict to the spatially coupled Curie-Weiss model as introduced in [98] and studied further in [35].

The Curie-Weiss (C-W) model in magnetic field is arguably among the most simple examples that present a first order phase transition. The C-W model is a system of  $N$  Ising spins  $S_i \in \{-1, +1\}$ , that are interacting according to the fully connected Hamiltonian

$$\mathcal{H}_{C-W}(\mathbf{S}) = -\frac{J}{N} \sum_{\langle i,j \rangle} S_i S_j - h \sum_{i=1}^N S_i, \quad (61)$$

where the notation  $\langle \cdot, \cdot \rangle$  is used to denote all unique pairs,  $J > 0$  is the ferromagnetic interaction strength and  $h \in \mathbb{R}$  is the external magnetic field.

Let us briefly remind what is obvious to everybody trained in statistical physics. For positive magnetic field  $h > 0$  the equilibrium magnetization  $m(J, h) > 0$  is positive, and vice versa. There exists a critical value of the interaction strength  $J_c = 1$  such that: for  $J < J_c$  the  $\lim_{h \rightarrow 0^+} m(J, h) = \lim_{h \rightarrow 0^-} m(J, h) = 0$ , and for  $J > J_c$  we have  $\lim_{h \rightarrow 0^+} m(J, h) > 0 > \lim_{h \rightarrow 0^-} m(J, h)$ . The latter is a first order phase transition, in the ‘‘low temperature’’ regime  $J > J_c$  the system keeps a non-zero magnetization even at zero magnetic field  $h$ . There exists a spinodal value of the magnetic field

$$h_s(J) = \sqrt{J(J-1)} - \operatorname{atanh} \left( \sqrt{\frac{J-1}{J}} \right), \quad (62)$$

with the following properties: If the magnetizations are initialized to negative values and the magnetic field is of strength  $0 < h < h_s(J)$ , then both local physical dynamics and local inference algorithms, such as the Gibbs sampling, will stay at negative magnetization  $m^-(J, h) < 0$  for time exponentially large in the size of the system. The spinodal

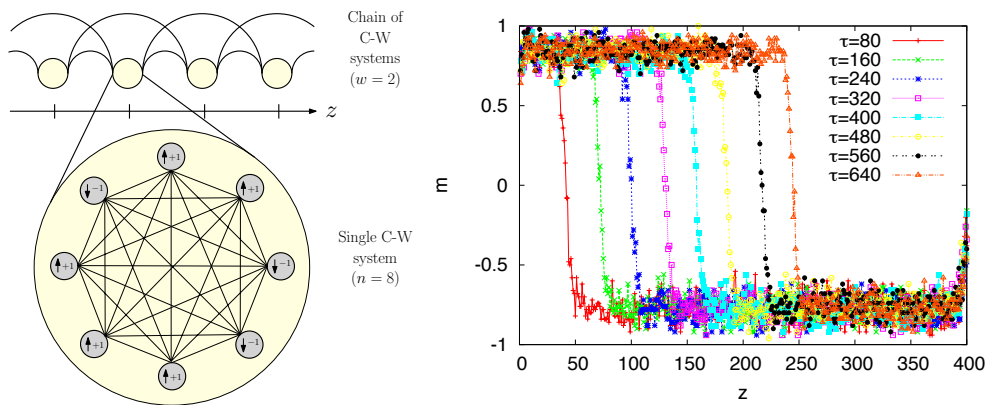


FIG. 7. Left: A schematic graphical representation of the spatially coupled C-W model. A chain of C-W models interacting within a certain range  $w$  ( $w = 2$  in the figure). In the zoomed part the fully-connected structure of the single C-W model is shown. A connection between C-W models along the chain indicates connections between all spins contained in both models. Right: The propagating wave obtained by Monte-Carlo heat-bath simulation for the following parameters:  $J = 1.4$ ,  $L = 400$ ,  $n = 100$ ,  $h = 0.05$ ,  $w = 5$ ,  $w_{\text{seed}} = 10$  and  $h_{\text{seed}} = 0.3$ . Simulations were performed using random sequential update and therefore time must be rescaled by  $\tau = t/N$ . The figure is taken from [35].

value of the magnetic field  $h_s(J)$  acts as an algorithmic barrier to equilibration, when initialized at  $S_i = -1$  for all  $i = 1, \dots, N$ , and hence to successful inference. For  $h > h_s(J)$  it is, on the other hand, easy to reach the equilibrium magnetization  $m^+(J, h)$ .

### 1. Spatially coupled Curie-Weiss model

We introduce here the construction from [98] that might not appear very transparent at first. But its idea is really simple. We create a one-dimensional chain of C-W models, put a nucleation seed somewhere and let the sub-systems interact in order to ensure that the nucleation proceeds to the whole chain.

As illustrated in Fig. 7, we consider a one-dimensional chain of  $(2L + 1)$  C-W systems, where each of the C-W system has  $n$  spins (referred to as a “block”) and is labelled by the index  $z \in \{-L, \dots, L\}$ . The result is that a configuration  $\mathbf{S}$  of the full system is now given by the values of  $N = n(2L + 1)$  spins, each labelled by a compound index:

$$\mathbf{S} = \{S_{iz} \in \{+1, -1\} : i \in \{1, \dots, n\}, z \in \{-L, \dots, L\}\}. \quad (63)$$

In a similar way, the uniform external magnetic field  $h$  for a single system is replaced by an external field profile  $h_z$ . As far as the coupling is concerned, every spin not only connects to all spins in the same location  $z$  but also all spins within  $w$  blocks from  $z$ . The corresponding Hamiltonian is then

$$\mathcal{H}_{n,L}(\mathbf{S}) = -\frac{1}{n} \sum_{\langle iz, jz' \rangle} J_{zz'} S_{iz} S_{jz'} - \sum_{z=-L}^L h_z \sum_{i=1}^n S_{iz}. \quad (64)$$

The couplings between spins are  $J_{zz'} = Jg(|z - z'|/w)/w$ , where the function  $g$  satisfies the following condition  $g(|x|) = 0, \forall |x| > 1$  and we choose its normalization to be  $\frac{1}{w} \sum_{z=-\infty}^{+\infty} g(w^{-1}|z|) = 1$ .

In order to ensure that the system *nucleates*, we must increase the field  $h_z$  at some point on the chain. We choose the magnetic field profile in such a way that  $h_z = h_{\text{seed}} > h_{\text{sp}}$  in some small region given by  $z \in \{0, \dots, w_{\text{seed}}\}$ . Everywhere else,  $h_z = h \ll h_{\text{sp}}$ , such that the average field strength is still small. To illustrate the nucleation in Fig. 7 we initialize to  $S_{iz} = -1$  everywhere and let the system evolve under Monte-Carlo dynamics. We indeed observe a nucleation “wave” that invades the whole system in a time proportional to the number of blocks. The system can be designed in a such a way that the spinodal regime entirely disappears.

### D. A brief history of time indices in the TAP equations

In the physics of disordered system, the historically first form of iterative procedure that was used to compute marginals (local magnetizations) in a densely connected spin glass model are the Thouless-Anderson-Palmer (TAP)

equations [222]. In the early statistical physics works on error correcting codes TAP equations were used for decoding. The primary goal of the paper by Kabashima and Saad [119], who pointed out the connection between belief propagation and Bethe approximation, was to compare the performance of TAP and BP. In dense systems the fixed points of both BP and TAP agree. However, it was reported e.g. in [115, 116] that TAP equations did not converge in some cases even when BP does and there is no replica symmetry breaking. With the renewed interest in message passing of dense systems that followed the work of Donoho, Maleki and Montanari on compressed sensing [68], it is definitely worth making some up-to-date remarks on the TAP equations and their convergence.

The fixed point of the TAP equations

$$m_i = \tanh \left[ \beta h + \beta \sum_{j=1}^N J_{ij} m_j - \beta^2 m_i \sum_{j=1}^N J_{ij}^2 (1 - m_j^2) \right] \quad (65)$$

describes the replica symmetric marginals of the following fully connected spin glass Hamiltonian

$$\mathcal{H}_{SK}(\mathbf{S}) = - \sum_{\langle i,j \rangle} J_{ij} S_i S_j - h \sum_i S_i, \quad (66)$$

where  $J_{ij}$  are independent random variables of zero mean and variance  $\tilde{J}/N$ . Hence a typical value of  $J_{ij} = O(1/\sqrt{N})$ .

Fixed points of the TAP equations are stationary points of the corresponding TAP free energy [222]. Derived as such, TAP equations do not include any time-indices and were mostly iterated in the simplest form of having time  $t-1$  on all magnetizations on the right hand side, and  $t$  on the left hand side. At the same time, as we said above, number of authors reported that TAP equations have problems to converge even when BP does converge and replica symmetry is not broken [115, 116]. No satisfactory explanation for this existed in the literature until very recently [26]. The reason behind this non-convergence was that the time indices were wrong and when done correctly, convergence is restored, and on sufficiently dense systems TAP equations behave as nicely as BP. This was first noticed by Bolthausen [26], who proved convergence of TAP with the right time indices in non-zero magnetic field (and out of the glassy spin glassy phase). His paper inspired the work of [19, 68] but otherwise passed quite unnoticed. Here we shall re-derive TAP as a large degree limit of BP and clarify this issue of time indices.

Let us go back to the belief propagation for sparse graphs eq. (50). Define message  $m_{i \rightarrow j}^t \equiv \tanh(h + \beta \sum_{k \neq j} u_{k \rightarrow i}^{k-t})$ . Recall that  $J_{ij}$ , and hence also  $u$ , is of order  $O(1/\sqrt{N})$  and expand to the leading order. BP then becomes

$$m_{i \rightarrow j}^t = \tanh \left( \beta h + \beta \sum_{k \neq j} J_{ki} m_{k \rightarrow i}^{t-1} \right). \quad (67)$$

In this dense-graph message passing there is not yet any surprise concerning time indices. The TAP equations are closed on full magnetizations (not cavity ones) defined as

$$m_i^t = \tanh \left( \beta h + \beta \sum_k J_{ki} m_{k \rightarrow i}^{t-1} \right). \quad (68)$$

In order to write the TAP equations we need to write messages in terms of the marginals up to all orders that contribute to the final equations. We get by Taylor expansion with respect to the second term

$$m_{i \rightarrow j}^t = \tanh \left( \beta h + \beta \sum_k J_{ki} m_{k \rightarrow i}^{t-1} - \beta J_{ij} m_{j \rightarrow i}^{t-1} \right) \approx m_i^t - \beta J_{ij} m_{j \rightarrow i}^{t-1} [1 - (m_i^t)^2], \quad (69)$$

which leads to the iterative TAP equations

$$m_i^t = \tanh \left\{ \beta h + \beta \sum_j J_{ij} m_j^{t-1} - \beta^2 m_i^{t-2} \sum_j J_{ij}^2 [1 - (m_j^{t-1})^2] \right\}. \quad (70)$$

Observe the time index  $(t-2)$  before the last sum, which is not intuitive on the first sight. These equations are the ones written and analyzed by Bolthausen [26].

In his proof Bolthausen's showed that the behavior of these iterative equations can be followed using what can be called the *state evolution* of the TAP algorithm, at least outside of the spin glass phase (the algorithm does *not*

converge inside the spin glass phase). It works as follows: we consider the interactions  $J_{ij}$  to have zero mean and variance  $\tilde{J}/N$ . Going back to eq. (68), the argument of the tanh is a sum of independent variables (by the assumptions of belief propagation) and thus follows a Gaussian distribution. Denoting  $m$  and  $q$  the mean and the variance of this distribution of messages, two self-consistent equations can be derived

$$m^t = \frac{1}{\sqrt{2\pi}} \int e^{-z^2/2} \tanh\left(\beta z \tilde{J} \sqrt{q^{t-1}} + \beta h\right) dz \quad (71)$$

$$q^t = \frac{1}{\sqrt{2\pi}} \int e^{-z^2/2} \tanh^2\left(\beta z \tilde{J} \sqrt{q^{t-1}} + \beta h\right) dz \quad (72)$$

The fixed point of these equations provides the well known replica symmetric solution for the magnetization and the spin overlap in the Sherrington-Kirkpatrick model, as was first derived in [215]. Since this is the correct solution outside the spin glass phase (above the so-called dAT line [57], it is reassuring to see that we have a convergent algorithm that will find the marginals fast in the densely connected case. We will return to this observation in section VB when we will discuss inference in densely connected models.

Note also that eqs. (71-72) correspond to a parallel update where all magnetizations are updated at the same time. Very often, it has been found that such update might be problematic for convergence and that one should update spins one at a time for better convergence properties. This, also, will be discussed in VB when discussing for the AMP algorithm [154]. In the case one chooses randomly at each time which spin should be updated, then one can still use eq. (70) with a careful book-keeping of the time-indices. The state evolution eqs. (72) become in that case differential equations in time. Instead of  $q^t + 1 = f(q^t)$  as in eqs. (72) we have now  $dq/dt = f(q^t) - q^t$  in the continuous time limit. We show an example of the behavior of these two approaches in Fig. 8. While in this case the parallel update was faster, we will see that sometimes the other one could be preferable because it is smoother and avoids e.g. the overshoot we see in the first iteration of the parallel update.

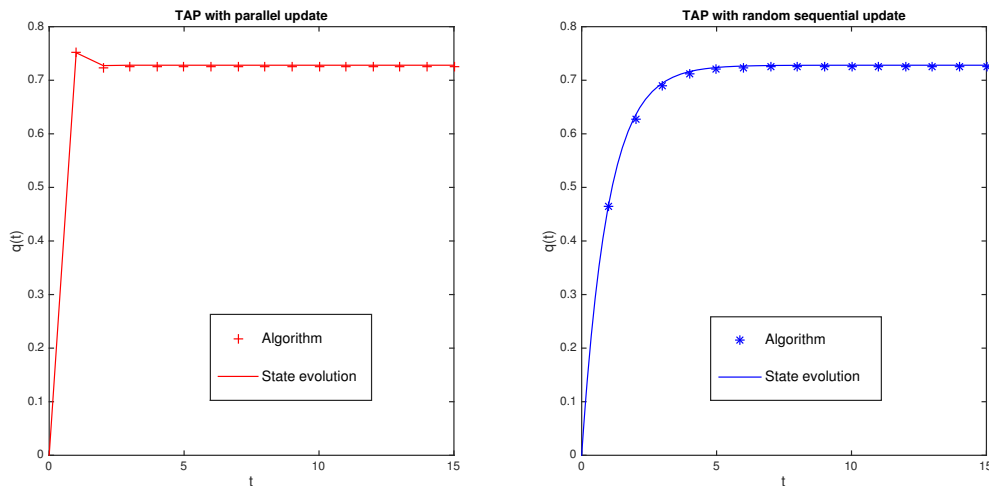


FIG. 8. State evolution versus actual simulation for the TAP equations in the Sherrington-Kirkpatrick with parallel update (left) and random sequential one (right), for a spin glass system with  $N = 5000$ ,  $1/\beta = T = 3$ ,  $\tilde{J} = 1$  and  $h = 4$ . The variance  $q$  of the distribution of messages is shown. In both cases, the state evolution equations (with the iterative form on the left and the differential one on the right) perfectly describes the evolution of the algorithm.



#### IV. CLUSTERING OF NETWORKS AND COMMUNITY DETECTION

Clustering is one of the most commonly studied problems in machine learning. The goal is to assign data points to  $q$  clusters in a way that the cluster is somehow representative of the properties of the points inside it. About 15 years ago a large number of scientists got interested in the research of the so-called complex networks, i.e. sets of nodes where some pairs are connected by edges, arising in a wide range of settings. A natural question followed: How to cluster networks, i.e. assign nodes of a graph in groups such that the largest possible part of the edges can be explain by a set of affinities between the clusters (instead of between the nodes themselves). Typically, one considers a number of clusters much smaller than the number of nodes. Part of the motivation for studying this question came from studies of social networks which resulted in the name for this problem: *community detection*.

##### A. Biased overview of community detection

The literature on community detection is vast and there is a number of reviews that make a great effort in putting the existing works in chronological and merits perspective, e.g. [77]. Here we give a perspective biased towards the approach of statistical physics of disordered systems.

The community detection is as follows: We are given a graph  $G(V, E)$  of  $N$  nodes and  $M$  edges. We search to assign the nodes into  $q$  groups, calling the assignment  $s_i \in \{1, \dots, q\}$ ,  $i = 1, \dots, N$ . In the most commonly considered assortative setting, the goal is that there are many edges between nodes in the same group and few edges among the groups. Traditionally, in statistics or machine learning, this problem would be solved by a spectral relaxation. One takes a matrix associated to the graph, its adjacency, Laplacian or others, and compute its largest (or smallest) eigenvalues and associated eigenvectors. The elements of these eigenvectors would then reveal in a *visible* way the community structure [64, 75], for more details see the nice review [227].

An influential set of works on community detection is due to Mark Newman and collaborators who introduced the so-called *modularity* function [51, 86, 182]

$$Q = \frac{1}{2M} \sum_{\langle i, j \rangle} \left( A_{ij} - \frac{d_i d_j}{2M} \right) \delta_{s_i, s_j}, \quad (73)$$

where the sum is over all distinct pairs of nodes,  $d_i$  is the degree of node  $i$ . Community detection is then done by finding an assignment of nodes that maximizes this modularity. Optimizing the modularity is a NP-hard problem. In practice, however, many efficient heuristic algorithms were suggested for this task, see e.g. the review [77].

The modularity-based community detection brings some nice connections to statistical mechanics and spin glasses. Reichardt and Bornholdt [199] pointed out that modularity maximization can be seen as a case of finding a ground state of a particular Potts spin glass. In order to assess the statistical significance of community structure found by maximizing the modularity, ref. [199] estimated the maximum value of modularity on a random graph, as the null model. Indeed, on sparse random graphs the maximum value of modularity can be very large even when no community structure whatsoever is present. To give an example, results on random graph partitioning [237] teach us that a random 3-regular graph can be divided into two groups of roughly equal size in such a way that only about 11% of edges is between the groups. This will visually look as a very good community structure with high modularity. Yet there were no communities in the process that created the random graph. The need to compare the value of modularity to a null model is not very satisfying. Ideally, one would like to have a method that would be able to tell that the underlying graph does not contain any communities if it did not.

Let us assume that we believe there were  $q$  communities taking respectively fraction  $n_a$  of nodes,  $a = 1, \dots, q$ ,  $\sum_a n_a = 1$ , with roughly  $c_{ab} n_a n_b N$  edges between groups  $a$  and  $b$ , and  $c_{aa} n_a^2 N/2$  edges inside group  $a$ ,  $c_{ab}$  is a system size independent  $q \times q$  matrix. The above very natural assumption is called the sparse *stochastic block model* (SBM) [107, 230], and is commonly considered in this setting. As Bayesian probability theory teaches us, the best possible way of inferring the hidden communities is to enumerate all assignments of nodes into communities that have roughly the above sizes and respective number of edges between groups. Subsequently one averages over all such assignments (factoring away the global permutational symmetry between groups). This way one ends up with probabilities for a given node to belong to a given group. For a truly random graph these probabilities will not be different from the fractions  $n_a$ .

From a computationally complexity point of view, enumerating exactly assignments as above is even harder than finding optimal values of a cost function such as the modularity. However, from a statistical physics point of view evaluating the above averages is equivalent to computation of local magnetizations in the corresponding Potts glass model. Notice, for instance, that the planted coloring [139] is simply a special case of the stochastic block model

( $c_{aa} = 0$ , and  $c_{ab} = c_{cd}$  for all  $a \neq b, c \neq d$ ). The corresponding asymptotically exact analysis of the stochastic block model has been done in [59, 60] as we shall summarize in the rest of this section.

### B. Asymptotically exact analysis of the SBM

We explained all the methodology needed for the asymptotic analysis of the SBM on the example planted spin glass in section II. In this section we consider again the teacher student scenario where the teacher generates the observed graph from the stochastic block model. We denote  $\theta = \{n_a, c_{ab}\}$  the set of parameters of the SBM. We remind that  $n_a$  is the fraction of nodes taken by group  $a$ ,  $a = 1, \dots, q$ , and  $c_{ab}/N$  is the probability a given node in group  $a$  connects to a given node in group  $b$ . Again we denote by  $\theta^*$  the actual values that the teacher used to generate the graph  $G$ . The graph is represented by its adjacency matrix  $A_{ij}$ , with  $N$  nodes and  $M$  edges. Further  $s_i \in \{1, \dots, q\}$  are the Potts spins denoting assignment into groups.

The posterior likelihood of the SBM reads

$$P(\mathbf{s}|\mathbf{G}, \theta) = \frac{1}{Z(\mathbf{G}, \theta)} \prod_{i=1}^N \mathbf{n}_{s_i} \prod_{\langle i,j \rangle} (\mathbf{c}_{s_i s_j})^{\mathbf{A}_{ij}} \left( \mathbf{1} - \frac{\mathbf{c}_{s_i s_j}}{N} \right)^{1-\mathbf{A}_{ij}} \quad (74)$$

where the second product is over all distinct pairs, and we included a constant  $N^{-M}$  into the partition function. We need to evaluate the maximum-mean-overlap (MMO) estimator (15) in order to find a configuration that maximizes the number of nodes that are assigned into the same group as the planted configuration. In a physics language we would rather think of the corresponding Potts model Hamiltonian

$$\mathcal{H}(G, \theta, \mathbf{s}) = \sum_{i=1}^N \log \mathbf{n}_{s_i} + \sum_{\langle i,j \rangle} \left[ \mathbf{A}_{ij} \log \mathbf{c}_{s_i s_j} + (\mathbf{1} - \mathbf{A}_{ij}) \log \left( \mathbf{1} - \frac{\mathbf{c}_{s_i s_j}}{N} \right) \right] \quad (75)$$

and the MMO estimator turns out to be computed from the local magnetizations of this Potts model.

When the parameters  $\theta^*$  are not known, we need to learn them according to the lines of section II A 4. We write the posterior distribution on the parameters  $P(\theta|G)$  and notice that it is concentrated around the maximum of the partition function  $Z(G, \theta)$ . We then iteratively maximize this partition function by imposing the Nishimori conditions

$$n_a = \frac{1}{N} \sum_{i=1}^N \mathbb{E}(\delta_{s_i, a}), \quad (76)$$

$$c_{ab} = \frac{1}{N n_a n_b} \sum_{(ij) \in E} \mathbb{E}(\delta_{a, s_i} \delta_{b, s_j}) \quad \text{when } a \neq b, \quad (77)$$

$$c_{aa} = \frac{2}{N n_a^2} \sum_{(ij) \in E} \mathbb{E}(\delta_{a, s_i} \delta_{a, s_j}). \quad (78)$$

This learning algorithm was called expectation maximization learning in [59]. The expectations were computed using belief propagation or Gibbs sampling as will be discussed subsequently. But even if the expectations were computed exactly this parameter learning algorithms depends strongly on the initial choice for the parameters  $\theta$ . It gets easily blocked in a local maxima of the partition function. The size of the space of initial conditions that need to be explored to find the global maximum is independent of  $N$ , but in practice this is a problem and completely general models  $c_{ab}$  are not so easy to learn. A considerable improvement can be obtained when the learning is initialized based on the result of spectral clustering. This procedure was suggested in [242] and works nicely, in particular in conjunction with the best known spectral clustering techniques [137] as will be discussed in sec. IV D

Two algorithms that are (in the Bayes-optimal setting) asymptotically exact for computing the marginals and the expectations in (76-78) were proposed in [59, 60]. One is the Gibbs sampling or Markov chain Monte Carlo, another is belief propagation (BP). We explicit here the belief propagation, because it can also be used very directly to understand behavior of the system and phase transitions in the thermodynamic limit. Note that the BP algorithm for the SBM was written by [100] but in that work the parameters were fixed ad-hoc, not in the Bayes optimal way nor by learning. Moreover, the algorithm was tested on a network of only 128 nodes, which is too small to observe any phase transitions.

Belief propagation for posterior distribution (74) is written in terms of the so-called messages  $\psi_{s_i}^{i \rightarrow j}$  that are defined as probabilities that node  $i$  is assigned to group  $s_i$  conditioned on the absence of edge  $(ij)$ . Assuming asymptotic

conditional independence of the probabilities  $\psi_{s_k}^{k \rightarrow i}$  for  $k \neq j, i$ , the iterative equations read

$$\psi_{s_i}^{i \rightarrow j} = \frac{1}{Z^{i \rightarrow j}} n_{s_i} \prod_{k \neq i, j} \left[ \sum_{s_k} c_{s_i s_k}^{A_{ik}} \left(1 - \frac{c_{s_i s_k}}{N}\right)^{1 - A_{ik}} \psi_{s_k}^{k \rightarrow i} \right], \quad (79)$$

where  $Z^{i \rightarrow j}$  is a normalization constant ensuring that  $\sum_{s=1}^q \psi_s^{i \rightarrow j} = 1$ . We further notice that because of the factor  $1/N$ , messages on non-edges  $(ij) \notin E$  depend only weakly on the target node and hence in the leading order the BP equations simplify into

$$\psi_{s_i}^{i \rightarrow j} = \frac{1}{Z^{i \rightarrow j}} n_{s_i} e^{-h_{s_i}} \prod_{k \in \partial i \setminus j} \left[ \sum_{s_k} c_{s_k s_i} \psi_{s_k}^{k \rightarrow i} \right], \quad (80)$$

where we denote by  $\partial i$  the set of neighbors of  $i$ , and define an auxiliary external field as

$$h_{s_i} = \frac{1}{N} \sum_{k=1}^N \sum_{s_k} c_{s_k s_i} \psi_{s_k}^k, \quad (81)$$

where  $\psi_{s_i}^i$  is the BP estimate of the marginal probability of node  $i$

$$\psi_{s_i}^i = \frac{1}{Z^i} n_{s_i} e^{-h_{s_i}} \prod_{j \in \partial i} \left[ \sum_{s_j} c_{s_j s_i} \psi_{s_j}^{j \rightarrow i} \right], \quad (82)$$

with  $Z^i$  being again a normalization. In order to find a fixed point of Eq. (80) we update the messages  $\psi^{i \rightarrow j}$ , recompute  $\psi^j$ , update the field  $h_{s_i}$  by adding the new contribution, subtracting the old one, and repeat.

Once a fixed point of the BP equations is reached, its associated free energy (log-likelihood)  $f_{\text{BP}} = -\log Z(G, \theta)/N$  reads

$$f_{\text{BP}}(G, \theta) = -\frac{1}{N} \sum_i \log Z^i + \frac{1}{N} \sum_{(i,j) \in E} \log Z^{ij} - \frac{c}{2}, \quad (83)$$

where

$$Z^{ij} = \sum_{a < b} c_{ab} (\psi_a^{i \rightarrow j} \psi_b^{j \rightarrow i} + \psi_b^{i \rightarrow j} \psi_a^{j \rightarrow i}) + \sum_a c_{aa} \psi_a^{i \rightarrow j} \psi_a^{j \rightarrow i} \quad \text{for } (i, j) \in E \quad (84)$$

$$Z^i = \sum_{s_i} n_{s_i} e^{-h_{s_i}} \prod_{j \in \partial i} \sum_{s_j} c_{s_j s_i} \psi_{s_j}^{j \rightarrow i}. \quad (85)$$

In [59, 60] it is argued that the above equations can be used to analyze the asymptotic performance of the Bayes optimal inference in SBM,  $\theta = \theta^*$ . The analysis goes as follows: Let us iterate BP (80) from two different initializations

- Random initialization, for each  $(ij) \in E$  we chose  $\psi_s^{i \rightarrow j} = n_a + \epsilon_s^{i \rightarrow j}$  where  $\epsilon_s^{i \rightarrow j}$  is a small zero-sum perturbation,  $\sum_s \epsilon_s^{i \rightarrow j} = 0$ .
- Planted initialization, each message is initialized as  $\psi_s^{i \rightarrow j} = \delta_{s, s_i^*}$ , where  $s_i^*$  is the actual assignment of node to groups (that is known only for the purpose of analysis).

The free energy (83) is computed for the two corresponding fixed points. The fixed point with smaller free energy (larger likelihood) corresponds asymptotically to the performance of the Bayes-optimal inference. The asymptotic here is in the sense that the difference between the Bayes-optimal and the BP marginals goes to zero as  $N \rightarrow \infty$ . This is an important and nontrivial property, because in general analysis of Bayes optimal inference in such a high-dimensional setting is very difficult (sharp-P hard). Note that the asymptotic exactness of BP is so far only a conjecture. Rigorous results showing the asymptotic exactness of BP are so far only partial, either at relatively high average degrees [179], or in related problems for very low average degrees [171], or e.g. in ferromagnets [61].

Another property of belief propagation that makes it very convenient for the analysis of phase transitions and asymptotic properties is the fact that BP, in a sense, ignores some part of the finite size effects. Let us compare to Markov chain Monte Carlo. Consider a set of parameters where the two initializations of BP do not give the same fixed point. Even if we iterate BP for infinite time we will have two different fixed points. On the other hand in

Monte Carlo Gibbs sampling for a system of size  $N$  we will eventually always find the lower free energy state. The time needed is in general exponentially large in  $N$ , but decreases as the free energy barrier gets smaller and therefore locating the spinodal threshold precisely from finite system size simulations can be involved. Another manifestation of this property is that in the paramagnetic phase on a graph with  $N$  nodes and  $M$  edges the free energy given by BP is always the same number. Whereas the exact (finite  $N$ ) free energy typically has some fluctuations.

In SBM belief propagation provides asymptotically an exact analysis of the Bayes-optimal inference. In the case where the model or its parameters  $\theta$  are mismatching the ones that generated the graph, this is not true in general. The most striking example here is the MAP estimator, in other words the ground state of the corresponding Potts model. Modularity maximization is a special case of this setting. The ground state could also be estimated by BP if we introduce a temperature-like parameter  $1/\beta$  in the posterior and tune this temperature to zero. Related algorithm was discussed recently in the context of modularity-based community detection in [243]. However, as we decrease this temperature we will typically encounter a point  $\beta_{\text{SG}} > 1$  above which the replica symmetric approximation fails and the corresponding belief propagation marginals are not any longer asymptotically exact. When this phase transition at  $\beta_{\text{SG}}$  is continuous this will manifest itself as non-convergence of the BP algorithm. Note that depending on the set of parameters this spin glass phase can be correlated to the original assignment (mixed phase) or not (pure spin glass phase). This behavior is qualitatively the same as the one seen in the phase diagram presented in Fig. 2. In the above sense it is hence easier to compute the marginals at the Bayes-optimal value of the parameters (that may need to be learned as described above) than to compute the ground state (or maximize the modularity) that is typically glassy.

### C. Examples of phase transitions in the SBM

The asymptotic analysis of the stochastic block model as described above leads to the discovery of phase transitions. The most striking picture arises in the case when the parameters of the model are such that the average degree is the same in every group. In a sense this is the hardest case for inference, because if groups differ in their average degree then a simple histogram on degrees gives some information about the correct assignment into groups.

Mathematically, the same average degree condition is expressed as

$$\sum_b c_{ab} n_b = c \quad \forall b = 1, \dots, q, \quad (86)$$

where  $c$  is the average degree. It is straightforward to see that when (86) holds then the following

$$\psi_s^{i \rightarrow j} = n_s \quad (87)$$

is always a (so-called *uniform*) fixed point (in general not the only one) of the belief propagation (80).

Let us now return to the concept of quiet planting explained for the planted spin glass in sec. II B 3 and note that all we needed for quiet planting to work was precisely the existence of such a uniform fixed point. It is hence straightforward that the phase transitions described in sections II A 3 and II C 3 exist also in Bayes-optimal inference in the stochastic block model. Let us give the example of assortative community structure with  $q = 4$  equally sized groups,  $n_a = 1/q$  for all  $a = 1, \dots, q$ , average degree  $c = 16$ , and affinity parameters such that  $c_{aa} = c_{\text{in}}$  and  $c_{ab} = c_{\text{out}}$  for all  $a \neq b$ . We define a noise-like parameter  $\epsilon = c_{\text{out}}/c_{\text{in}}$ . When  $\epsilon = 0$  the model generates four entirely disconnected groups, and when  $\epsilon = 1$  the generation process corresponds to an Erdős-Rényi graph with no information on the community structure. Without having any experience with phase transition and quiet planting one might anticipate that whenever  $\epsilon < 1$  the Bayes optimal inference will give a better overlap than a random assignment of nodes into groups. This expectation is wrong and the phase transition that happens instead is illustrated in Fig. 9.

For other values of parameters we can observe the triplet of discontinuous phase transition discussed in sec. II C 3. Actually, the planted coloring example, that was presented in Fig. 4, is a case of the stochastic block model with  $q = 5$  equally sized groups and extremely dis-assortative structure  $c_{\text{in}} = 0$ .

For general case of the sparse SBM the order of the phase transition, and the locations of the dynamical  $c_d$  and detectability  $c_c$  phase transitions, have to be analyzed case by case mostly numerically. However, the spinodal transition has a neat analytical expression in the case of the same average degree in every group (86). This expression is obtained as in sec. II C 1 by analyzing the local stability of the uniform fixed point. Belief propagation (80) linearized around this fixed point reads

$$\epsilon_a^{i \rightarrow j} = \sum_{b=1}^q \sum_{k \in \partial i \setminus j} T_{ab} \epsilon_b^{k \rightarrow i}, \quad (88)$$

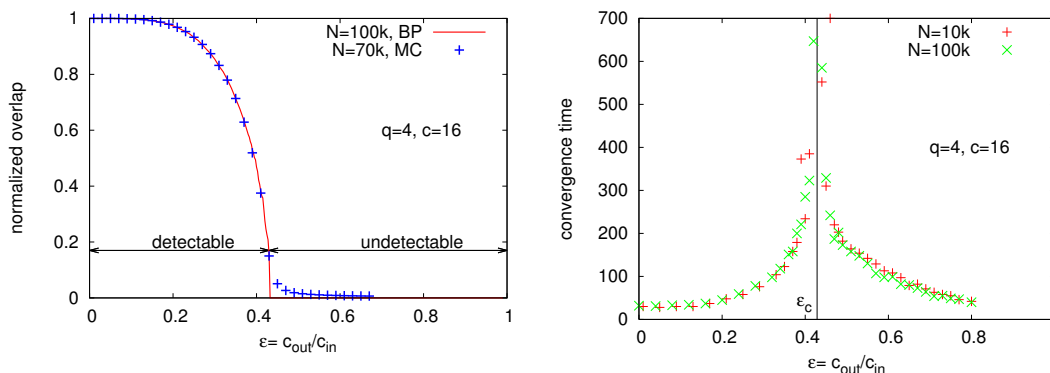


FIG. 9. Left: Normalized overlap between the MMO estimator and the original assignment to groups. We compare the BP result to Monte Carlo Gibbs sampling. Both agree well, but we see the absence of finite size corrections in BP in the undetectable phase. Right: The BP convergence time, illustrating the critical slowing down around the phase transition. Figures are both taken from [59].

where the  $q \times q$  matrix  $T_{ab}$  is defined as

$$T^{ab} = n_a \left( \frac{c_{ab}}{c} - 1 \right). \quad (89)$$

The phase transition where the paramagnetic fixed point ceases to be locally stable happens when

$$c\lambda_T^2 = 1, \quad (90)$$

where  $\lambda_T$  is the largest eigenvalue of the matrix  $T$ . In case of equally sized groups in the *assortative-diagonal* case where  $c_{aa} = c_{\text{in}}$  and  $c_{ab} = c_{\text{out}}$  for  $a \neq b$ , we obtain the now well known expression for the spinodal phase transition

$$|c_{\text{in}} - c_{\text{out}}| = q\sqrt{c}. \quad (91)$$

When the difference between  $c_{\text{in}}$  and  $c_{\text{out}}$  is larger BP detects communities and gives asymptotically the Bayes-optimal overlap. When the difference is smaller BP fails. Depending on the parameters and the order of the phase transition the detectability phase transition itself can either agree with (90) or happen at strictly smaller  $|c_{\text{in}} - c_{\text{out}}|$  giving rise to the hard phase discussed in sec. III B.

For the planted graph coloring (i.e. the extremely dis-assortative SBM,  $c_{\text{in}}=0$ ) the detectability phase transition is of second order for  $q \leq 3$  and of first order for  $q \geq 4$ . The spinodal transition happens at  $c_s = (q-1)^2$ . In the large  $q$  limit the dynamical and detectability phase transitions can be deduced from [235] while keeping in mind the concept of quiet planting

$$c_d = q(\log q + \log \log q) + O(1), \quad (92)$$

$$c_c = 2q \log q - \log q - 2 \log 2 + o(1). \quad (93)$$

For the assortative case  $c_{\text{in}} > c_{\text{out}}$  the phase transition is of second order for  $q \leq 4$  and of first order (although a very weak one for small  $q$ ) for  $q \geq 5$ . The limit of dense graphs (average probability for an edge to exist is  $p$ ,  $p_{\text{in/out}}$  are probabilities of connection within/between groups), and large number of groups  $q \rightarrow \infty$  was analyzed in [150] and is related to critical temperatures in the dense Potts glass [36, 91]. The regime in which both the dynamical and detectability appear is

$$N(p_{\text{in}} - p_{\text{out}})^2 = \gamma(q)p(1-p) \quad (94)$$

with the dynamical transitions at  $\gamma_d(q) = 2q \log q[1 + o(1)]$ , the detectability at  $\gamma_c(q) = 4q \log q[1 + o(1)]$ , and the spinodal threshold at  $\gamma_s(q) = q^2$ . In this limit we see that the hard phase between  $\gamma_s(q)$  and  $\gamma_c(q)$  is very wide (compared to the overall scale).

The prediction and location of these phase transition in the stochastic block model from [59, 60] was followed by a remarkable mathematical development where the location of the threshold was made rigorous for  $q = 2$  [158, 177, 178]. The detectable side was proven for generic  $q$  in [27].

To briefly comment on the case where the average degree of every group is not the same. The belief propagation is still conjectured to be asymptotically exact, but what concerns the phase transitions they get smeared. As recently studied in [244], the second order phase transitions disappear, and the first order phase transitions shrink into a multi-critical point beyond which they also disappear. The situation is similar as for the semi-supervised clustering, where the assignment of a fraction of nodes is known [245]. From a physics point of view it is relevant to note that this problem is an inference interpretation of the particle pinning that was recently used quite extensively for studies of structural glasses [39].

#### D. Spectral redemption in clustering sparse networks

A reader that did not skip section III A is now clearly anticipating the use of the non-backtracking matrix for spectral clustering of networks. Indeed in [137] the following spectral clustering method was proposed

- Construct the non-backtracking matrix

$$B_{i \rightarrow j, k \rightarrow l} = \delta_{il}(1 - \delta_{jk}). \quad (95)$$

and compute its largest (in module) eigenvalues until they start to have a non-zero complex part. Denote  $k$  the number of those large real eigenvalues.

- Consider the  $k$  corresponding  $2M$ -dimensional eigenvectors  $u_{i \rightarrow j}$  and create a set of  $N$ -dimensional vectors by resuming  $u_i = \sum_{k \in \partial i} u_{k \rightarrow i}$ . Then view the  $k$  vectors  $u_i$  as  $N$  points in  $k$  dimensional space and cluster those points into  $k$  groups using some off-the-shell clustering algorithm such as  $k$ -means.

Note in particular that  $k$  here is the estimator for the number of groups. Up to this point we were assuming that the number of groups was known. The performance of this non-backtracking based spectral algorithms compared to BP and other spectral algorithms on clustering of sparse graphs is illustrated in Fig. 10.

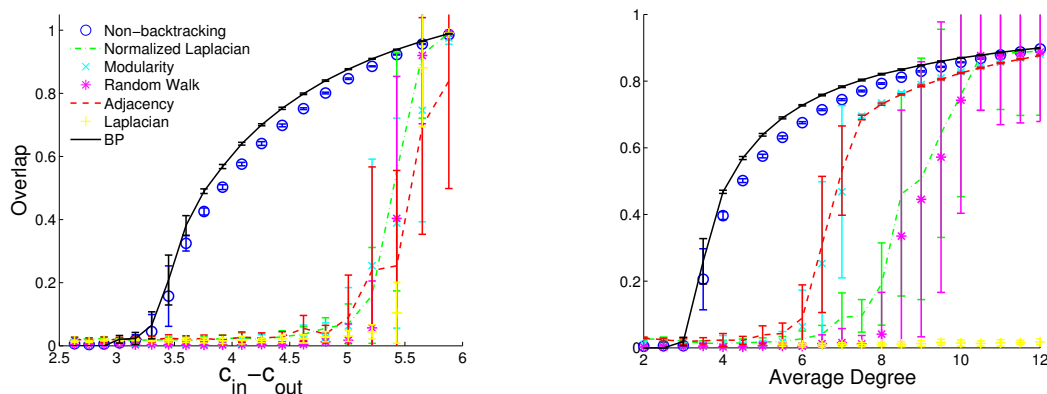


FIG. 10. The accuracy of spectral algorithms based on different linear operators, and of belief propagation, for two groups of equal size. On the left, we vary  $c_{\text{in}} - c_{\text{out}}$  while fixing the average degree  $c = 3$ ; the detectability transition given by occurs at  $c_{\text{in}} - c_{\text{out}} = 2\sqrt{3} \approx 3.46$ . On the right, we set  $c_{\text{out}}/c_{\text{in}} = 0.3$  and vary  $c$ ; the detectability transition is at  $c \approx 3.45$ . Each point is averaged over 20 instances with  $N = 10^5$ . The spectral algorithm based on the non-backtracking matrix  $B$  achieves an accuracy close to that of BP, and both remain large all the way down to the transition. Standard spectral algorithms based on the adjacency matrix, modularity matrix, Laplacian, normalized Laplacian, and the random walk matrix all fail well above the transition, giving a regime where they do no better than chance. Figure is taken from [137].

Ref. [137] analyzed the performance of the above algorithm on networks generated from the stochastic block model with equal average degree in every group. Large part of results that were not rigorous in [137] were very remarkably made rigorous in [27].

On a random graph taken from the configurational model, i.e. at random with a given degree distribution  $P(d)$ , in the limit of large size, the spectrum of the non-backtracking matrix is (except one eigenvalue) included inside a circle of radius  $\sqrt{\tilde{c}}$ . Here  $\tilde{c}$  is the average excess degree of the graph computed as

$$\tilde{c} = \frac{\sum_d d^2 P(d)}{\sum_d d P(d)} - 1. \quad (96)$$

The one eigenvalue that is not inside this circle is real and has value  $\tilde{c}$ . This random graph spectrum should be contrasted with the spectrum on the adjacency matrix (and other related ones) which for graphs with constant average and unbounded maximum degree is not even bounded in the thermodynamic limit.

Now, consider a graph generated by the SBM with average degree of every group the same. Denote  $\lambda_T$  an eigenvalue of the matrix  $T$ , eq. (89), then as long as  $\lambda_T > 1/\sqrt{\tilde{c}}$  the non-backtracking matrix will have a purely real eigenvalue at position  $c\lambda_T$ . This way we obtain up to  $q - 1$  additional eigenvalues on the real axes out of the circle of radius  $\sqrt{\tilde{c}}$ . Note that in the *assortative-diagonal* case the matrix  $T$  has  $q - 1$  degenerate eigenvalues  $\lambda_T = (c_{\text{in}} - c_{\text{out}})/(qc)$ , and therefore the non-backtracking matrix has a  $(q - 1)$ -times degenerate eigenvalue at  $(c_{\text{in}} - c_{\text{out}})/q$  which merges in the bulk below the spinodal phase transition. The spectrum on the non-backtracking operator is illustrated in Fig. 11.

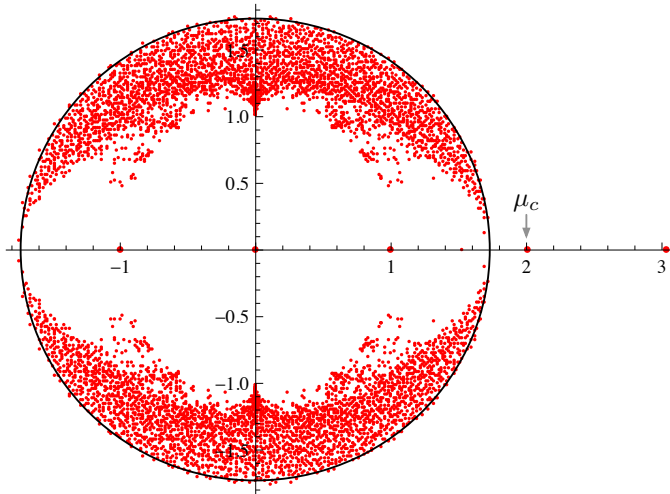


FIG. 11. The spectrum of the non-backtracking matrix  $B$  for a network generated by the block model with  $N = 4000$ ,  $c_{\text{in}} = 5$ , and  $c_{\text{out}} = 1$ . The leading eigenvalue is at  $c = 3$ , the second eigenvalue is close to  $\mu_c = (c_{\text{in}} - c_{\text{out}})/2 = 2$ , and the bulk of the spectrum is confined to the disk of radius  $\sqrt{\tilde{c}} = \sqrt{3}$ . The spectral algorithm that labels vertices according to the sign of  $B$ 's second eigenvector (summed over the incoming edges at each vertex) labels the majority of vertices correctly. Figure is taken from [137].

To compare properties of belief propagation and the non-backtracking (NB) based spectral clustering. The positive point for BP is that it gives slightly better overlap. Positive points for NB-spectral clustering is that it does not need to get any information about the model parameters nor about the number of groups. It works in time linear in the number of groups, as opposed to quadratic for BP. It should not be bothered by the presence of small loops which usually causes the failure of the Bethe approximation.

The only uncomfortable property of the non-backtracking matrix is that it can be rather large. This is actually not a problem at all because the spectrum (different from  $\pm 1$ ) of  $B$  can be computed from the spectrum of the following  $2N \times 2N$  matrix  $B'$  [137]

$$B' = \begin{pmatrix} 0 & D - \mathbf{1} \\ -\mathbf{1} & A \end{pmatrix}, \quad (97)$$

where  $A$  is the adjacency matrix and  $D$  is the diagonal matrix with  $D_{ii} = d_i$  being the degree of node  $i$ .

The matrix  $B'$  is smaller but still non-symmetric. The power method for computing largest eigenvalues works much better for symmetric matrices. In [207] it was suggested to use the so-called Bethe Hessian matrix defined as

$$\text{BH}(r) = (r^2 - 1)\mathbf{1} - rA + D, \quad (98)$$

with  $r = \sqrt{\tilde{c}}$  (or more general the squared root of the leading eigenvalue of (97) which is usually not problematic to compute) as a basis for spectral clustering. In particular, to take eigenvectors of all of its negative eigenvalues. Ref. [207] showed that this has all the advantages of the non-backtracking matrix while being  $N \times N$  and symmetric. The name Bethe Hessian is motivated by the relation between the Hessian of the Bethe free energy and this matrix [172, 200], which is particularly apparent when generalized to the weighted case.

### E. More on the non-backtracking operator

The non-backtracking operator as defined above is relatively well known in mathematics, often called the Hashimoto directed edges adjacency matrix [97]. It is used in a number of works as a tool in proofs, see e.g. [7, 17, 81, 121, 190, 217]. However to use it as a basis for a spectral algorithm it was first suggested in [137]. The idea of using the linearized BP was inspired by the earlier work of [54]. Since then a considerable number of papers on promising algorithmic applications of the non-backtracking matrix on sparse networks started appearing, see e.g. [157, 175, 240]. Here we briefly discuss selected contributions to this direction.

Looking at Fig. 11 we observe a very interesting structure in the bulk spectral density of the non-backtracking operator. Motivated by this, ref. [208] applied the cavity method designed to compute spectral density of non-Hermitian random matrices [203] to study the non-backtracking spectral density. A phase transition in the spectral density was observed to happen on the boundary of the circle of radius  $\sqrt{\tilde{c}}$ . Such a phase transition is absent in the spectral density of traditional matrices such as the adjacency, Laplacian, random walk etc. This is no proof since we are only concerned with spectral density not with sub-dominantly numerous eigenvalues, but from a physics point of view a phase transition is a strong indication that the properties of the non-backtracking matrix on a random graph are fundamentally different from the traditional matrices. Ref. [208] also observed that the eigenvalues that are close to the center of the circle are not visible in the asymptotic calculation of the spectral density. Numerical investigations revealed that eigenvectors corresponding to these eigenvalues are localized. More detailed understanding of this localization and its physical consequences is an interesting direction of future work.

In [9] the non-backtracking spectral clustering method was generalized to clustering of sparse hypergraphs. These are graphs where instead of connected pair of nodes, one connects  $k$ -uples of nodes. Interestingly, using the non-backtracking based spectral method detection can be done also e.g. in plated constraint satisfaction problems without even knowing the form of the corresponding constraints. Moreover, for the same reasons as in clustering, the method works down to previously computed spinodal thresholds [239]. It was also observed that the overlap (performance) of the spectral method is always a continuous function of the noise parameter, even if the Bayes optimal belief propagation has a strongly discontinuous transition. This further supports our previous suggestion that the spectral methods are extremely useful to point towards the right direction, but message passing based methods should then be used to improve the precision. Note that the hypergraph clustering can also be formulated as tensor factorization that became recently popular in connection with interdependent networks or networks with different kinds of edges that are referred to as multiplexes in the literature on complex networks.

Another exciting application of the non-backtracking matrix or the Bethe Hessian is the matrix completion problem [209]. In matrix completion one aims to estimate a low-rank matrix from a small random sample of its entries. This problem became popular in connection to collaborative filtering and related recommendation systems. Of course, the fewer entries are observed the harder the problem is. Ref. [209] shows that with the use of the non-backtracking matrix the number of entries from which the low rank structure is detectable is smaller than with other known algorithms. The way the matrix completion problem is approached is by realizing that a Hopfield model with Hebb learning rule can be viewed as a rank  $r$  structure that is able to recover the  $r$  patterns as distinct thermodynamic phases [108]. We hence view the observed entries of the low-rank matrix to complete as a sparse Hopfield model and estimate the patterns from the leading eigenvectors of the corresponding Bethe Hessian. In a second stage we use this as a initialization for more standard matrix completion algorithms in the spirit of [124], and achieve overall better performance.

Another problem where the leading eigenvalue of the non-backtracking matrix is relevant is percolation on networks [123]. In percolation we start with a graph  $G$  and remove each of its edges with probability  $1 - p$ . Then we look at the largest component of the remaining graph and ask if it covers an extensive fraction of all nodes. The value of  $p_c$  below which the giant component does not exist anymore with high probability is called the percolation threshold. The percolation thresholds were computed for many geometries including random graphs. A remarkable result concerns any sequence of dense graphs for which it was proven that the threshold is given by the inverse of the leading eigenvalue of the adjacency matrix [25]. This result does not extend to sparse graphs, where a counter-example is given by random regular graphs where the leading eigenvalue is the degree whereas the percolation threshold is inverse of the degree minus one. Based on a message passing algorithm for percolation [123] argue that on a class of sparse locally tree-like graphs the percolation threshold is given by the inverse of the leading eigenvalue of the non-backtracking matrix. Specifying for what exact class of graphs this result holds is still an open problem. Ref. [123] also proved that the non-backtracking matrix provides a lower bound on the percolation threshold for a generic graph (with the exception of trees). An analogous result was obtained independently by [96]. Due to these results, the non-backtracking matrix was used to study percolation on real networks [175, 192, 202].



## F. Deceptiveness of the variational Bayes method

Both in physics and computer science a very common and popular method for approximate bayesian inference is the naive mean field method, often called variational Bayesian inference [20, 188]. For clustering of sparse networks generated by the stochastic block model this method was studied e.g. in [45, 106]. Away from the detectability threshold the variational Bayes method gives very sensible results. On the one hand, deep in the undetectable phase (very small  $|c_{\text{in}} - c_{\text{out}}|$ ) the predicted magnetizations are close to zero, reflecting the undetectability. On the other hand, deep in the detectable phase the variational Bayesian method is able to estimate the correct group assignment, and is statistically consistent as proven in [45]. The performance of variational Bayes in the neighborhood of the detectability transition was studied in [242]. The conclusions of the comparison to belief propagation are quite interesting. It is not surprising that BP is more precise and converges faster on sparse graphs. What was surprising is that the naive mean-field inference fails in a very deceptive way - the marginals it predicts are very biased towards a configuration that is not correlated with the planted (ground truth) configuration. Ref. [242] quantified this by introducing the so-called illusive overlap and compared it to the actual one. This means that it is extremely dangerous to use naive mean-field for testing statistical significance of the results it provides and this could have profound consequences beyond the problem of clustering networks. Especially when trying to use the variational Bayes method in the vicinity of the corresponding detectable threshold, i.e. in regimes where number of samples is barely sufficient for estimation. Monte Carlo Markov chain method do not have this problem, but are in general slower.

## G. Real networks are not generated by the SBM

Our study of clustering of networks is asymptotically exact for the case when the networks were generated by the stochastic block model. In view of actual data sets and realistic applications this is never the case.

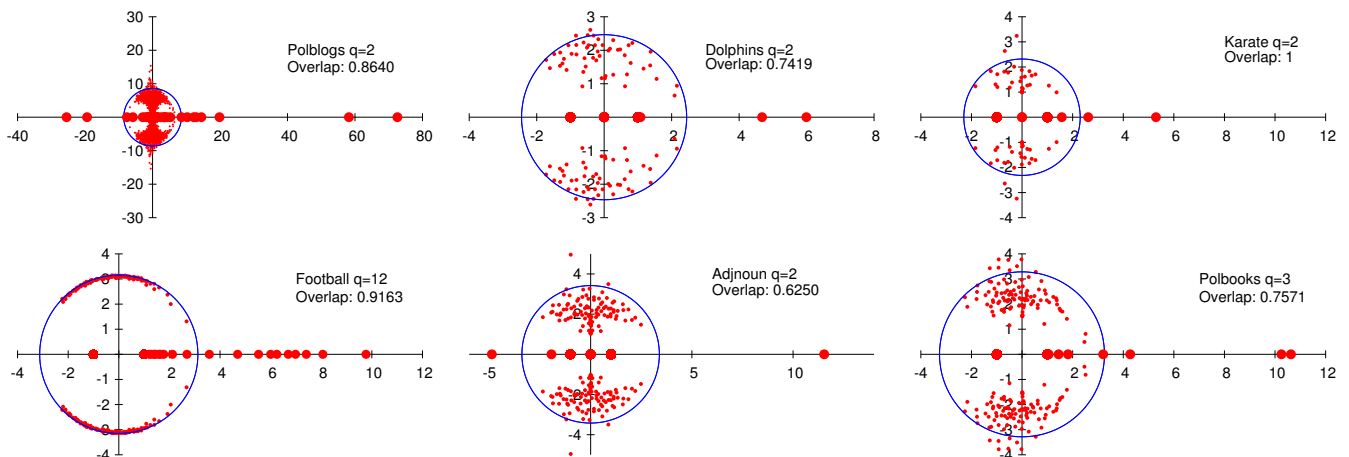


FIG. 12. Spectrum of the non-backtracking matrix in the complex plane for some real networks commonly used as benchmarks for community detection, taken from [6, 86, 130, 151, 181, 234]. The radius of the circle is the square root of the largest eigenvalue, which is a heuristic estimate of the bulk of the spectrum. The overlap is computed using the signs of the second eigenvector for the networks with two communities, and using  $k$ -means for those with three and more communities. The non-backtracking operator detects communities in all these networks, with an overlap comparable to the performance of other spectral methods. As in the case of synthetic networks generated by the stochastic block model, the number of real eigenvalues outside the bulk appears to be a good indicator of the number  $q$  of communities. Figure taken from [137].

One important discrepancy between the stochastic block model and real networks is that the later often have communities with a broad degree distribution whereas degree distribution of every group generated by the SBM is Poissonian. A variant of the stochastic block model that takes the degree distribution into account is the so-called degree corrected stochastic block model [122]. An asymptotically exact belief propagation can be also easily written for this model, see [232]. Ref. [232] have also shown that the corresponding Bethe free energy is a great tool for model selection between the canonical and degree corrected stochastic block models, and that classical model selection criteria do not apply to this problem because of the limited information per degree of freedom. Interestingly the BP for degree-corrected SBM also leads to the same non-backtracking matrix upon linearization.

There are of course many more discrepancies between real networks and those generated by the (degree corrected) SBM. However, when observing the spectrum of the non-backtracking operator on some of the commonly used benchmarks for community detection, we conclude that its properties we derived for the SBM basically stay conserved also in these examples, see Fig. 12. To conclude, let us quote the British mathematician and Bayesian statistician George E. P. Box (1919-2013): "Essentially, all models are wrong, but some are useful".

## V. LINEAR ESTIMATION AND COMPRESSED SENSING

The inference problem addressed in this section is the following. We observe a  $M$  dimensional vector  $y_\mu$ ,  $\mu = 1, \dots, M$  that was created depending component-wise on a linear projection of an unknown  $N$  dimensional vector  $x_i$ ,  $i = 1, \dots, N$  by a known matrix  $F_{\mu i}$

$$y_\mu = f_{\text{out}} \left( \sum_{i=1}^N F_{\mu i} x_i \right), \quad (99)$$

where  $f_{\text{out}}$  is an output function that might include noise. Examples are the additive white Gaussian noise (AWGN) output given by  $f_{\text{out}}(x) = x + w$  with  $w$  being random Gaussian variables, or linear threshold output where  $f_{\text{out}}(x) = \text{sign}(x + \kappa)$ , with  $\kappa$  being a threshold value.

The goal in linear estimation is to infer  $\mathbf{x}$  from the knowledge of  $\mathbf{y}$ ,  $F$  and  $f_{\text{out}}$ . An alternative way of representing the output function  $f_{\text{out}}$  is to denote  $z_\mu = \sum_{i=1}^N F_{\mu i} x_i$  and talk about likelihood of observing a given vector  $\mathbf{y}$  given  $\mathbf{z}$

$$P(\mathbf{y}|\mathbf{z}) = \prod_{\mu=1}^M P_{\text{out}}(y_\mu|z_\mu). \quad (100)$$

To give in perspective the immense number of important applications the above setting, let us give an illustrative example of medical diagnostics. Consider we have data about  $M$  cancer-patients that took a given treatment. The  $y_\mu$  is a variable saying up to what level the treatment was effective for a patient  $\mu$ . Our goal is to predict the outcome of the treatment for a new patient that did not take it yet. To do that we collect medical and personal data about each of the  $M$  patients, their medical history, family situation, but also for instance Facebook feeds, where did they work, what sport they did in their life, what education they have, how they rate their relationship with their wife, and all kinds of other information that on first sight is totally unrelated to the eventual outcome of the treatment. This information is collected in the vector  $\vec{F}_\mu$ . We aim to find a set of coefficients  $x_i$  such that the observations  $y_\mu$  can be well explained by  $z_\mu = \sum_{i=1}^N F_{\mu i} x_i$  for some  $P_{\text{out}}(y_\mu|z_\mu)$ .

In the way we set the problem it is reasonable to think that most patient-attributes will have no effect on the outcome of the treatment, i.e. for many  $i$  the  $x_i$  will be close to zero. In a method, called LASSO (stands for *least absolute shrinkage and selection operator*) [223], that is used everyday for similar type of problems (in banking or insurance industry for instance) the coefficients  $x_i$  are such that

$$\text{LASSO : } \min_{\mathbf{x}} \left[ \sum_{\mu=1}^M \left( y_\mu - \sum_{i=1}^N F_{\mu i} x_i \right)^2 + \lambda \sum_{i=1}^N |x_i| \right], \quad (101)$$

where  $\lambda$  is a regularization parameter that controls the trade-off between a good fit and sparsity of the vector  $\mathbf{x}$ . The advantage of LASSO is that it is a convex problem that can be solved efficiently and with strong guarantees using linear programming. LASSO and related linear regression problems are well studied in statistics and machine learning, instead of reviewing the literature we refer the reader to the excellent textbook [99].

LASSO can be framed in the Bayesian probabilistic setting by considering

$$P_{\text{out}}(y_\mu|z_\mu) = \frac{1}{\sqrt{2\pi}\Delta} e^{-\frac{(y_\mu - \sum_{i=1}^N F_{\mu i} x_i)^2}{2\Delta}} \quad (102)$$

and prior of  $x_i$  being the Laplace distribution

$$P_X^{\ell_1}(x_i) = e^{-\lambda|x_i|}/2. \quad (103)$$

Another sparsity inducing prior is a combination of strict zeros and fraction  $\rho$  of non-zeros

$$P_X(x_i) = \rho\phi(x_i) + (1 - \rho)\delta(x_i), \quad (104)$$

where  $\phi(x_i)$  is the distribution of non-zero elements. Linear programming does not work for priors such as (104), but the probabilistic framework is more general in this aspect.

In many applications the output variables  $y_\mu$  are binary (interpreted in the above example as the treatment worked or did not), then the most commonly considered output distribution is logistic function. The conditional dependence then is

$$P_{\text{out}}^{\text{logistic}}(y_\mu = 1|z_\mu) = \frac{1}{1 + e^{-z_\mu}}. \quad (105)$$

Example of the linear estimation setting that is the best known in statistical physics is the perceptron [204]. In perceptron, components of the unknown vector  $\mathbf{x}$  are interpreted as synaptic weights (that are in general not sparse). The rows of the matrix  $F$  are patterns presented to the perceptron. The measurements  $y_\mu$  are binary and correspond to classification of the patterns (think of some patterns being pictures of cats  $y_\mu = +1$  and the others being pictures of dogs  $y_\mu = -1$ ). The goal is to learn the synaptic weights  $x_i$  in such a way that  $\sum_i F_{\mu i} x_i > 0$  when  $y_\mu = +1$ , and  $\sum_i F_{\mu i} x_i < 0$  when  $y_\mu = -1$ .

Here we will adopt the Bayesian probabilistic framework for the above linear estimation problem. This is in general much more algorithmically involved than the convex relaxations of the problem, and consequently less widely studied. The cases where interesting theoretical analysis can be done are limited to special classes of matrices  $F_{\mu i}$  (mostly with random iid elements, but see discussion in section VE). Although (as always) the resulting algorithms can be used as heuristic tools for more general data  $F_{\mu i}$ . One problem where the above linear estimation problem involves matrix  $F_{\mu i}$  with random iid elements is *compressed sensing* [65] to which we consacrate next sections.

### A. Compressed sensing

Compressed sensing, a special case of the above linear estimation setting, is triggering a major evolution in signal acquisition. Most signals of interest are compressible and this fact is widely used to save storage place. But so far compression is made only once the full signal is measured. In many applications (e.g. medical imaging using MRI or tomography) it is desirable to reduce the number of measurements as much as possible (to reduce costs, time, radiation exposition dose etc.). It is hence desirable to measure the signal directly in the compressed format. Compressed sensing is a concept implementing exactly this idea by designing new measurement protocols and sparse signal reconstruction algorithms. In compressed sensing one aims to infer a sparse  $N$ -dimensional vector  $\mathbf{x}$  from the smallest possible number  $M$  of its linear projections  $\mathbf{y} = F\mathbf{x}$ . The  $M \times N$  measurement matrix  $F$  is to be designed.

Most commonly used techniques in compressed sensing are based on a development that took place in 2006 thanks to the works of Candes, Tao, and Donoho [40, 41, 65]. They proposed to find the vector  $\mathbf{x}$  satisfying the constraints  $\mathbf{y} = F\mathbf{x}$  which has the smallest  $\ell_1$  norm (i.e., the sum of the absolute values of its components). This  $\ell_1$  minimization problem can be solved efficiently using linear programming techniques. They also suggested using a random matrix for  $F$ . This is a crucial point, as it makes the  $M$  measurements random and incoherent. Incoherence expresses the idea that objects having a sparse representation must be spread out in the domain in which they are acquired, just as a Dirac or a spike in the time domain is spread out in the frequency domain after a Fourier transform. These ideas have led to a fast, efficient and robust algorithm, and this  $\ell_1$ -reconstruction is now widely used, and has been at the origin of the burst of interest in compressed sensing over the last decade.

It is possible to compute exactly the performance of  $\ell_1$ -reconstruction in the limit  $N \rightarrow \infty$ , and the analytic study shows the appearance of a sharp phase transition [68, 70]. For any signal with density  $\rho = K/N$ , where  $K$  is the number of non-zero elements, the  $\ell_1$ -reconstruction gives the exact signal reconstruction with probability one only if the measurement rate,  $\alpha = M/N$ , is above the so-called Donoho-Tanner line,  $\alpha > \alpha_{\ell_1}(\rho) > \rho$ , see Fig. 14 black dashed line.

However, without taking into account the computational time, sparse signal reconstruction from random linear projections is possible whenever  $\alpha > \rho$  (this can be done for instance by exhaustively checking all possible positions of non-zero elements and trying to invert the reduced system of linear equations). A challenging question is whether there is a compressed sensing design and a computationally tractable algorithm that can achieve reconstruction down to such low measurement rates. In a series of works [132, 134], complemented by impressive rigorous proof of [66], this question was answered positively under the assumption that the empirical distribution of the non-zero elements of the signal is known. This major contribution to the theory of compressed sensing is explained below and uses many of the statistical physics elements from section II.

### B. Approximate message passing

Approximate message passing (AMP) is the algorithmic procedure behind the work of [132, 134] on linear estimation and compressed sensing. Origins of AMP trace back to statistical physics works on the problem of code division multiple access (CDMA) [115]. What is call today the generalized approximate message passing (G-AMP) algorithm, i.e. generalization to an arbitrary element-wise output function, was derived for a first time in connection to perceptron neural network in [120]. For some reason, however, this work was not remarked by the community. The opinion that this type of algorithm has invincible convergence problem prevailed in the literature until [32] where the authors demonstrated impressive performance of a related message passing algorithm for learning in binary perceptron. AMP is closely related to relaxed-belief propagation (r-BP) of Rangan [194], the algorithm of [32] can actually be seen

as a special case of r-BP. Donoho, Maleki and Montanari introduced AMP for compressed sensing [68], they also established the name. Very remarkably, the rigorous proof of its performance for random matrices  $F$  was done in [18, 19]. A comprehensive generalization to arbitrary priors and element-wise output function is due to Rangan [195], who established the name *generalized approximate message passing* for the version with a general output channel.

As is clear from the earlier papers [115], AMP is very closely related to the TAP equations [222] presented in section III D. The main difference between TAP and AMP is that TAP was originally derived for a model with Ising spins and pairwise interactions, whereas AMP is for continuous variables and  $N$ -body interactions.

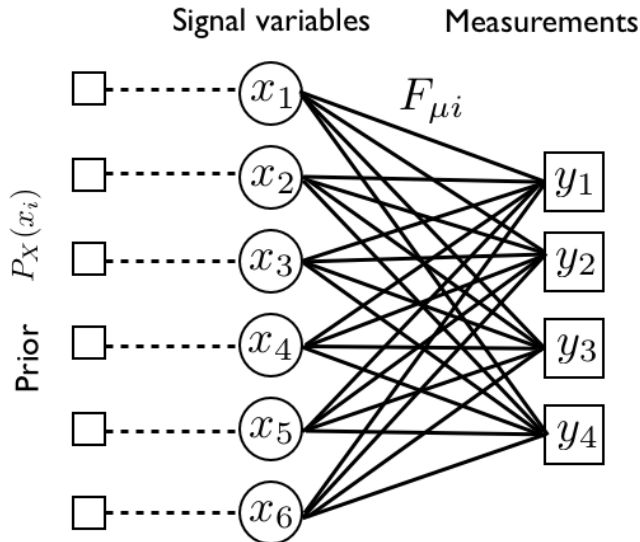


FIG. 13. Factor graph of the linear estimation problem corresponding to the posterior probability (106).

A detailed statistical physics derivation of the AMP algorithm was presented in [134] for the Gaussian output channel, and for general output as a part of yet more general problem of matrix factorization in [118]. Here we describe the main elements for the reader to understand where the resulting algorithm comes from.

We are given the posterior distribution

$$P(\mathbf{x}|\mathbf{y}, F) = \frac{1}{Z} \prod_{\mu=1}^M P_{\text{out}}(y_{\mu}|z_{\mu}) \prod_{i=1}^N P_X(x_i), \quad \text{where} \quad z_{\mu} = \sum_{i=1}^N F_{\mu i} x_i, \quad (106)$$

where the matrix  $F_{\mu i}$  has random independent entries (not necessarily identically distributed) with mean and variance  $O(1/N)$ . This posterior probability distribution corresponds to a graph of interactions  $y_{\mu}$  between variables (spins)  $x_i$  called the *graphical model* as depicted in Fig. 13.

A starting point in the derivation of AMP is to write the belief propagation algorithm corresponding to this graphical model. The matrix  $F_{\mu i}$  and measurements  $y_{\mu}$  play the role of quenched disorder. As long as the elements of  $F_{\mu i}$  are independents and of order  $O(1/\sqrt{N})$  the corresponding system is a mean field spin glass. In the Bayes-optimal case (i.e. when the prior is matching the true empirical distribution of the signal) the fixed point of belief propagation with lowest free energy then provides the asymptotically exact marginals of the above posterior probability distribution. This BP is not computationally tractable, because every interaction involves  $N$  variables, and the resulting belief propagation equations involve  $(N - 1)$ -uple integrals. Two tricks enable the derivation of the tractable AMP algorithm. The first trick is a Fourier decomposition of the output probability  $P_{\text{out}}(y|z)$  thanks to which the  $(N - 1)$ -uple integral factorizes into a product of  $N - 1$  integrals. The second trick is that each of the interactions  $y_{\mu}$  depends on each of the variables  $x_i$  only via the product  $F_{\mu i} x_i$ . Given the  $F_{\mu i} = O(1/\sqrt{N})$  this dependence is weak and a Taylor expansion in  $F_{\mu i}$  leads to a form in which the equation close only on the means and variances of the belief propagation messages. This results in the so-called the relaxed-belief-propagation (r-BP) [194]. This form of equations is tractable and involves a pair of means and variances for every pair variable-interaction.

The r-BP can be simplified further without changing the leading order behavior of the marginals by realizing that the dependence of the messages on the target node is weak. After the corresponding Taylor expansion the corrections

add up into the so-called *Onsager reaction terms* [222]. The final G-AMP iterative equations are written in terms of means  $a_i$  and their variances  $c_i$  for each of the variables  $x_i$ . The whole derivation is done in a way that the leading order of the marginal  $a_i$  are conserved. Given the BP was asymptotically exact for computations of the marginals so will be the G-AMP in computations of the means and variances. The final G-AMP equations read

$$V_\mu^t = \sum_{i=1}^N F_{\mu i}^2 c_i(t), \quad (107)$$

$$\omega_\mu^t = \sum_{i=1}^N F_{\mu i} a_i(t) - g_{\text{out}}(\omega_\mu^{t-1}, y_\mu, V_\mu^{t-1}) \sum_{i=1}^N F_{\mu i}^2 c_i(t), \quad (108)$$

$$(\Sigma_i^t)^{-1} = - \sum_{\mu=1}^M F_{\mu i}^2 \partial_\omega g_{\text{out}}(\omega_\mu^t, y_\mu, V_\mu^t), \quad (109)$$

$$T_i^t = \Sigma_i^t \left[ \sum_{\mu=1}^M F_{\mu i} g_{\text{out}}(\omega_\mu^t, y_\mu, V_\mu^t) - a_i(t) \sum_{\mu=1}^M F_{\mu i}^2 \partial_\omega g_{\text{out}}(\omega_\mu^t, y_\mu, V_\mu^t) \right], \quad (110)$$

$$a_i(t+1) = f_a(\Sigma_i^t, T_i^t), \quad (111)$$

$$c_i(t+1) = \Sigma_i^t \partial_T f_a(\Sigma_i^t, T_i^t), \quad (112)$$

where we denote by  $\partial_\omega$  ( $\partial_T$ ) the partial derivative with respect to variable  $\omega$  ( $T$ ). We define the input function as

$$f_a(\Sigma, T) = \frac{\int dx x P_X(x) e^{-\frac{(x-T)^2}{2\Sigma}}}{\int dx P_X(x) e^{-\frac{(x-T)^2}{2\Sigma}}}, \quad (113)$$

and the output function as

$$g_{\text{out}}(\omega, y, V) = \frac{\int dz (z - \omega) P_{\text{out}}(y|z) e^{-\frac{(z-\omega)^2}{2V}}}{V \int dz P_{\text{out}}(y|z) e^{-\frac{(z-\omega)^2}{2V}}}. \quad (114)$$

An important aspect of these equations to note is the index  $t - 1$  in the Onsager reaction term in eq. (108) that is crucial for convergence and appears for the same reason as in the TAP equations in sec. III D. Note that the whole algorithm is comfortably written in terms of matrix multiplications only, this is very useful for implementation where fast linear algebra can be used.

Using the usual Bethe approach, one can also compute the corresponding potential, and show that these message passing equations actually aim to minimize the following Bethe free energy [133, 198, 226]:

$$\begin{aligned} \mathcal{F}_{\text{var}}^{\text{Bethe}}(T, \Sigma) &= \sum_i D_{\text{KL}}(Q_i || P_X) + \sum_\mu D_{\text{KL}}(\mathcal{M}_\mu || P_{\text{out}}) \\ &+ \frac{1}{2} \sum_\mu [\log 2\pi V_\mu^* + 1 + V_\mu^* \partial_\omega g_{\text{out}}(\omega_\mu^*, y_\mu, V_\mu^*)], \end{aligned} \quad (115)$$

with  $V_\mu^*$  and  $\omega_\mu^*$  satisfying their respective fixed-point conditions, and where the two Kullback-Leibler divergences are taken with respect to probability distributions

$$\mathcal{M}_\mu(z; \omega_\mu^*, y_\mu, V_\mu^*) = \frac{1}{\mathcal{Z}_{\mathcal{M}}} P_{\text{out}}(y_\mu|z) \frac{1}{\sqrt{2\pi V_\mu^*}} e^{-\frac{(z-\omega_\mu^*)^2}{2V_\mu^*}} \quad (116)$$

$$Q_i(x; T_i, \Sigma_i) = \frac{1}{\mathcal{Z}_{\mathcal{Q}}} P_X(x) e^{-\frac{(x-T_i)^2}{2\Sigma_i}}, \quad (117)$$

where  $\mathcal{Z}_{\mathcal{M}}$  and  $\mathcal{Z}_{\mathcal{Q}}$  are the corresponding normalizations. Clearly these two probability distributions are related to the denominators in (113) and (114).

### 1. Note of convergence and parameter learning

When G-AMP converges, its performance in terms of mean-squared error is usually considerably better than performance of other existing algorithms. The AMP equations are proven to converge in the idealized setting of large

system, random iid matrix  $F$  with zero mean entries, and when the prior  $P_X$  either corresponds to the empirical distribution of the actual signal  $\mathbf{x}^*$  or to the convex relaxation of the problem [18, 19]. However, for mismatched signal distribution, for non-random matrices, positive mean random matrices or small system-sizes they might have unpleasant convergence issues.

Justified by the promise of strikingly better performance, it is an important subject of current research how to make the G-AMP algorithm the most robust possible, while keeping its performance and speed. Several recent works inscribe in this line. In [38] it was identified why AMP has convergence problems for the simple case of iid matrices with elements of non-zero mean. For mean of the matrix elements larger than some critical value, there is an anti-ferromagnetic-like (i.e. corresponding to a negative eigenvalue of the Hessian matrix) instability of the Nishimori line. Finite size always causes a slight mismatch between the true and the empirical distribution of the signal, and hence a slight deviation from the Nishimori line. The instability amplifies the deviation and causes the iteration of the AMP equation to fail and go far away from the Nishimori line. Even though we know that in the Bayes-optimal case the correct fixed point must satisfy the Nishimori conditions.

Inspired by this understanding, we need to stabilize the Nishimori line in order to improve the convergence. We observed that randomization of the update is doing just that. Combining the sequential update while keeping track of the correct time-indexes Ref. [154] designed the so-called Swept-AMP (SWAMP). Ref. [134] studied the expectation-maximization learning of parameters for the compressed sensing problem when the number of parameters is small, typically finite while the system size grows. Since the parameters learning is precisely imposing the validity of the Nishimori conditions, this is another way that greatly stabilizes the Nishimori line and improves the convergence.

Another way of stabilizing the Nishimori line is to slow down the iterations via dumping, i.e. when updating a message we take a linear combination of the new and old value. Such dumping can, however, slow down the iteration considerably. In order to avoid a drastic slow-down we take advantage of the following related development.

Authors of [133] study the Bethe free energy associated to G-AMP and wrote a variational form of the Bethe free energy (115) for which the G-AMP fixed points are local minima (not only generic stationary points such as saddles). This free energy can be optimized directly leading to provably converging (but considerably slower) method to find the fixed points. This variational Bethe free energy can be used to slow down the iterations in a way to keep decreasing the free energy - this we call adaptative dumping in [226]. Ref. [226] also describes a mean-removal procedure that greatly improves stability of the implementation. Other groups suggested several closely related convergence improvements [197, 198].

Combining the above implementation features - adaptive dumping, sequential update, mean removal and parameter learning - leads to the current state-of-the art implementation of the G-AMP algorithm for linear estimation problems.

## 2. Examples of priors and outputs

The G-AMP algorithm is written for a generic prior on the signal  $P_X$  (as long as it factorized over elements) and a generic element-wise output channel  $P_{\text{out}}$ . The algorithm depends on the specific form of those only trough the function  $f_a$  and  $g_{\text{out}}$  defined by (113) and (114). It is useful for give a couple of explicit examples.

The sparse prior that is the most commonly considered in probabilistic compressed sensing is the Gauss-Bernoulli, when in (104) we have  $\phi(x) = \mathcal{N}(\bar{x}, \sigma)$ . For this prior the input function  $f_a$  reads

$$f_a^{\text{Gauss-Bernoulli}}(\Sigma, T) = \frac{\rho e^{-\frac{(T-\bar{x})^2}{2(\Sigma+\sigma)}} \frac{\sqrt{\Sigma}}{(\Sigma+\sigma)^{\frac{3}{2}}} (\bar{x}\Sigma + T\sigma)}{(1-\rho)e^{-\frac{T^2}{2\Sigma}} + \rho \frac{\sqrt{\Sigma}}{\sqrt{\Sigma+\sigma}} e^{-\frac{(T-\bar{x})^2}{2(\Sigma+\sigma)}}}, \quad (118)$$

The most commonly considered output channel is simply additive white Gaussian noise (AWGN) (102). The output function then reads

$$g_{\text{out}}^{\text{AWGN}}(\omega, y, V) = \frac{y - \omega}{\Delta + V}. \quad (119)$$

As we anticipated above, the example of linear estimation that was most broadly studied in statistical physics is the case of the perceptron problem discussed in detail e.g. in [228]. In perceptron each of the  $M$   $N$ -dimensional patterns  $F_\mu$  is multiplied by a vector of synaptic weights  $x_i$  in order to produce an output  $y_\mu$  according to

$$y_\mu = 1 \quad \text{if} \quad \sum_{i=1}^N F_{\mu i} x_i > \kappa, \quad (120)$$

$$y_\mu = -1 \quad \text{otherwise}, \quad (121)$$

where  $\kappa$  is a threshold value independent of the pattern. The perceptron is designed for classification of patterns, i.e. one starts with a training set of patterns and their corresponding outputs  $y_\mu$  and aims to learn the weights  $x_i$  in such a way that the above relation between patterns and outputs is satisfied. To relate to the linear estimation problem above, let us consider the perceptron problem in the teacher-student scenario where the teacher perceptron generated the output  $y_\mu$  using some ground-truth set of synaptic weights  $x_i^*$ . The student perceptron knows only the patterns and the outputs and aims to learn the weights. How many patterns are needed for the student to be able to learn the synaptic weights reliably? What are efficient learning algorithms?

In the simplest case where the threshold is zero,  $\kappa = 0$  one can redefine the patterns  $F_{\mu i} \leftarrow F_{\mu i} y_\mu$  in which case the corresponding redefined output is  $y_\mu = 1$ . The output function in that case reads

$$g_{\text{out}}^{\text{perceptron}}(\omega, V) = \frac{1}{\sqrt{2\pi V}} \frac{e^{-\frac{\omega^2}{2V}}}{H\left(-\frac{\omega}{\sqrt{V}}\right)}, \quad (122)$$

where

$$H(x) = \int_x^\infty \frac{dt}{\sqrt{2\pi}} e^{-\frac{t^2}{2}}. \quad (123)$$

Note also that the perceptron problem formulated this way is closely related to what is called 1-bit compressed sensing in signal processing literature [30, 231].

In physics a case of perceptron that was studied in detail is that of binary synaptic weights  $x_i \in \{\pm 1\}$  [83, 84, 94]. To take that into account in the G-AMP we consider the binary prior  $P_X(x) = [\delta(x-1) + \delta(x+1)]/2$  which leads to the input function

$$f_a^{\text{binary}}(\Sigma, T) = \tanh\left(\frac{T}{\Sigma}\right). \quad (124)$$

It should be noted that an algorithm that is extremely close to G-AMP was written for a mathematically closely related problem CDMA in [115]. However, the time-indices were not treated correctly in that paper and that causes serious convergence problems. A message passing form of the algorithm, related to r-BP, was written and used very successfully for the binary perceptron learning in [32].

Note also that in [120] the G-AMP was written for the perceptron problem with the correct time-indices and good performance was illustrated on the CDMA problem. However, for an unknown reason, that paper did not have any impact of the research community and many of its results waited to be rediscovered in the connection to compressed sensing much later [69, 195].

### C. State evolution and phase transitions

The performance of the G-AMP algorithm above can be analyzed in the limit of large size, for matrices with independent entries. The corresponding analysis was baptized *state evolution* in [69]. Rigorous results on the state evolution are in [18, 19]. Statistical physics derivation of the state evolution is given in [134] and is formally very related to the state evolution of the TAP equation in sec. III D. The main point in the derivation of the state evolution is not to start from the G-AMP algorithm but from its message passing form (which is an intermediate step in the derivation of G-AMP before the number of message is reduced in the TAP fashion). One then recalls that in belief propagation we assumed conditional independence of incoming messages which translates into independence of terms present in sums of an extensive number of terms in the message passing. Central limit theorem is then used and only the mean and variance of these terms matters. One simply needs to keep track of the evolution of this mean and variance,

In statistical physics terms the state evolution exactly corresponds to the derivation of replica symmetric equations via the cavity method. Since the cavity and replica methods always yield the same result, the state evolution equations are exactly equivalent to the equations stemming from the replica method for the corresponding problem. For compressed sensing this is illustrated in [134]. Another example is that all the replica symmetric equations for the perceptron problem and related results, e.g. in [228], can be obtained as a special case of the G-AMP state evolution.

In the Bayes optimal case, i.e. prior distribution matching the empirical distribution of the true signal, the state evolution leads to the asymptotic Bayes optimal minimum mean squared error (MMSE) for the corresponding inference problem. Just as it did for the planted spin glass or the clustering of networks above. Since in linear estimation we are working with a fully connected graphical model the asymptotic analysis can be written in terms of only 3 scalar



parameters [134]. In the Bayes-optimal case, where Nishimori conditions hold, this further simplifies into a single scalar quantity defined as a large  $N$  limit of

$$m^t = \frac{1}{N} \sum_{i=1}^N a_i^2(t). \quad (125)$$

In order to write the equation for the Bayes-optimal MMSE for general output function we need to rewrite the output function using  $y = h(z, w)$  where  $w$  is a random variable distributed according to  $P_W(w)$ . Then

$$P_{\text{out}}(y|z) = \int dw P_W(w) \delta[y - h(z, w)] \quad (126)$$

with this definition the state evolution reads

$$m^{t+1} = \int dx P_X(x) \int d\xi \frac{e^{-\frac{\xi^2}{2}}}{\sqrt{2\pi}} f_a^2 \left( \frac{1}{\alpha \hat{m}^t}, x + \frac{\xi}{\sqrt{\alpha \hat{m}^t}} \right), \quad (127)$$

$$\hat{m}^t = - \int dw P_W(w) \int dp dz \frac{e^{-\frac{p^2}{2m^t}} e^{-\frac{(z-p)^2}{2(\rho_0 - m^t)}}}{2\pi \sqrt{m^t(\rho_0 - m^t)}} \partial_p g_{\text{out}}(p, h(z, w), \rho_0 - m^t), \quad (128)$$

where we denote  $\rho_0 = NE_F(F^2)E_{P_X}(x^2)$ . For the sparse prior (104) where the non-zero elements have second moment equal to  $\bar{x}^2$  and matrix  $F$  having iid element of zero mean and variance  $1/N$  we get  $\rho_0 = \rho \bar{x}^2$ . For the usual AWGN output (102) the second equation then simplifies considerably into

$$\hat{m}^t = \frac{1}{\Delta + \rho \bar{x}^2 - m^t}. \quad (129)$$

The mean-squared error of the AMP estimator is then  $\text{MSE} = \rho \bar{x}^2 - m^t$ . To evaluate the performance of AMP that is initialized in a way unrelated to the unknown signal, the state evolution is iterated till convergence starting from  $m^{t=0} = \rho^2 \bar{x}^2$ , where  $\bar{x}$  is the mean of the distribution  $\phi(x)$  in (104).

The free entropy can be also written as a function of the MSE  $E$ . In the case of the AWGN channel with variance  $\Delta$ , for instance, it reads [134]:

$$\begin{aligned} \Phi(E) = & -\frac{\alpha}{2} - \frac{\alpha}{2} \log(\Delta + E) - \frac{\alpha(\rho \bar{x}^2 - E)}{2(\Delta + E)} \\ & + \int ds P_X(s) \int \mathcal{D}z \log \left\{ \int dx e^{\frac{\alpha}{\Delta + E} x(s - \frac{x}{2}) + zx \frac{\sqrt{\alpha}}{\sqrt{\Delta + E}}} P_X(x) \right\}. \end{aligned} \quad (130)$$

In Fig. 14 we plot down to what measurement rate  $\alpha = M/N$  does AMP recover the signal of density  $\rho$  for several distributions of non-zero signal elements  $\phi(x)$ . We observe a first order phase transition that does depend on the distribution of non-zeros. The corresponding line is always better than the  $\ell_1$  transition, as shown in [67] where the distribution maximizing the spinodal line for Bayes-optimal inference was computed.

Ref. [134] further studied how is the inference performance influenced by measurement noise, mismatch between the prior and the actual signal distribution, how the performance changes under expectation maximization learning of the parameters, such as  $\rho$  or mean  $\bar{x}$  and variance  $\sigma$  of the signal distribution. Ref. [13] explored the role of approximately sparse signals when the  $\delta(x_i)$  in (104) is replaced by a narrow Gaussian. Influence of an uncertainty in the elements of the matrix  $F$  was studied in [135]. As expected from statistical physics where in the presence of disorder first order phase transitions become weaker, second order or disappear entirely, the same happens to the first order phase transition in compressed sensing under presence of various kinds of noise. Qualitative results are illustrated in [13, 134, 135].

Many examples of problems for which the replica analysis has been done and can be seen as a special case of the present state evolution can be found in the literature, see e.g. the works on perceptron and CDMA.

#### D. Spatial coupling

As discussed in section III B if nothing is changed about the graphical model corresponding to compressed sensing, the 1st order phase transition presented in Fig. 14 causes a barrier that is conjectured to be unbeatable with any

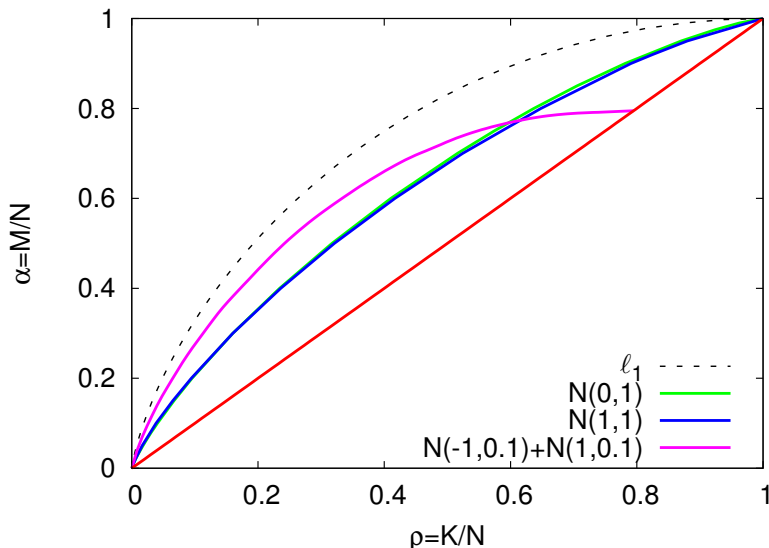


FIG. 14. Phase diagram for the AMP reconstruction in the optimal Bayesian case when the signal model is matching the empirical distribution of signal elements. The elements of the  $M \times N$  measurement matrix  $F$  are iid variables with zero mean and variance  $1/N$ . The spinodal transition  $\alpha_s(\rho)$  is computed with the state evolution and plotted for the following signal distributions:  $\phi(x) = \mathcal{N}(0,1)$  (green),  $\phi(x) = \mathcal{N}(1,1)$  (blue)  $\phi(x) = [\mathcal{N}(-1,0.1) + \mathcal{N}(1,0.1)]/2$  (magenta). The data are compared to the Donoho-Tanner phase transition  $\alpha_{\ell_1}(\rho)$  (dashed) for  $\ell_1$  reconstruction that does not depend on the signal distribution, and to the theoretical limit for exact reconstruction  $\alpha = \rho$  (red).

polynomial algorithm. In an idealized setting of compressed sensing, however, the design of the measurement matrix  $F_{\mu i}$  is entirely up to us. Thanks to this compressed sensing belongs to the class of problems where spatial coupling can be successfully applied. This was the main point of ref. [132] where spatially coupled measurement matrices were designed that allowed AMP to reconstruct the signal in compressed sensing anytime the measurement rate  $\alpha$  is larger than the density of non-zero elements in the signal  $\rho$ , i.e. all the way above the red line in Fig. 14. This *threshold saturation* was soon after proven rigorously in [66]. We should note that spatial coupling for compressed sensing was considered even before in [144], but in that work the observed improvement was limited and it did not seem possible to achieve the information theoretic limit  $\alpha = \rho$ .

The spatially coupled matrices suggested in [132] are illustrated in Fig. 15. The mechanism of why the spinodal transition disappears with such spatially-coupled measurement matrices is physically exactly the same as for the spatially coupled Currie-Weiss model discussed in section III C. The first block of the matrix has larger effective measurement rate and plays the role of a nucleation seed. The interactions in the blocks next to the diagonal then ensure that the seed grows into the whole system. Ref. [134] discusses further the choice of parameters of the spatially coupled measurement matrices, other related designs and the effect of noise. With the goal of optimizing the spatially coupled matrices the properties of the nucleation and necessary properties of the seed in compressed sensing were studied in [37].

Nowadays there are several problems in the literature closely related to compressed sensing to which spatial coupling was applied. One of them is the group testing problem which is motivated by grouping blood samples to test for a very rare disease. Spatial coupling for group testing was suggested in [241]. In group testing the variables  $x_i$  are binary and the fraction of ones is very small. Tests group together a number of variables and output the number of ones present in each of the test-groups. The goal is to minimize the number of tests while being able to recover exactly which variables were positive (one) and which negative (zero). This problem is very closely related to the sparsely spread CDMA where the fraction of ones is considered to be  $1/2$ . For densely spread CDMA spatial coupling was considered in [210, 220].

Another problem formally very closely related to compressed sensing is the real valued error correction where the codeword is corrupted by gross errors on a fraction of entries and a small noise on all the entries. In [14] it was shown that the error correction and its robustness towards noise can be enhanced considerably using AMP and spatial coupling.

A similar application of these ideas has allowed for the development of the spatially coupled sparse superposition codes [11, 12, 15, 113, 205]. These are efficient coding schemes using exactly the compressed sensing setting with a

$$\begin{pmatrix} y \end{pmatrix} = \begin{pmatrix} F \end{pmatrix} \times \begin{pmatrix} s \end{pmatrix}$$

■ : unit coupling  
■ : coupling  $J_1$   
■ : coupling  $J_2$   
 : no coupling (null elements)

FIG. 15. Example of a spatially coupled measurement matrix  $F$  for compressed sensing. The elements of the matrix are taken independently at random, their variance has the block diagonal structure as illustrated in the figure. The figure is taken from [134].

twist: the variables are  $L$ -dimensional and are forced to point into one corner of the  $L$ -hypercube. These codes, with the associated AMP decoder, have been shown to be fast and reliable, and actually reach the Shannon limit for the AWGN channel in the large  $L$  limit.

## E. Non-random matrices and non-separable priors

### 1. Structured priors

AMP as described above uses the empirical distribution of signal elements. A natural question is whether its performance can be improved further if more information is known about the signal. There are works that have investigated this question and combined AMP with more complex, structured priors. Utilizing such structured priors is key to leveraging many of the advancements recently seen in statistical signal representation. For instance techniques such hybrid AMP [196, 211] have shown promising results. In those works, an additional graphical model is introduced in order to take into account the correlation between variables. The improvement, for instance for image denoising, can be spectacular.

Another possible approach to structured prior is not to model the correlations directly, but instead to utilize a bipartite construction via hidden variables, as in the restricted Boltzmann machine (RBM) [103, 104]. If a binary RBM can be trained to model the support pattern of a given signal class, then the statistical description of the RBM admits its use within AMP, as was shown recently in [224]. This is particularly interesting since RBMs are the building blocks of “deep belief networks” [21] and have recently sparked a surge of interest, partly because of the efficient algorithms developed to train them (e.g. contrastive divergence (CD) [104]). The possibility, shown in [224], to incorporate deep learned priors into generalized linear problems such as compressed sensing looks like a very promising one.

### 2. Orthogonal matrices

Using non-random matrices for the linear projection is crucial to explore the range of applicability. There have been, again, a collection of works in this direction, for instance in the analysis of the so-called perceptron learning with correlated pattern (which form the sensing matrix) [117, 216].

Another interesting strategy is given by the recent work S-AMP that extends the approximate message-passing algorithm to general matrix ensembles when there is a certain well-defined large system size limit, based on the S-transform (in free probability) of the spectrum of the measurement matrix [34]. Older works, in fact, already used a similar approach for the CDMA problem [219].

### 3. Reconstruction in discrete tomography

Reconstruction of signal in x-ray computed tomography (CT) is another problem that belongs to the class of linear estimation. The matrix  $F_{\mu i}$  corresponding to computer tomography has very particular structure. Classical reconstruction algorithms such as filtered back-projection require the corresponding linear system to be sufficiently determined. Therefore, the number of measurements needed is generally close to the number of pixels to be reconstructed. Nevertheless, many applications would benefit from being able to reconstruct from a smaller number of angles. Ref. [88] designed and tested a message passing algorithm that is adapted to the measures performed in CT and is able to provide reliable reconstruction with a number of measurements that is smaller than what required by previous techniques. This algorithm is another nice example of how inspiration from physics can provide a promising algorithmic approach.

Each measurement in x-ray CT is well approximated by a sum of absorption coefficient of the material under investigation along a straight line of the corresponding x-ray. Let us discretize the object under study into small elements, and assign a discrete value  $x_i \in \{1, \dots, q\}$  of the absorption coefficient to every small element  $i$ . One component of measurement in CT is then

$$y_\mu = \sum_{i \in \mu} x_i, \quad (131)$$

where the sum is over all elements that lie on the line  $\mu$ . The structural information that in general allows us to decrease the number of measurement is that mostly two pixels that lie next to each other have the same value. This expectation is represented in the following posterior distribution

$$P(\mathbf{x}|\mathbf{y}) = \frac{1}{Z} \prod_{\mu=1}^M \left[ \delta \left( y_\mu - \sum_{i \in \mu} x_i e^{J_\mu \sum_{(ij) \in \mu} \delta_{x_i, x_j}} \right) \right], \quad (132)$$

where the notation  $(ij) \in \mu$  means the elements  $i$  and  $j$  are next to each other on the line corresponding to measurement  $\mu$ ,  $J_\mu$  is the interaction constant.

Ref. [88] writes belief propagation algorithm for estimating marginals of this posterior distribution. However, one update of this belief propagation involves intractable sums over all configurations of variables on one line. We realize that these sums correspond to the partition functions of one-dimensional Potts model with fixed magnetization. One-dimensional line is a tree and for trees partition functions can be computed exactly with belief propagation. We use this to design an algorithm that uses BP within BP. The resulting implementation is comparably fast as the competing convex relaxation based algorithms and provides better reconstruction and robustness to noise. We believe that overall the algorithm suggested in [88] provides a promising perspective for reconstruction in x-ray computed tomography.

## F. Optics in complex media

Finally, we would like to close the loop with physics and mention one explicit physics experiment in the field of compressed optics where AMP and related tools have been especially useful.

Wave propagation in complex media is a fundamental problem in physics, be it in acoustics, optics, or electromagnetism. In optics, it is particularly relevant for imaging applications. Indeed, when light passes through a multiple-scattering medium, such as a biological tissue or a layer of paint, ballistic light is rapidly attenuated, preventing conventional imaging techniques, and random scattering events generate a so-called speckle pattern that is usually considered useless for imaging.

Recently, however, wavefront shaping using spatial light modulators has emerged as a unique tool to manipulate multiply scattered coherent light, for focusing or imaging in scattering media [176]. This makes it possible to measure the so-called transmission matrix of the medium [191], which fully describes light propagation through the linear medium, from the modulator device to the detector. Interestingly, these transmission matrices, due to the fact that they account for the multiple scattering and interference, are essentially iid random matrices [191], which is exactly what AMP technics have been designed for.

An important issue in most such recent experiments lies in accessing the amplitude and phase of the output field, that in optics usually requires a holographic measurement, i.e., with the use of a second reference beam. The phase and amplitude of the measured field can then be extracted by simple linear combinations of interference patterns with a phase shifted or off-axis reference. This however poses the unavoidable experimental problem of the interferometric stability of the reference arm. In order to be able to avoid entirely the use of the reference beam, we need to solve a

problem that looks like compressed sensing: finding  $\mathbf{x}$  (sparse or binary) such that  $\mathbf{y} = |F\mathbf{x}|$  where  $F$  is complex and iid. Combining the GAMP and the SWAMP approach for phase retrieval [154, 212], it has been possible to precisely do this, and to calibrate efficiently, and to perform a reference-less measurement of the transmission matrix of a highly scattering material. Within this framework, the work of [71] showed that the transfer matrix can still be retrieved for an opaque material (a thin layer of white paint), and then can be used for imaging or focusing, using the opaque complex material as a lens. This was experimentally validated.

As a result the full complex-valued transmission matrix of a strongly scattering material can be estimated, up to a global phase, with a simple experimental setup involving only real-valued inputs and outputs in combination with the technics presented in this review. We believe this illustrates the power of the technics presented in this review, and shows that not only does statistical physics provide interesting perspective to inference problems, but also that inference technics can be in return useful for physics experiments.

## VI. PERSPECTIVES

The authors' research that is covered in this review was mostly obtained following the strategy

- (a) Pick an interesting statistical inference problem.
- (b) Consider it in some simple (usually random) setting.
- (c) Analyze the corresponding phase diagram in that setting in order to gain new insight about the problem.
- (d) Reconsider the algorithmic approaches in the light of the analysis and come up with new algorithmic ideas for the problem under investigation.

This strategy, a typical one for physicists, showed up as rather fruitful.

In today's scientific landscape the number of very interesting data-driven problems is considerable and in the author's opinion, we have little risk of running out of interesting problems to pick in the starting point (a).

Point (b) might seem the simplest, but it is on the contrary quite crucial. Computer science and related fields mostly aim at understanding the worst possible setting or to prove something under weakest possible conditions. Analysis in a random setting usually does not seem generic enough to be of considerable interest. In machine learning and more applied parts of computer science the focus is on a couple of benchmark-datasets (such as e.g. the MNIST database). Simple models that aim to represent reasonably well the generic situation is really a domain of physical sciences. This is how progress in physics is made, and in our opinion this is transferable to other fields as well.

In point (c), physicists can use with large effectiveness tools and methods from statistical physics of disordered systems such as glasses and spin glasses. The advantage of these methods is that, unlike any other existing generic method, they are able to describe the Bayes-optimal probabilistic inference. The disadvantage is that they are not fully rigorous and therefore sometimes viewed with dismissal or skepticism. On the other hand, rigorous proofs of results obtained with the cavity and replica method is a great mathematical challenge and many partial results were obtained that have led to new mathematical tools making the whole probability theory more powerful. One of the goals of the presented research is to transfer the physics reasoning and insight to mathematicians in order to help them to craft plausible proof strategies.

Concerning, finally, point (d), we hope that all the work presented within this review demonstrates that indeed the physics insight and deeper understanding brings promising algorithmic ideas. What is, perhaps, more challenging is to push such ideas into actual applications.

The authors believe that the above strategy has a lot to offer and will lead to discovery of many interesting results also in the future. We hope this review will help trigger activity in this direction.

## ACKNOWLEDGEMENTS

We would like to express our gratitude to all our colleagues with whom many of the results presented here have been obtained. In particular, we wish to thank Maria-Chiara Angelini, Jean Barbier, Francesco Caltagirone, T. Castellani, Michael Chertkov, Andrea Crisanti, Leticia F. Cugliandolo, Laurent Daudet, Aurelien Decelle, Angelique Drémeau, Laura Foini, Silvio Franz, Sylvain Gigan, Emmanuelle Guillard, Jacob E. Jensen, Yoshiyuki Kabashima, Brian Karrer, Lukas Kroc, Srinivas Kudekar, Jorge Kurchan, Marc Lelarge, Antoine Liutkus, Thibault Lesieur, Luca Leuzzi, André Manoel, David Martina, Marc Mézard, Andrea Montanari, Christopher Moore, Richard G. Morris, Elchanan Mossel, Joe Neeman, Mark Newman, Hidetoshi Nishimori, Boshra Rajaei, Sundeep Rangan, Joerg Reichardt, Federico Ricci-Tersenghi, Alaa Saade, David Saad, Ayaka Sakata, Francois Sausset, Christophe Schülke, Guilhem Semerjian, Cosma R. Shalizi, David Sherrington, Alan Sly, Phil Schniter, Eric W. Tramel, Rudiger Urbanke, Massimo Vergassola, Jeremy Vila, Xiaoran Yan, Sun Yifan, Francesco Zamponi, Riccardo Zecchina and Pan Zhang.

Finally, we also wish to thank Alena and Julie for their continuous support and for letting us work, if only from time to time, on this review.

## FUNDINGS

Part of the research leading to the presented results has received funding from the European Research Council under the European Union's 7<sup>th</sup> Framework Programme (FP/2007-2013/ERC Grant Agreement 307087-SPARCS).

- 
- [1] Emmanuel Abbe, Afonso S Bandeira, Annina Bracher, and Amit Singer. Decoding binary node labels from censored edge measurements: Phase transition and efficient recovery. *Network Science and Engineering, IEEE Transactions on*, 1(1):10–22, 2014.
  - [2] Emmanuel Abbe and Andrea Montanari. Conditional random fields, planted constraint satisfaction and entropy concentration. In *Approximation, Randomization, and Combinatorial Optimization. Algorithms and Techniques*, pages 332–346. Springer, 2013.
  - [3] Dimitris Achlioptas and Amin Coja-Oghlan. Algorithmic barriers from phase transitions. In *Foundations of Computer Science, 2008. FOCS'08. IEEE 49th Annual IEEE Symposium on*, pages 793–802. IEEE, 2008.
  - [4] Dimitris Achlioptas and Christopher Moore. The asymptotic order of the random  $k$ -sat threshold. *focs*, 00:779, 2002.
  - [5] Dimitris Achlioptas and Yuval Peres. The threshold for random  $K$ -SAT is  $2^k \log 2 - o(k)$ . *Journal of the American Mathematical Society*, 17(4):947–973, 2004.
  - [6] Lada A Adamic and Natalie Glance. The political blogosphere and the 2004 us election: divided they blog. In *Proceedings of the 3rd international workshop on Link discovery*, pages 36–43. ACM, 2005.
  - [7] Noga Alon, Itai Benjamini, Eyal Lubetzky, and Sasha Sodin. Non-backtracking random walks mix faster. *Communications in Contemporary Mathematics*, 9(04):585–603, 2007.
  - [8] Noga Alon, Michael Krivelevich, and Benny Sudakov. Finding a large hidden clique in a random graph. *Random Structures and Algorithms*, 13(3-4):457–466, 1998.
  - [9] Maria Chiara Angelini, Francesco Caltagirone, Florent Krzakala, and Lenka Zdeborová. Spectral detection on sparse hypergraphs. *arXiv preprint arXiv:1507.04113*, 2015.
  - [10] Victor Bapst, Guilhem Semerjian, and Francesco Zamponi. Effect of quantum fluctuations on the coloring of random graphs. *Physical Review A*, 87(4):042322, 2013.
  - [11] Jean Barbier and Florent Krzakala. Replica analysis and approximate message passing decoder for superposition codes. In *Information Theory (ISIT), 2014 IEEE International Symposium on*, pages 1494–1498. IEEE, 2014.
  - [12] Jean Barbier and Florent Krzakala. Approximate message-passing decoder and capacity-achieving sparse superposition codes. *arXiv preprint arXiv:1503.08040*, 2015.
  - [13] Jean Barbier, Florent Krzakala, Marc Mézard, and Lenka Zdeborová. Compressed sensing of approximately-sparse signals: Phase transitions and optimal reconstruction. In *Communication, Control, and Computing (Allerton), 2012 50th Annual Allerton Conference on*, pages 800–807. IEEE, 2012.
  - [14] Jean Barbier, Florent Krzakala, Lenka Zdeborová, and Pan Zhang. Robust error correction for real-valued signals via message-passing decoding and spatial coupling. In *Information Theory Workshop (ITW), 2013 IEEE*, pages 1–5. IEEE, 2013.
  - [15] Jean Barbier, Christophe Schülke, and Florent Krzakala. Approximate message-passing with spatially coupled structured operators, with applications to compressed sensing and sparse superposition codes. *Journal of Statistical Mechanics: Theory and Experiment*, 2015(5):P05013, 2015.
  - [16] Wolfgang Barthel, Alexander K Hartmann, Michele Leone, Federico Ricci-Tersenghi, Martin Weigt, and Riccardo Zecchina. Hiding solutions in random satisfiability problems: A statistical mechanics approach. *Physical review letters*, 88(18):188701, 2002.

- [17] Hyman Bass. The Ihara-Selberg zeta function of a tree lattice. *International Journal of Mathematics*, 3(06):717–797, 1992.
- [18] Mohsen Bayati, Marc Lelarge, Andrea Montanari, et al. Universality in polytope phase transitions and message passing algorithms. *The Annals of Applied Probability*, 25(2):753–822, 2015.
- [19] Mohsen Bayati and Andrea Montanari. The dynamics of message passing on dense graphs, with applications to compressed sensing. *Information Theory, IEEE Transactions on*, 57(2):764–785, 2011.
- [20] Matthew James Beal. *Variational algorithms for approximate Bayesian inference*. University of London, 2003.
- [21] Yoshua Bengio. Learning deep architectures for AI. *Foundations and Trends® in Machine Learning*, 2(1):1–127, 2009.
- [22] Quentin Berthet and Philippe Rigollet. Computational lower bounds for sparse pca. *arXiv preprint arXiv:1304.0828*, 2013.
- [23] H. A. Bethe. Statistical physics of superlattices. *Proc. Roy. Soc. London A*, 150:552–575, 1935.
- [24] Giulio Biroli and Jean-Philippe Bouchaud. The random first-order transition theory of glasses: a critical assessment. *Structural Glasses and Supercooled Liquids: Theory, Experiment, and Applications*, pages 31–113, 2012.
- [25] Béla Bollobás, Christian Borgs, Jennifer Chayes, Oliver Riordan, et al. Percolation on dense graph sequences. *The Annals of Probability*, 38(1):150–183, 2010.
- [26] Erwin Bolthausen. An iterative construction of solutions of the TAP equations for the Sherrington–Kirkpatrick model. *Communications in Mathematical Physics*, 325(1):333–366, 2014.
- [27] Charles Bordenave, Marc Lelarge, and Laurent Massoulié. Non-backtracking spectrum of random graphs: community detection and non-regular ramanujan graphs. *arXiv preprint arXiv:1501.06087*, 2015.
- [28] J.-P. Bouchaud, L. Cugliandolo, J. Kurchan, and M. Mézard. Out of equilibrium dynamics in spin glasses and other glassy systems. In A. P. Young, editor, *Spin Glasses and Random Fields*. World Scientific, Singapore, 1998.
- [29] Jean-Philippe Bouchaud and Marc Potters. *Theory of financial risk and derivative pricing: from statistical physics to risk management*. Cambridge university press, 2003.
- [30] Petros T Boufounos and Richard G Baraniuk. 1-bit compressive sensing. In *Information Sciences and Systems, 2008. CISS 2008. 42nd Annual Conference on*, pages 16–21. IEEE, 2008.
- [31] DR Bowman and K Levin. Spin-glass theory in the bethe approximation: Insights and problems. *Physical Review B*, 25(5):3438, 1982.
- [32] A. Braunstein and R. Zecchina. Learning by Message Passing in Networks of Discrete Synapses. *Physical Review Letters*, 96(3):030201, 2006.
- [33] T Tony Cai, Tengyuan Liang, and Alexander Rakhlin. Computational and statistical boundaries for submatrix localization in a large noisy matrix. *arXiv preprint arXiv:1502.01988*, 2015.
- [34] Burak Cakmak, Ole Winther, and Bernard H Fleury. S-amp: Approximate message passing for general matrix ensembles. In *Information Theory Workshop (ITW), 2014 IEEE*, pages 192–196. IEEE, 2014.
- [35] Francesco Caltagirone, Silvio Franz, Richard G Morris, and Lenka Zdeborová. Dynamics and termination cost of spatially coupled mean-field models. *Physical Review E*, 89(1):012102, 2014.
- [36] Francesco Caltagirone, Giorgio Parisi, and Tommaso Rizzo. Dynamical critical exponents for the mean-field potts glass. *Physical Review E*, 85(5):051504, 2012.
- [37] Francesco Caltagirone and Lenka Zdeborová. Properties of spatial coupling in compressed sensing. *arXiv preprint arXiv:1401.6380*, 2014.
- [38] Francesco Caltagirone, Lenka Zdeborová, and Florent Krzakala. On convergence of approximate message passing. In *Information Theory (ISIT), 2014 IEEE International Symposium on*, pages 1812–1816. IEEE, 2014.
- [39] Chiara Cammarota and Giulio Biroli. Ideal glass transitions by random pinning. *Proceedings of the National Academy of Sciences*, 109(23):8850–8855, 2012.
- [40] Emmanuel J Candè and Michael B Wakin. An introduction to compressive sampling. *Signal Processing Magazine, IEEE*, 25(2):21–30, 2008.
- [41] Emmanuel J Candes and Terence Tao. Near-optimal signal recovery from random projections: Universal encoding strategies? *Information Theory, IEEE Transactions on*, 52(12):5406–5425, 2006.
- [42] JM Carlson, JT Chayes, L Chayes, JP Sethna, and DJ Thouless. Bethe lattice spin glass: the effects of a ferromagnetic bias and external fields. i. bifurcation analysis. *Journal of statistical physics*, 61(5-6):987–1067, 1990.
- [43] JM Carlson, JT Chayes, James P Sethna, and DJ Thouless. Bethe lattice spin glass: the effects of a ferromagnetic bias and external fields. ii. magnetized spin-glass phase and the de almeida-thouless line. *Journal of statistical physics*, 61(5-6):1069–1084, 1990.
- [44] Tommaso Castellani, Florent Krzakala, and Federico Ricci-Tersenghi. Spin glass models with ferromagnetically biased couplings on the Bethe lattice: analytic solutions and numerical simulations. *The European Physical Journal B-Condensed Matter and Complex Systems*, 47(1):99–108, 2005.
- [45] Alain Celisse, Jean-Jacques Daudin, Laurent Pierre, et al. Consistency of maximum-likelihood and variational estimators in the stochastic block model. *Electronic Journal of Statistics*, 6:1847–1899, 2012.
- [46] Patrick Charbonneau, Yuliang Jin, Giorgio Parisi, Beatriz Seoane, and Francesco Zamponi. Numerical detection of the gardner transition in a mean-field glass former. *arXiv preprint arXiv:1501.07244*, 2015.
- [47] Patrick Charbonneau, Yuliang Jin, Giorgio Parisi, and Francesco Zamponi. Hopping and the stokes–einstein relation breakdown in simple glass formers. *Proceedings of the National Academy of Sciences*, 111(42):15025–15030, 2014.
- [48] Patrick Charbonneau, Jorge Kurchan, Giorgio Parisi, Pierfrancesco Urbani, and Francesco Zamponi. Fractal free energy landscapes in structural glasses. *Nature communications*, 5, 2014.



- [49] Peter Cheeseman, Bob Kanefsky, and William M. Taylor. Where the Really Hard Problems Are. In *Proc. 12th IJCAI*, pages 331–337, San Mateo, CA, USA, 1991. Morgan Kaufmann.
- [50] M Chertkov, L Kroc, F Krzakala, M Vergassola, and L Zdeborová. Inference in particle tracking experiments by passing messages between images. *Proceedings of the National Academy of Sciences*, 107(17):7663–7668, 2010.
- [51] Aaron Clauset, Mark EJ Newman, and Cristopher Moore. Finding community structure in very large networks. *Physical review E*, 70(6):066111, 2004.
- [52] Amin Coja-Oghlan. Graph partitioning via adaptive spectral techniques. *Combinatorics, Probability and Computing*, 19(02):227–284, 2010.
- [53] Amin Coja-Oghlan and André Lanka. Finding planted partitions in random graphs with general degree distributions. *SIAM Journal on Discrete Mathematics*, 23(4):1682–1714, 2009.
- [54] Amin Coja-Oghlan, Elchanan Mossel, and Dan Vilenchik. A spectral approach to analysing belief propagation for 3-colouring. *Combinatorics, Probability and Computing*, 18(06):881–912, 2009.
- [55] A Crisanti, H Horner, and H-J Sommers. The spherical-p-spin interaction spin-glass model. *Zeitschrift für Physik B Condensed Matter*, 92(2):257–271, 1993.
- [56] L. F. Cugliandolo and J. Kurchan. Analytical solution of the off-equilibrium dynamics of a long-range spin glass model. *Phys. Rev. Lett.*, 71:173, 1993.
- [57] J. R. L. de Almeida and D. J. Thouless. Stability of the Sherrington-Kirkpatrick solution of a spin-glass model. *J. Phys. A*, 11:983–990, 1978.
- [58] Bruno De Finetti. Theory of probability. a critical introductory treatment. 1979.
- [59] Aurelien Decelle, Florent Krzakala, Cristopher Moore, and Lenka Zdeborová. Asymptotic analysis of the stochastic block model for modular networks and its algorithmic applications. *Physical Review E*, 84(6):066106, 2011.
- [60] Aurelien Decelle, Florent Krzakala, Cristopher Moore, and Lenka Zdeborová. Inference and phase transitions in the detection of modules in sparse networks. *Physical Review Letters*, 107(6):065701, 2011.
- [61] Amir Dembo, Andrea Montanari, et al. Ising models on locally tree-like graphs. *The Annals of Applied Probability*, 20(2):565–592, 2010.
- [62] Arthur P Dempster, Nan M Laird, and Donald B Rubin. Maximum likelihood from incomplete data via the em algorithm. *Journal of the royal statistical society. Series B (methodological)*, pages 1–38, 1977.
- [63] Yash Deshpande and Andrea Montanari. Finding hidden cliques of size  $\sqrt{N/e}$  in nearly linear time. *Foundations of Computational Mathematics*, pages 1–60, 2015.
- [64] William E Donath and Alan J Hoffman. Lower bounds for the partitioning of graphs. *IBM Journal of Research and Development*, 17(5):420–425, 1973.
- [65] David L Donoho. Compressed sensing. *Information Theory, IEEE Transactions on*, 52(4):1289–1306, 2006.
- [66] David L Donoho, Adel Javanmard, and Alessandro Montanari. Information-theoretically optimal compressed sensing via spatial coupling and approximate message passing. *Information Theory, IEEE Transactions on*, 59(11):7434–7464, 2013.
- [67] David L Donoho, Iain Johnstone, and Alessandro Montanari. Accurate prediction of phase transitions in compressed sensing via a connection to minimax denoising. *Information Theory, IEEE Transactions on*, 59(6):3396–3433, 2013.
- [68] David L Donoho, Arian Maleki, and Andrea Montanari. Message-passing algorithms for compressed sensing. *Proceedings of the National Academy of Sciences*, 106(45):18914–18919, 2009.
- [69] David L. Donoho, Arian Maleki, and Andrea Montanari. Message-passing algorithms for compressed sensing. *Proc. Natl. Acad. Sci.*, 106(45):18914–18919, 2009.
- [70] David L Donoho and Jared Tanner. Sparse nonnegative solution of underdetermined linear equations by linear programming. *Proceedings of the National Academy of Sciences of the United States of America*, 102(27):9446–9451, 2005.
- [71] Angélique Drémeau, Antoine Liutkus, David Martina, Ori Katz, Christophe Schülke, Florent Krzakala, Sylvain Gigan, and Laurent Daudet. Reference-less measurement of the transmission matrix of a highly scattering material using a dmd and phase retrieval techniques. *Optics express*, 23(9):11898–11911, 2015.
- [72] Andreas Engel and Christian P. L. Van den Broeck. *Statistical Mechanics of Learning*. Cambridge University Press, New York, NY, USA, 2001.
- [73] Vitaly Feldman, Will Perkins, and Santosh Vempala. On the complexity of random satisfiability problems with planted solutions. *arXiv preprint arXiv:1311.4821*, 2013.
- [74] A. J. Felstrom and K.S. Zigangirov. Time-varying periodic convolutional codes with low-density parity-check matrix. *IEEE Trans. Inf. Theory*, 45(6):2181–2191, 1999.
- [75] Miroslav Fiedler. Algebraic connectivity of graphs. *Czechoslovak mathematical journal*, 23(2):298–305, 1973.
- [76] Laura Foini, Florent Krzakala, and Francesco Zamponi. On the relation between kinetically constrained models of glass dynamics and the random first-order transition theory. *Journal of Statistical Mechanics: Theory and Experiment*, 2012(06):P06013, 2012.
- [77] Santo Fortunato. Community detection in graphs. *Physics Reports*, 486(3):75–174, 2010.
- [78] S. Franz, M. Mézard, F. Ricci-Tersenghi, M. Weigt, and R. Zecchina. A ferromagnet with a glass transition. *Europhys. Lett.*, 55:465, 2001.
- [79] Silvio Franz and Giorgio Parisi. Phase diagram of coupled glassy systems: A mean-field study. *Phys. Rev. Lett.*, 79(13):2486–2489, Sep 1997.
- [80] Silvio Franz and Giorgio Parisi. Quasi-equilibrium in glassy dynamics: an algebraic view. *Journal of Statistical Mechanics: Theory and Experiment*, 2013(02):P02003, 2013.
- [81] Joel Friedman. *A proof of Alon’s second eigenvalue conjecture and related problems*. American Mathematical Soc., 2008.
- [82] R. G. Gallager. *Information theory and reliable communication*. John Wiley and Sons, New York, 1968.

- [83] E Gardner and B Derrida. Optimal storage properties of neural network models. *Journal of Physics A: Mathematical and General*, 21(1):271, 1988.
- [84] E Gardner and B Derrida. Three unfinished works on the optimal storage capacity of networks. *Journal of Physics A: Mathematical and General*, 22(12):1983, 1989.
- [85] A Georges, D Hansel, P Le Doussal, and J-P Bouchaud. Exact properties of spin glasses. ii. nishimori's line: new results and physical implications. *Journal de Physique*, 46(11):1827–1836, 1985.
- [86] Michelle Girvan and Mark EJ Newman. Community structure in social and biological networks. *Proceedings of the national academy of sciences*, 99(12):7821–7826, 2002.
- [87] Paul M Goldbart, Nigel Goldenfeld, and David Sherrington. Stealing the gold—a celebration of the pioneering physics of sam edwards. *Stealing the Gold—A Celebration of the Pioneering Physics of Sam Edwards*, by Paul M Goldbart, Nigel Goldenfeld and David Sherrington, pp. 458. Foreword by Paul M Goldbart, Nigel Goldenfeld and David Sherrington. Oxford University Press, Feb 2005. ISBN-10: 0198528531. ISBN-13: 9780198528531, 1, 2005.
- [88] Emmanuelle Gouillart, Florent Krzakala, Marc Mézard, and Lenka Zdeborová. Belief-propagation reconstruction for discrete tomography. *Inverse Problems*, 29(3):035003, 2013.
- [89] Peter Grassberger and Jean-Pierre Nadal. *From statistical physics to statistical inference and back*. Kluwer Academic, 1994.
- [90] D. J. Gross, I. Kanter, and H. Sompolinsky. Mean-field theory of the potts glass. *Phys. Rev. Lett.*, 55(3):304–307, Jul 1985.
- [91] DJ Gross, I Kanter, and Haim Sompolinsky. Mean-field theory of the potts glass. *Physical review letters*, 55(3):304, 1985.
- [92] D.J. Gross and M. Mézard. The simplest spin glass. *Nucl. Phys. B*, 240:431, 1984.
- [93] F. Guerra and F. L. Toninelli. The thermodynamic limit in mean field spin glass models. 2002. cond-mat/0204280.
- [94] Géza Györgyi. First-order transition to perfect generalization in a neural network with binary synapses. *Physical Review A*, 41(12):7097, 1990.
- [95] Bruce Hajek, Yihong Wu, and Jiaming Xu. Computational lower bounds for community detection on random graphs. *arXiv preprint arXiv:1406.6625*, 2014.
- [96] Kathleen E Hamilton and Leonid P Pryadko. Tight lower bound for percolation threshold on an infinite graph. *Physical review letters*, 113(20):208701, 2014.
- [97] Ki-ichiro Hashimoto. Zeta functions of finite graphs and representations of p-adic groups. *Automorphic forms and geometry of arithmetic varieties.*, pages 211–280, 1989.
- [98] S Hamed Hassani, Nicolas Macris, and Ruediger Urbanke. Chains of mean-field models. *J. Stat. Mech.: Theor. and Exp.*, page P02011, 2012.
- [99] Trevor Hastie, Robert Tibshirani, Jerome Friedman, and James Franklin. The elements of statistical learning: data mining, inference and prediction. *The Mathematical Intelligencer*, 27(2):83–85, 2005.
- [100] Matthew B Hastings. Community detection as an inference problem. *Physical Review E*, 74(3):035102, 2006.
- [101] Simon Heimlicher, Marc Lelarge, and Laurent Massoulié. Community detection in the labelled stochastic block model. 09 2012.
- [102] Itay Hen and AP Young. Exponential complexity of the quantum adiabatic algorithm for certain satisfiability problems. *Physical Review E*, 84(6):061152, 2011.
- [103] Geoffrey E. Hinton. Training products of experts by minimizing contrastive divergence. *Neural Computation*, 14(8):1771–1800, August 2002.
- [104] Geoffrey E. Hinton. A practical guide to training restricted boltzmann machines. Technical Report UTML TR 2010-003, University of Toronto, Toronto, Canada, August 2010.
- [105] Glen M Hocky, Ludovic Berthier, and David R Reichman. Equilibrium ultrastable glasses produced by random pinning. *The Journal of chemical physics*, 141(22):224503, 2014.
- [106] Jake M Hofman and Chris H Wiggins. Bayesian approach to network modularity. *Physical review letters*, 100(25):258701, 2008.
- [107] Paul W Holland, Kathryn Blackmond Laskey, and Samuel Leinhardt. Stochastic blockmodels: First steps. *Social networks*, 5(2):109–137, 1983.
- [108] John J Hopfield. Neural networks and physical systems with emergent collective computational abilities. *Proceedings of the national academy of sciences*, 79(8):2554–2558, 1982.
- [109] Yukito Iba. The nishimori line and bayesian statistics. *Journal of Physics A: Mathematical and General*, 32(21):3875, 1999.
- [110] Edwin T Jaynes. Information theory and statistical mechanics. *Physical review*, 106(4):620, 1957.
- [111] Mark Jerrum. Large cliques elude the metropolis process. *Random Structures & Algorithms*, 3(4):347–359, 1992.
- [112] Haixia Jia, Cristopher Moore, and Doug Strain. Generating hard satisfiable formulas by hiding solutions deceptively. In *Proceedings of the National Conference on Artificial Intelligence*, volume 20, page 384. Menlo Park, CA; Cambridge, MA; London; AAAI Press; MIT Press; 1999, 2005.
- [113] Antony Joseph and Andrew R Barron. Least squares superposition codes of moderate dictionary size are reliable at rates up to capacity. *Information Theory, IEEE Transactions on*, 58(5):2541–2557, 2012.
- [114] Ari Juels and Marcus Peinado. Hiding cliques for cryptographic security. *Designs, Codes and Cryptography*, 20(3):269–280, 2000.
- [115] Yoshiyuki Kabashima. A CDMA multiuser detection algorithm on the basis of belief propagation. *Journal of Physics A: Mathematical and General*, 36(43):11111, 2003.

- [116] Yoshiyuki Kabashima. Propagating beliefs in spin-glass models. *Journal of the Physical Society of Japan*, 72(7):1645–1649, 2003.
- [117] Yoshiyuki Kabashima. Inference from correlated patterns: a unified theory for perceptron learning and linear vector channels. In *Journal of Physics: Conference Series*, volume 95, page 012001. IOP Publishing, 2008.
- [118] Yoshiyuki Kabashima, Florent Krzakala, Marc Mézard, Ayaka Sakata, and Lenka Zdeborová. Phase transitions and sample complexity in bayes-optimal matrix factorization. *arXiv preprint arXiv:1402.1298*, 2014.
- [119] Yoshiyuki Kabashima and David Saad. Belief propagation vs. tap for decoding corrupted messages. *EPL (Europhysics Letters)*, 44(5):668, 1998.
- [120] Yoshiyuki Kabashima and Shinsuke Uda. A BP-based algorithm for performing Bayesian inference in large perceptron-type networks. In *Algorithmic Learning Theory*, pages 479–493. Springer, 2004.
- [121] David R Karger, Sewoong Oh, and Devavrat Shah. Iterative learning for reliable crowdsourcing systems. In *Advances in neural information processing systems*, pages 1953–1961, 2011.
- [122] Brian Karrer and Mark EJ Newman. Stochastic blockmodels and community structure in networks. *Physical Review E*, 83(1):016107, 2011.
- [123] Brian Karrer, MEJ Newman, and Lenka Zdeborová. Percolation on sparse networks. *Physical review letters*, 113(20):208702, 2014.
- [124] Raghunandan H Keshavan, Andrea Montanari, and Sewoong Oh. Matrix completion from a few entries. *Information Theory, IEEE Transactions on*, 56(6):2980–2998, 2010.
- [125] T.R. Kirkpatrick and D. Thirumalai. Dynamics of the structural glass transition and the  $p$ -spin-interaction spin-glass model. *Phys. Rev. Lett.*, 58:2091, 1987.
- [126] T.R. Kirkpatrick and D. Thirumalai.  $p$ -spin-interaction spin-glass models: Connections with the structural glass problem. *Phys. Rev. B*, 36:5388, 1987.
- [127] T.R. Kirkpatrick, D. Thirumalai, and P.G. Wolynes. Scaling concepts for the dynamics of viscous liquids near an ideal glassy state. *Phys. Rev. A*, 40:1045, 1989.
- [128] TR Kirkpatrick and PG Wolynes. Connections between some kinetic and equilibrium theories of the glass transition. *Physical Review A*, 35(7):3072, 1987.
- [129] TR Kirkpatrick and PG Wolynes. Stable and metastable states in mean-field potts and structural glasses. *Physical Review B*, 36(16):8552, 1987.
- [130] Valdis Krebs. Books about us politics. *unpublished*, <http://www.orgnet.com>, 2004.
- [131] F. Krzakala and J. Kurchan. A landscape analysis of constraint satisfaction problems. *Phys. Rev. E*, 76:021122, 2007.
- [132] F Krzakala, M Mézard, F Sausset, YF Sun, and L Zdeborová. Statistical-physics-based reconstruction in compressed sensing. *Physical Review X*, 2(2):021005, 2012.
- [133] Florent Krzakala, Andre Manoel, Eric W Tramel, and Lenka Zdeborova. Variational free energies for compressed sensing. In *Information Theory (ISIT), 2014 IEEE International Symposium on*, pages 1499–1503. IEEE, 2014.
- [134] Florent Krzakala, Marc Mézard, Francois Sausset, Yifan Sun, and Lenka Zdeborová. Probabilistic reconstruction in compressed sensing: algorithms, phase diagrams, and threshold achieving matrices. *Journal of Statistical Mechanics: Theory and Experiment*, 2012(08):P08009, 2012.
- [135] Florent Krzakala, Marc Mézard, and Lenka Zdeborová. Compressed sensing under matrix uncertainty: Optimum thresholds and robust approximate message passing. In *Acoustics, Speech and Signal Processing (ICASSP), 2013 IEEE International Conference on*, pages 5519–5523. IEEE, 2013.
- [136] Florent Krzakala, Marc Mézard, and Lenka Zdeborová. Reweighted belief propagation and quiet planting for random k-sat. *Journal on Satisfiability, Boolean Modeling and Computation*, 8:149, 2014.
- [137] Florent Krzakala, Cristopher Moore, Elchanan Mossel, Joe Neeman, Allan Sly, Lenka Zdeborová, and Pan Zhang. Spectral redemption in clustering sparse networks. *Proceedings of the National Academy of Sciences*, 110(52):20935–20940, 2013.
- [138] Florent Krzakala, Federico Ricci-Tersenghi, Lenka Zdeborová, Riccardo Zecchina, Eric W. Tramel, and Leticia F. Cugliandolo. *Statistical Physics, Optimization, Inference and Message-Passing Algorithms*. Oxford University Press, 2015.
- [139] Florent Krzakala and Lenka Zdeborová. Hiding quiet solutions in random constraint satisfaction problems. *Physical review letters*, 102(23):238701, 2009.
- [140] Florent Krzakala and Lenka Zdeborová. Following gibbs states adiabatically - the energy landscape of mean-field glassy systems. *EPL (Europhysics Letters)*, 90(6):66002, 2010.
- [141] Florent Krzakala and Lenka Zdeborová. On melting dynamics and the glass transition. i. glassy aspects of melting dynamics. *The Journal of chemical physics*, 134(3):034512, 2011.
- [142] Florent Krzakala and Lenka Zdeborová. On melting dynamics and the glass transition. ii. glassy dynamics as a melting process. *The Journal of chemical physics*, 134(3):034513, 2011.
- [143] Florent Krzakala and Lenka Zdeborová. Performance of simulated annealing in  $p$ -spin glasses. In *Journal of Physics: Conference Series*, volume 473, page 012022. IOP Publishing, 2013.
- [144] S. Kudekar and H.D. Pfister. The effect of spatial coupling on compressive sensing. In *Communication, Control, and Computing (Allerton)*, pages 347–353, 2010.
- [145] Shrinivas Kudekar, Thomas J Richardson, and Rüdiger L Urbanke. Threshold saturation via spatial coupling: Why convolutional ldpc ensembles perform so well over the bec. *IEEE Transactions on Information Theory*, 57(2):803–834, 2011.
- [146] C. Kwon and D. J. Thouless. Ising spin glass at zero temperature on the bethe lattice. *Phys. Rev. B*, 37, 1988.
- [147] Laurent Laloux, Pierre Cizeau, Jean-Philippe Bouchaud, and Marc Potters. Noise dressing of financial correlation matrices. *Physical review letters*, 83(7):1467, 1999.

- [148] M. Lelarge, L. Massoulié, and Jiaming Xu. Reconstruction in the labeled stochastic block model. In *Information Theory Workshop (ITW), 2013 IEEE*, pages 1–5, Sept 2013.
- [149] Michael Lentmaier, Arvind Sridharan, Daniel J Costello, and K Sh Zigangirov. Iterative decoding threshold analysis for ldpc convolutional codes. *IEEE Trans. Inf. Theory*, 56(10):5274–5289, 2010.
- [150] Thibault Lesieur, Florent Krzakala, and Lenka Zdeborová. Mmse of probabilistic low-rank matrix estimation: Universality with respect to the output channel. *arXiv preprint arXiv:1507.03857*, 2015.
- [151] David Lusseau, Karsten Schneider, Oliver J Boisseau, Patti Haase, Elisabeth Slooten, and Steve M Dawson. The bottlenose dolphin community of doubtful sound features a large proportion of long-lasting associations. *Behavioral Ecology and Sociobiology*, 54(4):396–405, 2003.
- [152] Zongming Ma, Yihong Wu, et al. Computational barriers in minimax submatrix detection. *The Annals of Statistics*, 43(3):1089–1116, 2015.
- [153] D. J. C. MacKay. *Information theory, inference, and learning algorithms*. Cambridge University Press, Cambridge, 2003.
- [154] Andre Manoel, Florent Krzakala, Eric Tramel, and Lenka Zdeborová. Swept approximate message passing for sparse estimation. In *Proceedings of the 32nd International Conference on Machine Learning (ICML-15)*, pages 1123–1132, 2015.
- [155] Romain Mari and Jorge Kurchan. Dynamical transition of glasses: From exact to approximate. *The Journal of chemical physics*, 135(12):124504, 2011.
- [156] Manuel Sebastian Mariani, Giorgio Parisi, and Corrado Rainone. Calorimetric glass transition in a mean-field theory approach. *Proceedings of the National Academy of Sciences*, 112(8):2361–2366, 2015.
- [157] Travis Martin, Xiao Zhang, and MEJ Newman. Localization and centrality in networks. *Physical Review E*, 90(5):052808, 2014.
- [158] Laurent Massoulié. Community detection thresholds and the weak Ramanujan property. In *Proceedings of the 46th Annual ACM Symposium on Theory of Computing*, pages 694–703. ACM, 2014.
- [159] Sharon Bertsch McGrayne. *The Theory That Would Not Die: How Bayes Rule Cracked the Enigma Code, Hunted Down Russian Submarines, and Emerged Triumphant from Two Centuries of Controversy by Sharon Bertsch McGrayne*. Yale University Press, 2011.
- [160] M. Mézard and G. Parisi. The bethe lattice spin glass revisited. *Eur. Phys. J. B*, 20:217, 2001.
- [161] M. Mézard and G. Parisi. The cavity method at zero temperature. *J. Stat. Phys.*, 111:1–34, 2003.
- [162] M. Mézard, G. Parisi, and M. A. Virasoro. SK model: The replica solution without replicas. *Europhys. Lett.*, 1:77–82, 1986.
- [163] M. Mézard, G. Parisi, and M. A. Virasoro. *Spin-Glass Theory and Beyond*, volume 9 of *Lecture Notes in Physics*. World Scientific, Singapore, 1987.
- [164] M. Mézard, G. Parisi, and R. Zecchina. Analytic and algorithmic solution of random satisfiability problems. *Science*, 297:812–815, 2002.
- [165] Marc Mezard and Andrea Montanari. *Information, physics, and computation*. Oxford University Press, 2009.
- [166] R. Monasson and R. Zecchina. Entropy of the K-satisfiability problem. *Phys. Rev. Lett.*, 76:3881–3885, 1996.
- [167] Rémi Monasson, Riccardo Zecchina, Scott Kirkpatrick, Bart Selman, and Lidror Troyansky. Determining computational complexity from characteristic “phase transitions”. *Nature*, 400(6740):133–137, 1999.
- [168] A. Montanari. Estimating random variables from random sparse observations. *European Transactions on Telecommunications*, 19(4):385–403, 2008.
- [169] A. Montanari and G. Semerjian. On the dynamics of the glass transition on bethe lattices. *J. Stat. Phys.*, 124:103–189, 2006.
- [170] A. Montanari and G. Semerjian. Rigorous inequalities between length and time scales in glassy systems. *J. Stat. Phys.*, 125:23, 2006.
- [171] Andrea Montanari and Devavrat Shah. Counting good truth assignments of random k-SAT formulae. In *Proceedings of the eighteenth annual ACM-SIAM symposium on Discrete algorithms*, pages 1255–1264. Society for Industrial and Applied Mathematics, 2007.
- [172] Joris M Mooij, Hilbert J Kappen, et al. Validity estimates for loopy belief propagation on binary real-world networks. In *NIPS*, 2004.
- [173] Cristopher Moore and Stephan Mertens. *The nature of computation*. Oxford University Press, 2011.
- [174] T. Mora. *Géométrie et inférence dans l’optimisation et en théorie de l’information*. PhD thesis, Université Paris-Sud, 2007. <http://tel.archives-ouvertes.fr/tel-00175221/en/>.
- [175] Flaviano Morone and Hernán A Makse. Influence maximization in complex networks through optimal percolation. *Nature*, 2015.
- [176] Allard P Mosk, Ad Lagendijk, Geoffroy Lerosey, and Mathias Fink. Controlling waves in space and time for imaging and focusing in complex media. *Nature photonics*, 6(5):283–292, 2012.
- [177] Elchanan Mossel, Joe Neeman, and Allan Sly. Stochastic block models and reconstruction. *arXiv preprint arXiv:1202.1499*, 2012.
- [178] Elchanan Mossel, Joe Neeman, and Allan Sly. A proof of the block model threshold conjecture. *arXiv preprint arXiv:1311.4115*, 2013.
- [179] Elchanan Mossel, Joe Neeman, and Allan Sly. Belief propagation, robust reconstruction and optimal recovery of block models. In *Proceedings of The 27th Conference on Learning Theory*, pages 356–370, 2014.
- [180] R. Mulet, A. Pagnani, M. Weigt, and R. Zecchina. Coloring random graphs. *Phys. Rev. Lett.*, 89:268701, 2002.

- [181] Mark EJ Newman. Finding community structure in networks using the eigenvectors of matrices. *Physical review E*, 74(3):036104, 2006.
- [182] Mark EJ Newman. Modularity and community structure in networks. *Proceedings of the National Academy of Sciences*, 103(23):8577–8582, 2006.
- [183] H. Nishimori. *Statistical Physics of Spin Glasses and Information Processing: An Introduction*. Oxford University Press, Oxford, UK, 2001.
- [184] Hidetoshi Nishimori. Exact results and critical properties of the ising model with competing interactions. *Journal of Physics C: Solid State Physics*, 13(21):4071, 1980.
- [185] Hidetoshi Nishimori. Internal energy, specific heat and correlation function of the bond-random ising model. *Progress of Theoretical Physics*, 66(4):1169–1181, 1981.
- [186]
- [187] L. Onsager. A two dimensional model with an order-disorder transition. *Phys. Rev*, 65, 1965.
- [188] Manfred Opper and David Saad. *Advanced mean field methods: Theory and practice*. MIT press, 2001.
- [189] J. Pearl. Reverend bayes on inference engines: A distributed hierarchical approach. In *Proceedings American Association of Artificial Intelligence National Conference on AI*, pages 133–136, Pittsburgh, PA, USA, 1982.
- [190] Henry D Pfister and Pascal O Vontobel. On the relevance of graph covers and zeta functions for the analysis of SPA decoding of cycle codes. In *Information Theory Proceedings (ISIT), 2013 IEEE International Symposium on*, pages 3000–3004. IEEE, 2013.
- [191] SM Popoff, G Lerosey, R Carminati, M Fink, AC Boccarda, and S Gigan. Measuring the transmission matrix in optics: an approach to the study and control of light propagation in disordered media. *Physical review letters*, 104(10):100601, 2010.
- [192] Filippo Radicchi. Predicting percolation thresholds in networks. *Physical Review E*, 91(1):010801, 2015.
- [193] Corrado Rainone, Pierfrancesco Urbani, Hajime Yoshino, and Francesco Zamponi. Following the evolution of hard sphere glasses in infinite dimensions under external perturbations: Compression and shear strain. *Physical review letters*, 114(1):015701, 2015.
- [194] Sundeep Rangan. Estimation with random linear mixing, belief propagation and compressed sensing. In *Information Sciences and Systems (CISS), 2010 44th Annual Conference on*, pages 1–6. IEEE, 2010.
- [195] Sundeep Rangan. Generalized approximate message passing for estimation with random linear mixing. In *Information Theory Proceedings (ISIT), 2011 IEEE International Symposium on*, pages 2168–2172. IEEE, 2011.
- [196] Sundeep Rangan, Alyson K Fletcher, Vivek K Goyal, and Philip Schniter. Hybrid approximate message passing with applications to structured sparsity. *arXiv preprint arXiv:1111.2581*, 2011.
- [197] Sundeep Rangan, Alyson K Fletcher, Philip Schniter, and Ulugbek Kamilov. Inference for generalized linear models via alternating directions and Bethe free energy minimization. *arXiv preprint arXiv:1501.01797*, 2015.
- [198] Sundeep Rangan, Philip Schniter, and Alyson Fletcher. On the convergence of approximate message passing with arbitrary matrices. In *Information Theory (ISIT), 2014 IEEE International Symposium on*, pages 236–240. IEEE, 2014.
- [199] Jörg Reichardt and Stefan Bornholdt. Statistical mechanics of community detection. *Physical Review E*, 74(1):016110, 2006.
- [200] F. Ricci-Tersenghi. The bethe approximation for solving the inverse ising problem: a comparison with other inference methods. *J. Stat. Mech.: Th. and Exp.*, page P08015, 2012.
- [201] Emile Richard and Andrea Montanari. A statistical model for tensor PCA. In *Advances in Neural Information Processing Systems*, pages 2897–2905, 2014.
- [202] Tim Rogers. Assessing node risk and vulnerability in epidemics on networks. *EPL (Europhysics Letters)*, 109(2):28005, 2015.
- [203] Tim Rogers and Isaac Pérez Castillo. Cavity approach to the spectral density of non-Hermitian sparse matrices. *Physical Review E*, 79(1):012101, 2009.
- [204] Frank Rosenblatt. The perceptron: a probabilistic model for information storage and organization in the brain. *Psychological review*, 65(6):386, 1958.
- [205] Cynthia Rush, Adam Greig, and Ramji Venkataramanan. Capacity-achieving sparse superposition codes via approximate message passing decoding. *arXiv preprint arXiv:1501.05892*, 2015.
- [206] Alaa Saade, Florent Krzakala, Marc Lelarge, and Lenka Zdeborová. Spectral detection in the censored block model. *to appear in Proc. of ISIT 2015, arXiv preprint arXiv:1502.00163*, 2015.
- [207] Alaa Saade, Florent Krzakala, and Lenka Zdeborová. Spectral clustering of graphs with the bethe hessian. In *Advances in Neural Information Processing Systems*, pages 406–414, 2014.
- [208] Alaa Saade, Florent Krzakala, and Lenka Zdeborová. Spectral density of the non-backtracking operator on random graphs. *EPL (Europhysics Letters)*, 107(5):50005, 2014.
- [209] Alaa Saade, Florent Krzakala, and Lenka Zdeborová. Matrix completion from fewer entries: Spectral detectability and rank estimation. *arXiv preprint arXiv:1506.03498*, 2015.
- [210] Christian Schlegel and Dmitri Truhachev. Multiple access demodulation in the lifted signal graph with spatial coupling. In *IEEE International Symposium on Information Theory Proceedings (ISIT)*, pages 2989–2993. IEEE, 2011.
- [211] Philip Schniter. Turbo reconstruction of structured sparse signals. In *Information Sciences and Systems (CISS), 2010 44th Annual Conference on*, pages 1–6. IEEE, 2010.
- [212] Philip Schniter and Sundeep Rangan. Compressive phase retrieval via generalized approximate message passing. *Signal Processing, IEEE Transactions on*, 63(4):1043–1055, 2015.

- [213] Bart Selman, David G. Mitchell, and Hector J. Levesque. Generating hard satisfiability problems. *Artif. Intell.*, 81(1-2):17–29, 1996.
- [214] C. E. Shannon. A mathematical theory of communication. *Bell System Tech. Journal*, 27:379–423, 623–655, 1948.
- [215] D. Sherrington and S. Kirkpatrick. Solvable model of a spin-glass. *Phys. Rev. Lett.*, 35:1792–1796, 1975.
- [216] Takashi Shinzato and Yoshiyuki Kabashima. Perceptron capacity revisited: classification ability for correlated patterns. *Journal of Physics A: Mathematical and Theoretical*, 41(32):324013, 2008.
- [217] Sasha Sodin. Random matrices, nonbacktracking walks, and orthogonal polynomials. *Journal of Mathematical Physics*, 48(12):123503, 2007.
- [218] YiFan Sun, Andrea Crisanti, Florent Krzakala, Luca Leuzzi, and Lenka Zdeborová. Following states in temperature in the spherical s+ p-spin glass model. *Journal of Statistical Mechanics: Theory and Experiment*, 2012(07):P07002, 2012.
- [219] Koujin Takeda, Shinsuke Uda, and Yoshiyuki Kabashima. Analysis of cdma systems that are characterized by eigenvalue spectrum. *EPL (Europhysics Letters)*, 76(6):1193, 2006.
- [220] Keigo Takeuchi, Toshiyuki Tanaka, and Tsutomu Kawabata. Improvement of BP-based CDMA multiuser detection by spatial coupling. In *IEEE International Symposium on Information Theory Proceedings (ISIT)*, pages 1489–1493. IEEE, 2011.
- [221] D. J. Thouless. Spin-glass on a Bethe lattice. *Phys. Rev. Lett.*, 56:1082–1085, 1986.
- [222] D. J. Thouless, P. W. Anderson, and R. G. Palmer. Solution of ‘solvable model of a spin-glass’. *Phil. Mag.*, 35:593–601, 1977.
- [223] Robert Tibshirani. Regression shrinkage and selection via the lasso. *Journal of the Royal Statistical Society. Series B (Methodological)*, pages 267–288, 1996.
- [224] Eric W Tramel, Angélique Drémeau, and Florent Krzakala. Approximate message passing with restricted boltzmann machine priors. *arXiv preprint arXiv:1502.06470*, 2015.
- [225] L. Viana and A. J. Bray. Phase diagrams for dilute spin-glasses. *J. Phys. C*, 18:3037–3051, 1985.
- [226] Jeremy Vila, Philip Schniter, Sundeeep Rangan, Florent Krzakala, and Lenka Zdeborová. Adaptive damping and mean removal for the generalized approximate message passing algorithm. *2015 IEEE International Conference on Acoustics, Speech and Signal Processing (ICASSP)*, pages 2021 – 2025, 2015.
- [227] Ulrike Von Luxburg. A tutorial on spectral clustering. *Statistics and computing*, 17(4):395–416, 2007.
- [228] Timothy LH Watkin, Albrecht Rau, and Michael Biehl. The statistical mechanics of learning a rule. *Reviews of Modern Physics*, 65(2):499, 1993.
- [229] J. Wehr and M. Aizenman. Fluctuations of extensive functions of quenched random couplings. *J. Stat. Phys.*, 60:287–306, 1990.
- [230] Harrison C White, Scott A Boorman, and Ronald L Breiger. Social structure from multiple networks. i. blockmodels of roles and positions. *American journal of sociology*, pages 730–780, 1976.
- [231] Yingying Xu, Yoshiyuki Kabashima, and Lenka Zdeborová. Bayesian signal reconstruction for 1-bit compressed sensing. *Journal of Statistical Mechanics: Theory and Experiment*, 2014(11):P11015, 2014.
- [232] Xiaoran Yan, Cosma Shalizi, Jacob E Jensen, Florent Krzakala, Cristopher Moore, Lenka Zdeborova, Pan Zhang, and Yaojia Zhu. Model selection for degree-corrected block models. *Journal of Statistical Mechanics: Theory and Experiment*, 2014(5):P05007, 2014.
- [233] J.S. Yedidia, W.T. Freeman, and Y. Weiss. Understanding belief propagation and its generalizations. In *Exploring Artificial Intelligence in the New Millennium*, pages 239–236. Science & Technology Books, 2003.
- [234] Wayne W Zachary. An information flow model for conflict and fission in small groups. *Journal of anthropological research*, pages 452–473, 1977.
- [235] L. Zdeborová and F. Krzakala. Phase transitions in the coloring of random graphs. *Phys. Rev. E*, 76:031131, 2007.
- [236] Lenka Zdeborová. Statistical physics of hard optimization problems1. *acta physica slovacica*, 59(3):169–303, 2009.
- [237] Lenka Zdeborová and Stefan Boettcher. A conjecture on the maximum cut and bisection width in random regular graphs. *Journal of Statistical Mechanics: Theory and Experiment*, 2010(02):P02020, 2010.
- [238] Lenka Zdeborová and Florent Krzakala. Generalization of the cavity method for adiabatic evolution of gibbs states. *Physical Review B*, 81(22):224205, 2010.
- [239] Lenka Zdeborová and Florent Krzakala. Quiet planting in the locked constraint satisfaction problems. *SIAM Journal on Discrete Mathematics*, 25(2):750–770, 2011.
- [240] Pan Zhang. Nonbacktracking operator for the Ising model and its applications in systems with multiple states. *Physical Review E*, 91(4):042120, 2015.
- [241] Pan Zhang, Florent Krzakala, Marc Mézard, and Lenka Zdeborová. Non-adaptive pooling strategies for detection of rare faulty items. In *Communications Workshops (ICC), 2013 IEEE International Conference on*, pages 1409–1414. IEEE, 2013.
- [242] Pan Zhang, Florent Krzakala, Jörg Reichardt, and Lenka Zdeborová. Comparative study for inference of hidden classes in stochastic block models. *Journal of Statistical Mechanics: Theory and Experiment*, 2012(12):P12021, 2012.
- [243] Pan Zhang and Cristopher Moore. Scalable detection of statistically significant communities and hierarchies, using message passing for modularity. *Proceedings of the National Academy of Sciences*, 111(51):18144–18149, 2014.
- [244] Pan Zhang, Cristopher Moore, and MEJ Newman. Community detection in networks with unequal groups. *arXiv preprint arXiv:1509.00107*, 2015.
- [245] Pan Zhang, Cristopher Moore, and Lenka Zdeborová. Phase transitions in semisupervised clustering of sparse networks. *Physical Review E*, 90(5):052802, 2014.